INVESTIGATION ON TORSIONAL BEHAVIOR OF CFRP STRENGTHENED SQUARE HOLLOW STEEL SECTION

NEWSHA ABDOLLAHI CHAHKAND

DISSERTATION SUBMITTED IN FULFILMENT OF THE REQUIREMENTS FOR THE DEGREE OF MASTER OF ENGINEERING SCIENCE

FACULTY OF ENGINEERING
UNIVERSITY OF MALAYA
KUALA LUMPUR

2013

UNIVERSITI MALAYA
ORIGINAL LITERARY WORK DECLARATION

Name of Candidate: Newsha Abdollahi Chahkand

Registration/Matric No: KGA100002

Name of Degree: Master's Degree

Title of Project Paper/Research Report/Dissertation/Thesis ("this Work"):

Investigation on Torsional Behavior of CFRP Strengthened Square Hollow Steel Section

Field of Study: Structures

I do solemnly and sincerely declare that:

(1) I am the sole author/writer of this Work;
(2) This Work is original;
(3) Any use of any work in which copyright exists was done by way of fair dealing and for permitted purposes and any excerpt or extract from, or reference to or reproduction of any copyright work has been disclosed expressly and sufficiently and the title of the Work and its authorship have been acknowledged in this Work;
(4) I do not have any actual knowledge nor do I ought reasonably to know that the making of this work constitutes an infringement of any copyright work;
(5) I hereby assign all and every rights in the copyright to this Work to the University of Malaya ("UM"), who henceforth shall be owner of the copyright in this Work and that any reproduction or use in any form or by any means whatsoever is prohibited without the written consent of UM having been first had and obtained;
(6) I am fully aware that if in the course of making this Work I have infringed any copyright whether intentionally or otherwise, I may be subject to legal action or any other action as may be determined by UM.

Candidate's Signature Date
Newsha Abdollahi Chahkand

Subscribed and solemnly declared before,

Witness's Signature Date

Name:
Designation

UNIVERSITI MALAYA
PERAKUAN KEASLIAN PENULISAN

Nama: Newsha Abdollahi Chahkand

No. Pendaftaran/Matrik: KGA100002

Nama Ijazah: Master's Degree

Tajuk Kertas Projek/Laporan Penyelidikan/Disertasi/Tesis ("Hasil Kerja ini"):

Investigation on Torsional Behavior of CFRP Strengthened Square Hollow Steel Section

Bidang Penyelidikan: Structures

Saya dengan sesungguhnya dan sebenarnya mengaku bahawa:

(1) Saya adalah satu-satunya pengarang/penulis Hasil Kerja ini;
(2) Hasil Kerja ini adalah asli;
(3) Apa-apa penggunaan mana-mana hasil kerja yang mengandungi hakcipta telah dilakukan secara urusan yang wajar dan bagi maksud yang dibenarkan dan apa-apa petikan, ekstrak, rujukan atau pengeluaran semula daripada atau kepada mana-mana hasil kerja yang mengandungi hakcipta telah dinyatakan dengan sejelasnya dan secukupnya dan satu pengiktirafan tajuk hasil kerja tersebut dan pengarang/penulisnya telah dilakukan di dalam Hasil Kerja ini;
(4) Saya tidak mempunyai apa-apa pengetahuan sebenar atau patut semunasabahnya tahu bahawa penghasilan Hasil Kerja ini melanggar suatu hakcipta hasil kerja yang lain;
(5) Saya dengan ini menyerahkan kesemua dan tiap-tiap hak yang terkandung di dalam hakcipta Hasil Kerja ini kepada Universiti Malaya ("UM") yang seterusnya mula dari sekarang adalah tuan punya kepada hakcipta di dalam Hasil Kerja ini dan apa-apa pengeluaran semula atau penggunaan dalam apa jua bentuk atau dengan apa juga cara sekalipun adalah dilarang tanpa terlebih dahulu mendapat kebenaran bertulis dari UM;
(6) Saya sedar sepenuhnya sekiranya dalam masa penghasilan Hasil Kerja ini saya telah melanggar suatu hakcipta hasil kerja yang lain sama ada dengan niat atau sebaliknya, saya boleh dikenakan tindakan undang-undang atau apa-apa tindakan lain sebagaimana yang diputuskan oleh UM.

Tandatangan Calon Tarikh

Newsha Abdollahi Chahkand

Diperbuat dan sesungguhnya diakui di hadapan,

Tandatangan Saksi Tarikh

Nama:

Jawatan:

ABSTRACT

Fiber Reinforced Polymer (FRP) is one of the most popular methods for structural repairing and strengthening due to several properties such as non-corroding, higher strength, lighter weight, fatigue resistant, high modulus of elasticity, and low density. Extensive studies have been carried out on strengthening of steel members in flexural, shear, buckling, tensile, enhancing fatigue life and enhancing stability of steel members with FRP. It was found that there was no published literature concerning the investigation of torsional behavior of steel structures strengthened with FRP.

This study examines the performance of Carbon Fiber Reinforced Polymer (CFRP) strengthened square hollow section (SHS) to withstand torsional moment using novel wrapping configurations of fiber reinforced polymer. Fifteen beam specimens were tested in order to investigate the effects of different number of layers and CFRP orientations on the performance of strengthened SHS under pure torsion. To investigate the effect of width to thickness ratio of SHS, two sets of specimens with different thickness were considered. In addition, theoretical predictions of ultimate torsional capacity of strengthened square hollow steel section beams were proposed based on classical torsion theory with modified geometric properties of the strengthened specimens.

The best strengthening scheme was obtained for the specimen with four layers of alternating spiral (-45º) and reverse-spiral (45º) arrangement of CFRP with respect to the longitudinal axis of the specimen. The experimental results showed that CFRP strengthening of torsional member was more effective on a beam with larger width to thickness ratio. In general, it was observed that the failure mode of specimens strengthened with spiral direction fiber orientation was splitting, while the failure mode of reverse-spiral direction was rupture and debonding. By comparing the experimental

results and the calculated values using the simplified expression, it was found that the values were in good agreement.

ABSTRAK

Polimer yang diperkuatkan dengan gentian (FRP) merupakan salah satu kaedah yang paling popular untuk memperbaiki dan mengukuhkan struktur disebabkan oleh beberapa sifat seperti tahan karat, kuat, ringan, tahan lama, modulus keanjalan yang tinggi, dan kepadatan yang rendah. Kajian yang menyeluruh telah dijalankan untuk memperkukuhkan anggota struktur keluli dalam lenturan, ricih, lengkokan, tegangan, memanjangkan hayat dan meningkatkan kestabilan bahagian keluli dengan polimer yang diperkuatkan dengan FRP. Kajian telah mendapati bahawa tidak ada literature yang diterbitkan berkenaan kajian kelakuan puntiran struktur keluli yang diperkukuhkan dengan FRP.

Kajian ini menguji prestasi keratan segi empat sama berongga (SHS) yang diperkukuhkan dengan polimer yang diperkuatkan dengan gentian karbon untuk menahan momen puntiran menggunakan konfigurasi pembalutan CFRP yang baru. Lima belas rasuk telah diuji bagi mengkaji kesan menggunakan nombor lapisan dan orientasi yang berbeza ke atas kebolehan CFRP memperkukuhkan SHS. Untuk mengkaji kesan nisbah kelebaran kepada ketebalan SHS, dua set spesimen dengan ketebalan yang berbeza telah diuji. Di samping itu, ramalan secara teori bagi keupayaan puntiran muktamad rasuk SHS yang diperkukuhkan dicadangkan berdasarkan teori puntiran klasik dengan mengubahsuai ciri-ciri geometrik spesimen yang diperkukuhkan.

Skema pengukuhan yang terbaik diperoleh daripada spesimen yang dibalut dengan susunan empat lapisan CFRP selang seli lingkaran (-45˚) dan lingkaran songsang (45˚) dari paksi melintang spesimen. Keputusan eksperimen menunjukkan bahawa pengukuhan anggotan puntiran dengan CFRP lebih berkesan pada yang mempunyai nisbah kelebaran kepada ketebalan yang lebih besar. Secara umum, telah diperhatikan bahawa mod kegagalan spesimen yang diperkukuhkan dengan orientasi gentian dalam arah lingkaran merupakan pembelahan (*splitting*), manakala mod kegagalan arah

lingkaran songsang merupakan pemecahan (*rupture*) dan nyahikatan (*debonding*). Dengan membanding keputusan eksperimen dan nilai-nilai yang dikira menggunakan ungkapan yang dipermudahkan, telah didapati bahawa nilai-nilai tersebut adalah sama.

I dedicate this Thesis to

My first teacher, MOM,

Dad,

&

My Husband,

Your love, sacrifice and patience have made this possible;

You have been there with me through the ups and downs.

I LOVE YOU

&

Thank you very much for your full support.

ACKNOWLEDGEMENTS

I would like to express my appreciation to my supervisors, Professor Ir. Dr. Mohd Zamin Jumaat and Associate Prof. Dr. Nor Hafizah Ramli Sulong for their advice, guidance, and valuable comments concerning this thesis. This project would not have been possible without them.

I would also like to thank the University of Malaya, which allowed me to continue my education and provided financial support for the research.

My special thanks to Encik Mansor Hitam (Laboratory Assistant, Heavy Structures lab.), Mr. Sreedharan A/l V.k.raman (Assistant Science Officer, Heavy Structures lab.), Encik Yusop Zain (Assistant Science Officer, Timber structure lab.), Encik Mohiddin Hamzah (Laboratory Assistant, Hydraulic Lab.), and all the administrative staff members at the Civil and Enviromental Engineering Department of University of Malaya whose contributions and supports have been invaluable.

I would like to thank the suppliers from the local and international companies. Thanks go to Mr. Pierre Favre, Marketing Manager of SIKA in Malaysia. Thanks also to Mr. Yap Cheng Ken, Service Engineer of GT Instruments company. Thanks go to Construction Research Institute of Malaysia (CREAM) and Malaysia Office of Pintas IP Group.

Last but not least, I would like to thank my family for their full support. Your love and sacrifice have made this possible.

Thank you.

TABLE OF CONTENTS

LIST OF FIGURES

LIST OF TABLES

LIST OF SYMBOLS AND ABBREVIATIONS

h: Height of section

b: Width of section

t: Thickness of section

L: Length of section

L_e: Effective Length

h_{eq}: Equivalent height

b_{eq}: Equivalent width

t_{eq}: Equivalent thickness

t_{fiber}: Thickness of fiber

r_{ext}: External corner radius

r_{int}: Internal corner radius

r_m: Mid-corner radius

$r_{ext,eq}$: Equivalent external corner radius

$r_{m,eq}$: Equivalent mid-corner radius

$A_{h:}$ Enclosed area

$A_{h,eq}$: Equivalent enclosed area

E_{CFRP}: Young's modulus of CFRP

E_{steel}: Young's modulus of the steel

τ_y: Shear stress

F_u: Ultimate tensile strength of steel

$T_{pl:}$ Plastic torsional capacity

$T_{pl,eq}$: Ultimate torsional capacity of the strengthened

1.0 INTRODUCTION

1.1 General

Retrofitting and rehabilitation of deteriorated structures are important in regions of high seismic activities. Over the last decade, strengthening and retrofitting of existing steel structures has become one of the important challenges for civil engineering. This study presents the torsional behavior of Carbon Fiber Reinforced Polymer strengthened steel beam specimens with square hollow sections (SHS). The problem statement, objectives of research, scope of work, and outline of the thesis are described in this chapter.

1.2 Problem statement

A conventional repair technique of steel bridges or steel structures commonly includes welding or bolting steel plates to the existing bridges or structures. Welded or bolted heavy steel plates can increase the dead load and decrease the durability of the existing steel bridges or structures. Thus, the need for using durable, resistant, flexible, light-weight materials and cost-effective methods for retrofitting is evident.

Advanced composite substances in the form of Fiber Reinforced Polymer (FRP) have many advantages compared to steel plates. Using FRP is one of the best methods for strengthening and rehabilitation of existing structures (Zhao and Zhang, 2007). Due to several properties such as non-corroding, higher strength, lighter weight, fatigue resistant, high modulus of elasticity, very low coefficient of thermal expansion, and low density, these composite materials have been used in various engineering aspects. As FRPs are becoming accessible at lower prices, a tendency towards using FRP as an alternative to welded steel plate is gaining significant momentum. This increasing momentum has forced advancements in this field and a large deal of research. Several researchers have reported employing CFRP for strengthened steel structures such as

tensile strengthening (Al-Zubaidy et al., 2012), flexural and shear strengthening (Bambach et al., 2009b; Haedir et al., 2010; and El-Tawil et al., 2011), repair of fatigue damage and enhancing fatigue life using CFRP (Tavakkolizadeh and Saadatmanesh, 2003b; and Kima and Harries, 2011), and enhancing stability of steel members with CFRP (Harries et al., 2009)

In the course of literature survey conducted by the author, it was found that there was no published literature concerning the investigation of torsional behavior of steel structures strengthened with FRP. This study attempts to fill the knowledge gap in this area. All conducted studies concerning torsional strengthening so far is related to concrete structures (Koutchoukali and Belarbi, 2001; Ronagh and Dux, 2003; Salom et al., 2004; Hii and Al-Mahaidi, 2005; Fang and Shiau, 2004; Ameli et al., 2007; Al-Mahaidi and Hii, 2007).

However, torsional behavior of structural steel is an important action, and is sometimes the major feature of design and analysis like in the case of curved bridge girders and eccentrically loaded beams. Natural disasters such as earthquake and wind or vortex shedding have repeatedly demonstrated the susceptibility of existing structures to damage by seismic effect. Due to seismic effect, there is a need for an efficient, cost-effective system which can be used for the repair and strengthening of steel highway bridge girders. In the United States of America, the Tacoma Narrows Bridge (1940), the Sunshine Skyway Bridge (1980), and the Silver Bridge (1967) were damaged by wind, storm and heavier loads (rush-hour traffic), which caused the torsional failure of the structure. Many bridges and building elements are subjected to significant equilibrium torsional moments that may require strengthening. A good example of this is the Westgate Bridge in Melbourne, Australia (Gosbell and Meggs, 2002). Hence, comprehensive information on torsional strengthening of steel structures is deemed important.

An experimental design of research was therefore set up in this study in order to gain a better understanding of the behavior of torsional strengthened steel specimens. In this thesis, the experimental procedure including details of specimens, test setup and the results obtained are explained. Influence of the important parameters that may affect the behavior of the strengthened specimens are also elaborated.

1.3 Objectives of research

In general, the objective of this thesis is to investigate the behavior of CFRP strengthened square hollow steel section beams under pure torsion. The specific objectives are described as follows:

a) To evaluate the behavior of strengthened steel beams by using CFRP in terms of torque-twist angle relation, torque-strain relation, and failure modes.
b) To compare the effects of different number of layers of CFRP wrap and CFRP wrap orientation.
c) To investigate the effect of width to thickness ratio of the square hollow steel section beams.
d) To propose a method based on theoretical prediction for determining the torsional capacity of CFRP-strengthened square hollow steel section beams.

1.4 Scope of work

The scope of this study was to explore the effect of adhesive bonded CFRP sheets on pure torsion behavior of SHS through experimental testing. SHS used in the tests had dimensions of 50×50 mm and different thickness of 3 and 4.5 mm. The total length of the beams was 1400 mm and the length of the test region was approximately 1160 mm. The steel sections were hot-formed square hollow sections. The CFRP sheets and epoxy

resins were supplied by Sika Kimia Sdn.Bhd. The CFRP used was SikaWrap®-200C while the epoxy used was Sikadur ®-330.

In total, fifteen SHS specimens strengthened using a novel wrapping configuration of fiber reinforced polymer were tested to withstand torsional moment. The ability of pure torsion strengthening of SHS using CFRP was investigated. In torsional strengthening, the effects of different number of layers of CFRP wrap on the whole structural behavior of the strengthened beams were investigated. In addition, the influence of different CFRP orientations were also examined. These included vertical, spiral and reverse-spiral wrap orientations.

Following extensive experimental work on different CFRP configurations and number of layers, theoretical predictions of ultimate torsional capacity of strengthened steel hollow sections were proposed. The basis of calculation was based on the classical torsion formula. Modified geometrical properties of CFRP strengthened steel sections were formulated. The formula were used to validate the torsional capacity of the strengthened SHS obtained in the experimental work.

1.5 Outline of the thesis

This thesis consists of five chapters. Details of the chapters are as follows:

In chapter One (Introduction), the problem statement, objectives of research, and scope of work are introduced.

Chapter Two (Literature Review) consists of 2 sections. First, a review of previous research on strengthening of steel members with FRP, including flexural strengthening, tensile strengthening, repair of fatigue damage and enhancing fatigue life using CFRP, enhancing stability of steel members with CFRP, and failure modes in CFRP bonded

steel system are presented. Second, literature review of research concerning torsional strengthening of concrete members with FRPs is reported.

In chapter Three, the experimental design is explained, which includes a complete description of the research methodology consisting of specifications of the specimens, preparation of the specimens, test setup and instrumentation.

In chapter Four (Results and Discussions), the findings from the experimental results are analysed and discussed. Theoretical predictions of ultimate torsional capacity of CFRP strengthened steel sections are proposed. Direct comparisons between experimental and theoretical values are presented.

In chapter Five (Conclusions), a summary of achievements from this study is given. In addition, some recommendations for future study, based on the findings of this investigation are presented.

2.0 LITERATURE REVIEW

2.1 Introduction

The utilization of FRP for strengthening existing structures is gaining universal acceptance and widely adopted. FRP is strong against corrosion; with lighter weight, higher strength, and low density, which explains why the usage of these composite materials has increased significantly. At present, based on literature review carried out by the author, no literature was found on investigation relating to torsional behavior of steel structure strengthened using FRP. All recent studies are related to torsional strengthening of concrete structures. Thus, this chapter comprises of two sections.

In the first section, the literatures review of previous research concerning the utilization of FRPs for strengthening of steel members is reported. The second section is a review of previous research concerning torsional strengthening of concrete members with FRPs.

2.2 Fiber Reinforced Polymer (FRP)

Fiber Reinforced Polymer (FRP) is a composite substance which consists of a polymer matrix with fibers. The fibers can be classified into fiberglass (GFRP), aramid (AFRP), or carbon (CFRP). The polymer can be a polyester thermosetting plastic, vinylester, or epoxy. Because of several properties such as higher corrosion resistance of composite materials, lighter weight and higher strength, these composite materials have been used in different types of engineering aspects.

Figure 2.1 shows the comparison of material properties between various FRPs and steel (Quake Wrap, 2008). It can be seen that CFRP have similar stiffness to steel, whereas GFRP and AFRP have lower stiffness match up to steel. Furthermore, CFRP has higher

tensile strength and modulus of elasticity compared to GFRP and AFRP. Table 2.1 shows the properties of carbon, glass and aramid fibers (Lam, 2008).

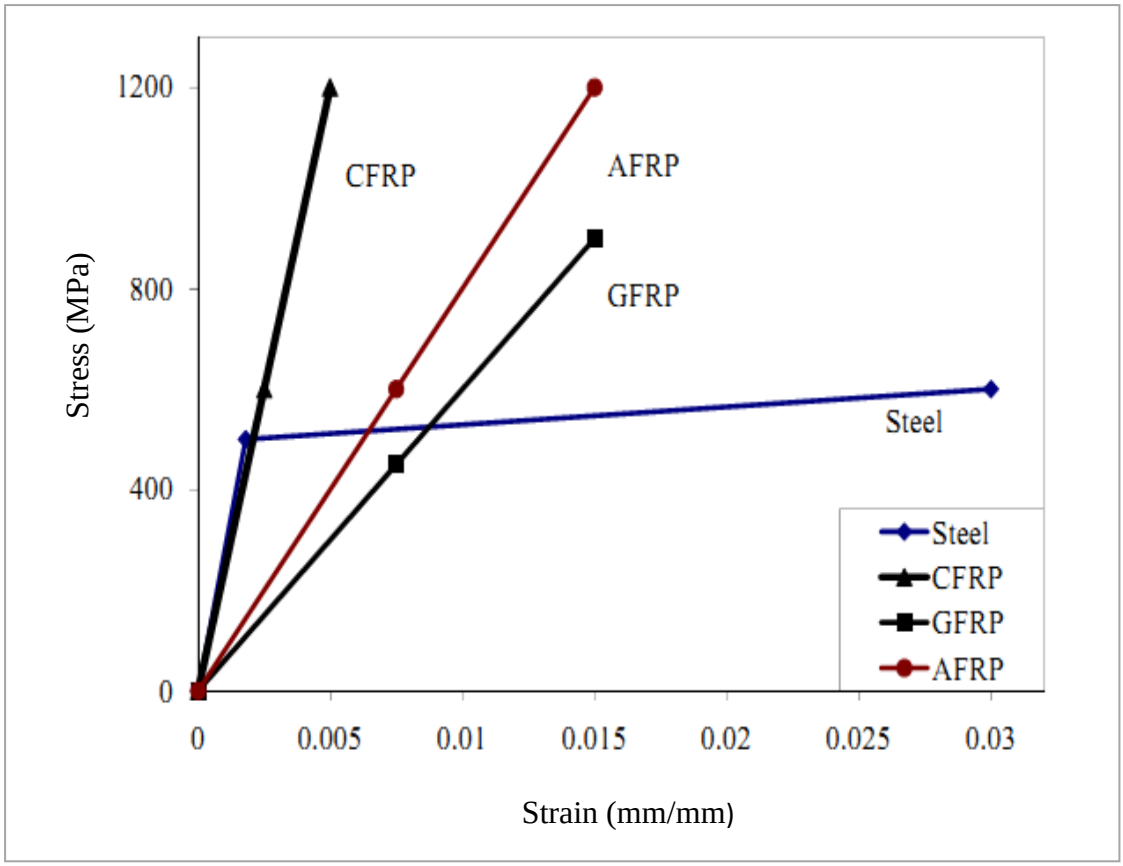

Figure 2.1 Comparison of stress-strain behavior of steel and FRPs (Quake Wrap, 2008)

Table 2.1: Typical properties of carbon, glass and aramid fibers (Lam, 2008)

Type of Fiber	Modulus of Elasticity GPa	Tensile Strength MPa	Ultimate Elongation
Carbon	290~400	2400~5700	0.3%~1.8%
Glass	72~87	3300~4500	4.8%~5.0%
Aramid	62~142	2410~3150	1.5%~4.4%

2.2.1 Carbon Fiber Reinforced Polymer (CFRP)

Carbon Fiber Reinforced Polymer (CFRP) is a composite substance reinforced by carbon fibers. The fibers can be either continuous or discontinuous. They have high

tensile strength which can reach 1000 ksi (7 GPa), very high modulus of elasticity (exceeding that of steel), low density: 114 lb/ft³ (1800 kg/m³), high ultimate strength, and properties enabling the material to be used in highly corrosive environments. CFRP can be classified based on its modulus of elasticity, as shown in Table 2.2 (Kopeliovich, web reference).

Table 2.2: Classification of CFRP based on modulus of elasticity

Classification	Modulus of Elasticity (E) / Tensile Strength (TS) (GPa)
UHM (Ultra High Modulus)	E >450
HM (High Modulus)	E= 350-450
IM (Intermediate Modulus)	E= 200-350
HT (High Tension and Low Modulus)	E<100 and TS>3
SHT (Super High Tension)	TS>4.5

Carbon fiber substances are normally produced in the form of dry fiber tow sheets. The sheets are impregnated by a saturating resin on-site using a wet lay-up method and are suitable for curved applications or highly irregular surfaces. For applications requiring a higher degree of strengthening, the carbon fibers can be pultruded into a procured laminate and bonded to the surface of the structure using a structural adhesive. The carbon fibers show a brittle failure mode which is considered as a disadvantage.

CFRP composite has two forms including CFRP wrap (CFRP dry fabric or CFRP fabric) and CFRP plate (CFRP laminate or CFRP strip). CFRP wrap can be wrapped around structural members, and is flexible. Polymer (adhesive) bonds the CFRP wrap to the structural members and the CFRP wrap is applied on the job site to produce the CFRP composite. CFRP plate is a pre-manufactured CFRP composite. CFRP plate is usually used to repair steel, because steel has a higher tensile elastic modulus.

2.3 Strengthening of Steel Members with FRP

Over two decades, CFRP has been applied to strengthen the various elements in steel structures. The applications of CFRP in strengthening steel structures include:

a) Tensile strengthening

b) Repair of fatigue damage and enhancing fatigue life

c) Enhancing stability of steel members

d) Steel-concrete and bridge girders

e) Fire-damaged steel elements

f) Flexural elements of steel structures

g) Concrete-filled steel sections

h) Compressive sections: circular, rectangular, and tube sections

The following sub-sections review existing studies on various applications of strengthening of steel members with FRP.

2.3.1 Flexural strengthening

There were number of studies related to strengthening of steel structures with FRP, particularly in the field of steel bridge girder.

Sen and Liby (1994) were the first to study potential applications of CFRP to steel members. In their study, steel-concrete composite girders were strengthened with CFRP plates. The results showed that the ultimate flexural capacities of composite beams were considerably increased by using the CFRP laminates. Estimated increase in their ultimate strengths ranged from 11 to 50 %, depending on the mode of failure and the yield strength of the specimen.

Mertz and Gillespie (1996) reported on the usage of CFRP for rehabilitation of deteriorated bridges, where about 40% of tension flange was corroded. The strengthening scheme is shown in Figure 2.2. The results showed 25% increase in stiffness and 100% increase in ultimate load-carrying capacity.

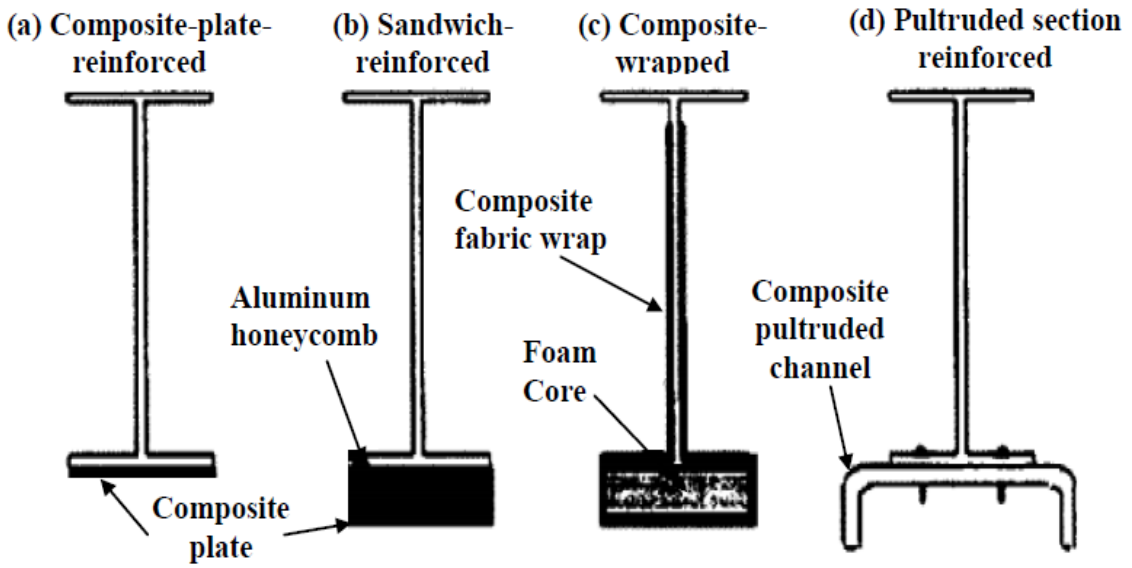

Figure 2.2 Small scaled specimens tested (Mertz and Gillespie, 1996)

Tavakkolizadeh and Saadatmanesh (2003a) used externally bonded CFRP sheets for strengthening steel-concrete composite girders under static loading. CFRP sheets with constant thickness and different number of layers of 1, 3, and 5 were used in the specimens as shown in Figure 2.3. The results showed that the ultimate load-carrying capacities of the girders with 1, 3, and 5 layers increased by 44, 51, and 76%, respectively. The study showed that as the number of CFRP layers increased, the efficiency for utilizing the CFRP sheet decreased.

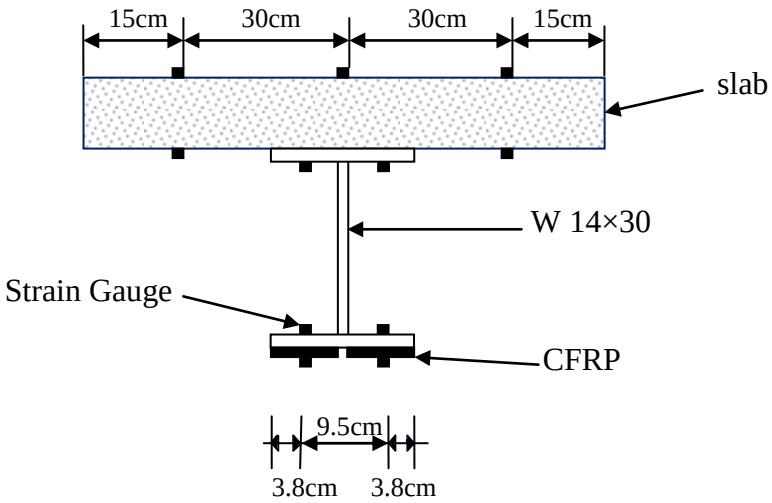

Figure 2.3 Cross sectional properties of composite girder (Tavakkolizadeh and Saadatmanesh, 2003a)

Photiou et al. (2006) investigated artificially degraded steel rectangular hollow section (RHS) beams in pure flexure with an eye towards performance of two types of fiber (carbon/glass) configurations. Their results showed that extending the fiber perimeter up to the webs of the beam provides a significant level of composite action among the two substances, which ensures enhanced post-yield implementation.

Lanier et al. (2009) investigated on steel monopoles strengthened with CFRP materials. The results showed that CFRP substances for strengthening steel monopoles that was installed to enhance their flexural strength and stiffness and can be easily designed.

Deng et al. (2011) investigated the flexural strength of steel–concrete composite beams reinforced with a prestressed CFRP plate. The results showed that the flexural strength was not influenced by the permanent load and the prestressing force when the failure was due to rupture of CFRP plate. However, the flexural strength increased with the co-existence of prestressing force when failure mode was due to crushing of concrete and decreased by the permanent load. The experimental, analytical and FE results are summarized in Table 2.3.

Table 2.3: Summary of experimental, analytical and FE results (Deng et al., 2011)

Specimens	Test results (KN)	Incremental deformation method (KN)	AASHTO method (KN)	Proposed method (KN)	FE analysis (KN)
One layer	528.0	470.4	459.9	479.6	507.0
Three layers	553.4	560.2	537.6	550.8	541.6
Five layers	645.8	596.3	585.6	645.0	598.2

2.3.2 Tensile strengthening

Several researchers have conducted studies on tensile strengthening of steel tubes and bolted joints using adhesively bonded CFRP plates.

Jiao and Zhao (2004) investigated on lap joint between Very High Strength (VHS) tubes through CFRP-epoxy strengthening system in axial tension (Figure 2.4). Three types of epoxy were used including Sikadur-330, Araldite 420, and Araldite Kit K138. The results showed that Araldite 420 was found to be suitable for welded VHS tubes strengthening with the CFRP product of SikaWrap®Hex-230C and also a minimum number of four layers of CFRP were used when strengthening with Araldite 420. Three kinds of failure modes were observed including adhesive failure, fiber tear and mixed failure.

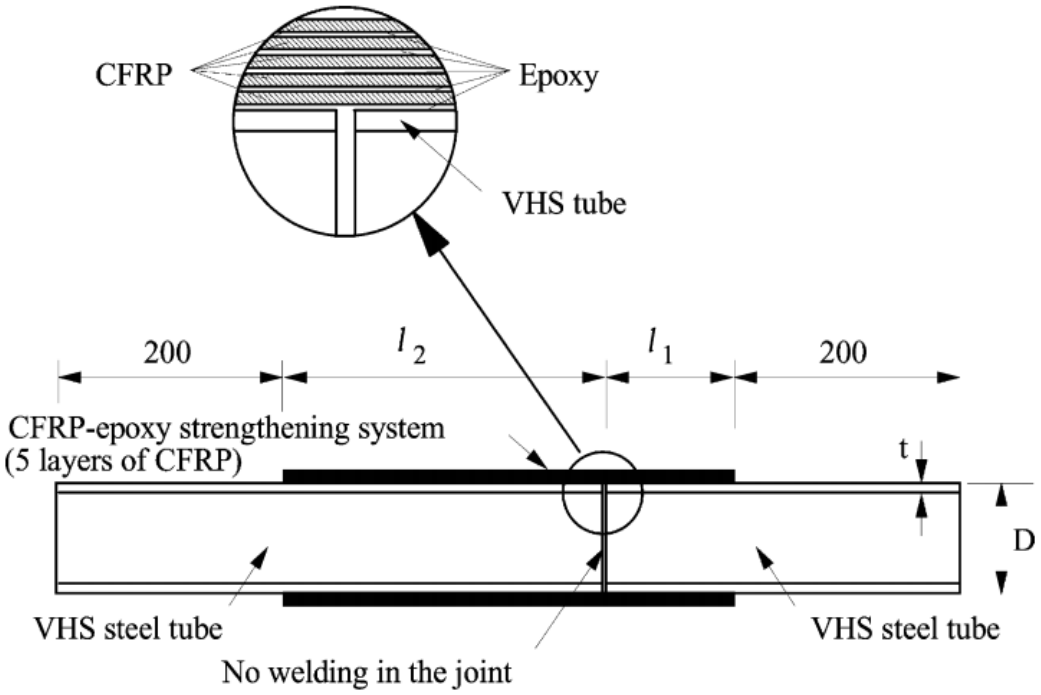

Figure 2.4 Lap joint configuration (Jiao and Zhao, 2004)

Fawzia et al. (2006) performed a series of tests to examine the behavior of Very High Strength (VHS) circular steel tubes strengthened with CFRP in axial tension. The study focused on the bond length between steel and fibers and number of fiber layers. A method to calculate the effective bond length was presented using the strain profile along the length and across the depth of the CFRP layers.

2.3.3 Repair of fatigue damage and enhancing fatigue life using CFRP

Several studies were carried out on fatigue crack propagation in steel members strengthened by CFRP.

Tavakkolizadeh and Saadatmanesh (2003b) used externally bonded CFRP laminates on the retrofitting of notched steel beams for medium cycle fatigue loading. The results showed that the CFRP laminates decreased the crack growth rate significantly; however CFRP patch tends to extend the fatigue life by more than three times.

Liu et al. (2006) investigated the direct tension fatigue behavior of bonded CFRP sheets used to create 'strap joints' between two steel plates. The results showed an apparent fatigue limit of 40% of the ultimate static strength of the strap joint specimens. Below this limit, the steel-CFRP bond behavior and specimen failure was not affected by the applied fatigue loads.

Liu et al. (2009) investigated the prediction of fatigue life for CFRP-strengthened steel plates (Figure 2.5). The fatigue crack growth was presented by a simple analytical method. Two types of fiber sheets were studied. They used normal modulus (E 1/4 240 GPa) and high modulus CFRP (E 1/4 640GPa) sheets. Both double-sided and single-sided repairs were investigated. The method could be used to estimate the fatigue life of CFRP sheets reinforced steel plates, crack growth rate and the stress intensity factors.

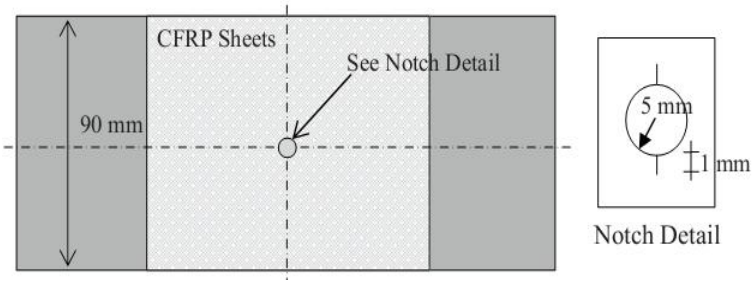

(a) Plan view

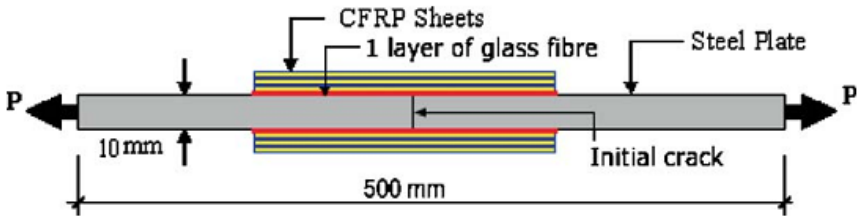

(b) Section view of two-side patched steel plates

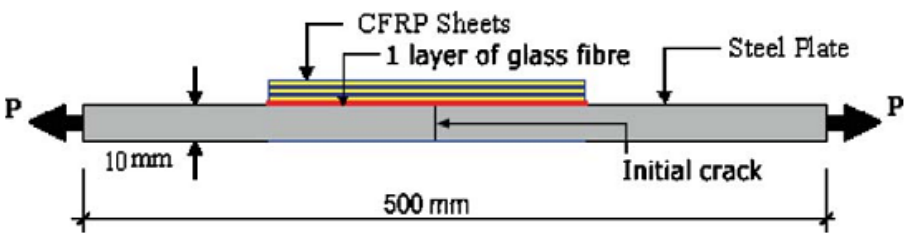

(c) Section view of single-side patched steel plates

Figure 2.5 Configuration of composites-repaired steel plates (Liu et al., 2009)

2.3.4 Enhancing stability of steel members with CFRP

Zhao et al. (2006) investigated the effect of CFRP on the web crippling capacity of cold formed Rectangular Hollow Section (RHS) (Figure 2.6). The study showed that CFRP increased the web crippling capacity particularly for RHS's with higher web depth- to-thickness ratios. The most important findings were: (i) improved restraints against web rotation, (ii) achievement of materials strain hardening and (iii) altering of failure mode from web buckling to web yielding. Greater increase in ultimate deformation for Type 3 and Type 5 was achieved for thinner RHS sections.

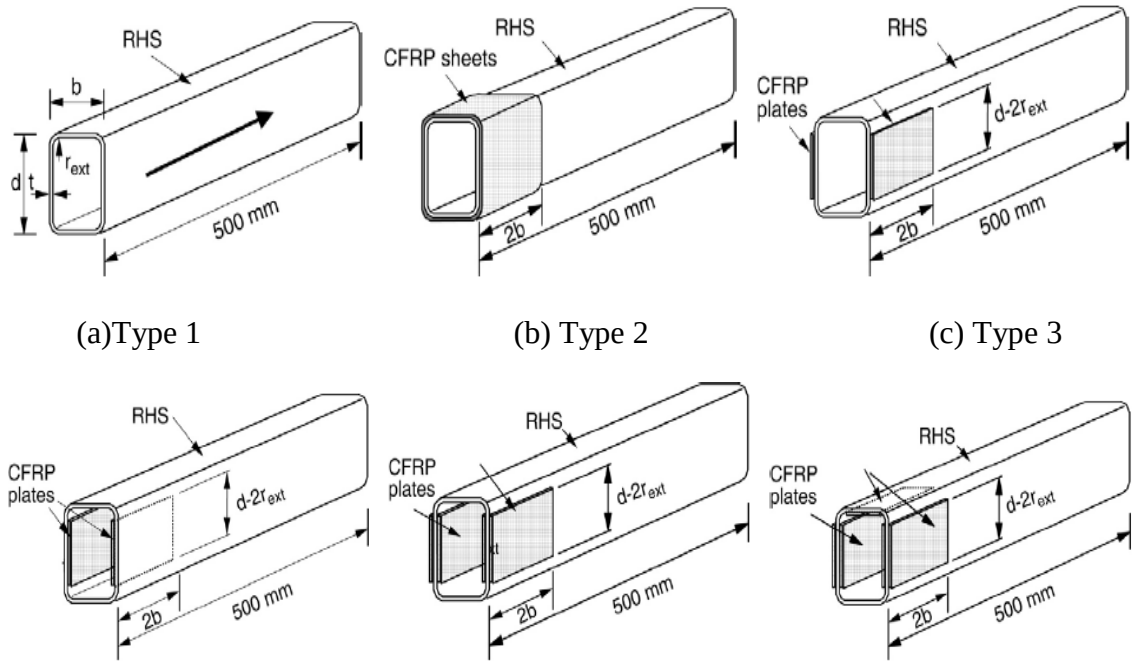

(a)Type 1 (b) Type 2 (c) Type 3

(d) Type 4 (e) Type 5 (f) Type 6

Figure 2.6 Various types of CFRP strengthening (Zhao et al., 2006)

Fernando et al. (2009) showed the results of a series of end bearing tests on CFRP-strengthened rectangular hollow strength (RHS) tubes. Different adhesives were used to connect CFRP plates to RHS tubes. The test results demonstrated that the adhesive properties have a strong effect on the behavior of such CFRP-strengthened RHS tubes. Four dissimilar failure modes were observed in the tests: (1) cohesion failure; (2) adhesion failure; (3) interlaminar failure of CFRP plates; (4) combined cohesion and

adhesion failure (Table 2.4). The tests also presented that for two adhesives of similar tensile strengths, the adhesive with a greater ultimate tensile strain leads to a larger peak load.

Table 2.4: Material properties of adhesive (Fernando et al., 2009)

Adhesive	Modulus of elasticity, E (MPa)	Ultimate stress, σ_u (MPa)	Ultimate strain, ε_u
A (FIFE- Tyfo)	3975	40.7	0.0111
B (Sika 30)	11.250	22.3	0.0030
C (Sika 330)	4820	31.3	0.0075
D (Araldite 2015)	1750	14.7	0.0151
E (Araldite 420)	1828	21.5	0.0289

Bambach et al. (2009a) used externally bonded CFRP on G450 cold-formed square hollow sections (SHS). The result demonstrated that the application of CFRP to slender sections delayed local buckling, resulting in significant increase in axial capacity of up to 2 times the capacity of the steel section alone, elastic buckling stress of up to 4 times that of the steel section alone, and strength-to-weight ratio of up to 1.5 times the compression members.

Haedir and Zhao (2011) used externally bonded CFRP sheets to strengthen short steel circular hollow section columns (Figure 2.7). It has been shown that the increase in the yield stress of the tube reduces the yield slenderness limit that defines a fully effective section. The results showed that the strength was improved for tubes strengthened with a higher amount of CFRP.

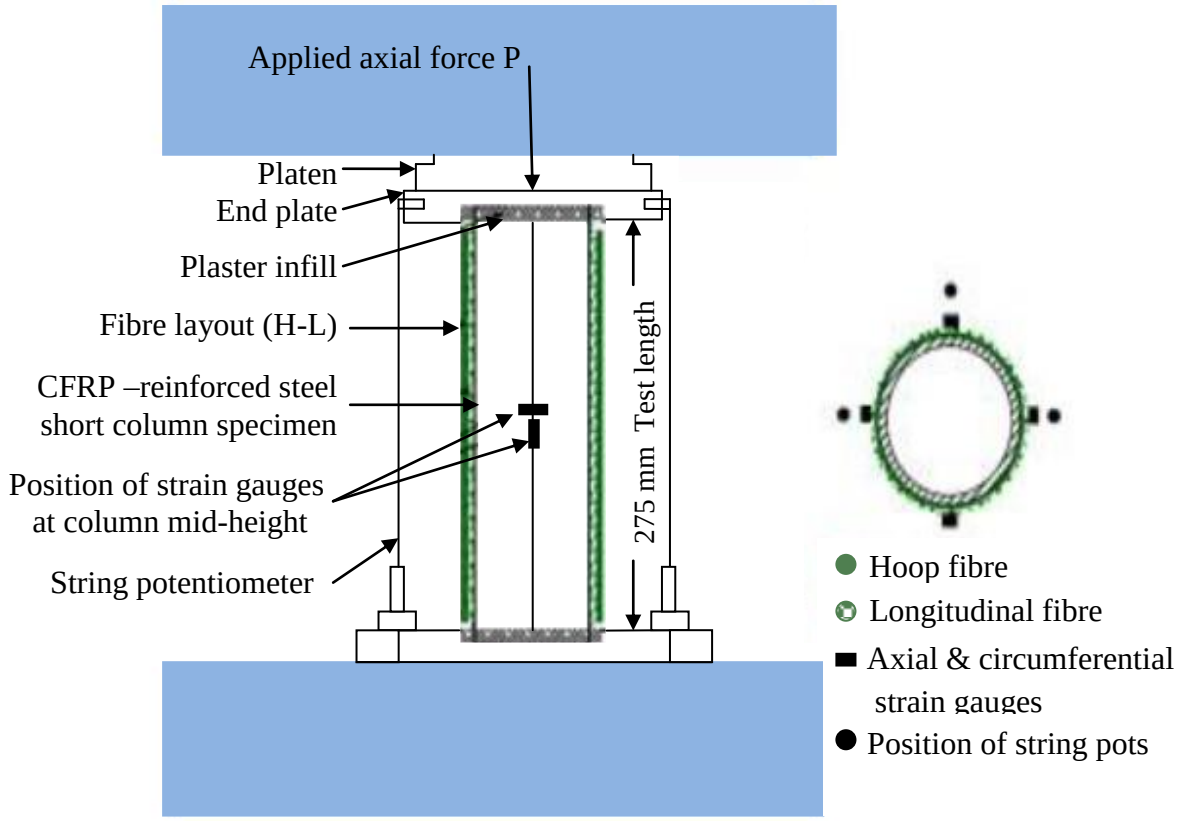

(a)Schematic

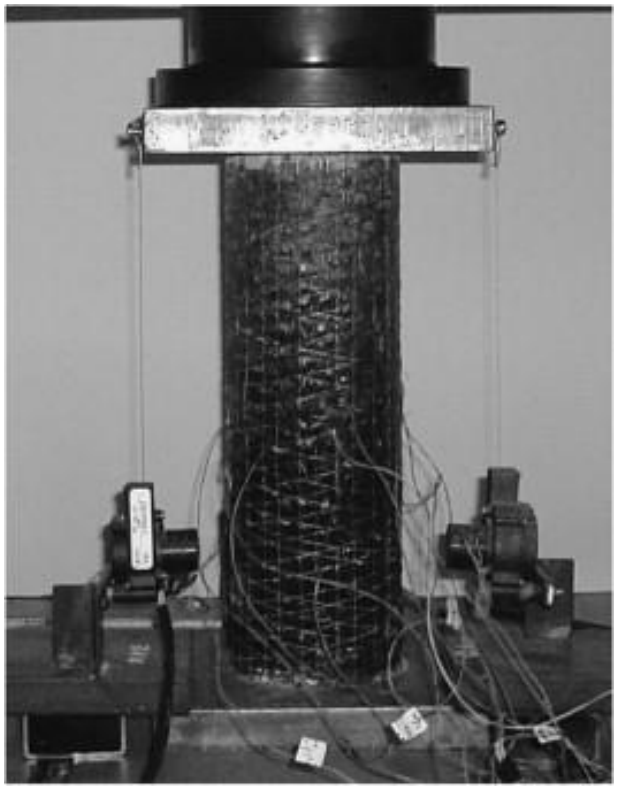

(b) CFRP reinforced steel short column detail

Figure 2.7 Experimental set-up and adopted instrumentation (Haedir and Zhao, 2011)

2.3.5 Failure modes in CFRP bonded steel system

Understanding the CFRP failure modes is helpful in delaying the failures and finding the solutions for avoiding brittle and earlier failure modes. Possible failure modes in a CFRP bonded steel system include:

(a) Steel and adhesive interface failure

(b) Adhesive layer failure

(c) CFRP and adhesive interface failure

(d) CFRP delamination

(e) CFRP rupture

(f) Steel yielding.

A schematic view of failure modes in CFRP bonded steel system are shown in Figure 2.8. The thickness of adhesive, type of adhesive and the modulus of elasticity of the CFRP sheets had significant influence on the failure modes (Zhao and Zhang, 2007).

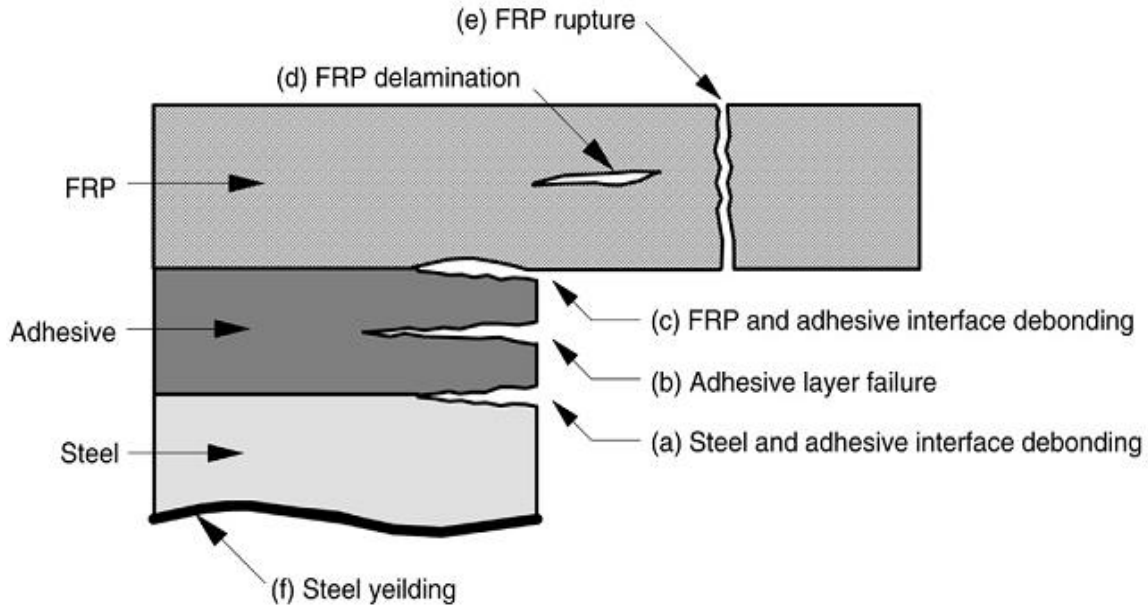

Figure 2.8 Schematic view of failure mode (Zhao and Zhang, 2007)

Buyukozturk et al. (2004) investigated on strengthening of both steel and reinforced concrete members. They indicated that failures of FRP flexural strengthened steel beams and reinforced concrete beams occur due to different methods, and related to the parameters of configuration strengthening. Their results showing the failure modes of FRP strengthened steel beams are as follows: (a) FRP debonding, (b) buckling of top flange in compression, (c) FRP rupture, and (d) buckling of web in shear.

Narmashiri et al. (2012) investigated the CFRP failure analysis of the flexural strengthened steel I-beams. Their results presented that failures of FRP flexural strengthened steel I-beams comprise: (a) below point load debonding (BD), (b) end debonding (ED), (c) below point load splitting (BS), and (4) end delamination (EDL). The occurrence of CFRP failure modes depended on the configuration strengthening and schedule.

2.4 Torsional strengthening of concrete members with FRPs

In this section, a review on torsional strengthening of concrete structures is presented in order to understand the performance of CFRP under torsion, which can be related to torsional strengthening of steel structures.

FRP as an external reinforcement is used widely to address the strength requirements related to shear and flexure in concrete structural systems. In comparison, relatively little is known about the effects of strengthening of concrete structures on torsional behavior.

Torsional cracks are formed due to a similar mechanism that is responsible for the formation of shear cracks. The major difference between torsional cracking and shear cracking lies in the pattern of the crack. The crack patterns formed in a beam under torsion and shear are shown in Figure 2.9. It can be observed in Figure 2.9a that shear

cracks follow similar directions on opposite sides of the beam. It can be seen in Figure 2.9b that in torsion, cracks have different directions on opposite sides and follow a spiral pattern (FIB-14, 2001).

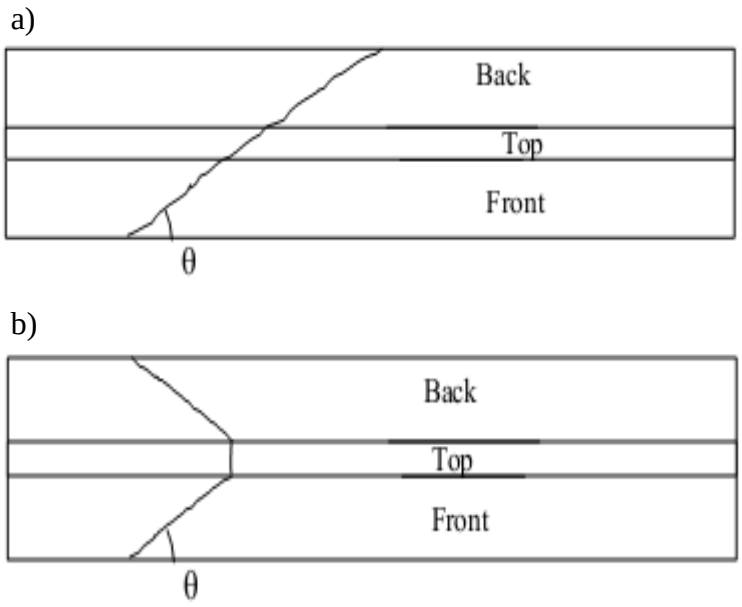

Figure 2.9 Crack patterns in, (a) beam under shear loading, (b) beam under torsional loading (FIB-14, 2001)

Therefore, a FRP material placed with the fibers forming an angle (θ) with respect to the longitudinal axis of the beam may be quite effective in reducing diagonal cracking on one side of the beam but ineffective on the other side. This point should be taken into account and highlighted in design (FIB-14, 2001).

Zhang et al. (2001) investigated CFRP strengthened concrete beams for which the wrapping was around the whole cross-section either in strip form or along the entire length. The width of strips and the number of wrapped layers were varied. The design of concrete structures based on the Chinese Code and CFRP wraps strengthening in determining the ultimate torsional capacity of the beams were proposed. Differences between the experimental torques and the predicted torques were up to 25%.

Ghobarah et al. (2002) investigated the torsional behavior of eleven concrete beams. Three beams were designated as control beams and eight beams were strengthened with two different types of FRP material, i.e. GFRP and CFRP. They strengthened the concrete beams with FRPs (fully wrapped) which were utilized in three configurations: 1) along the total length 2) inclined at 45° with respect to the beam axis, and 3) in strips. Their results showed that the fully wrapped configuration is better than using strips. They also showed that the 45° orientation of the fibers guarantees that the material is efficiently employed. Ghobarah et al. (2002) calculated torque-twist angle and compared the ultimate torsional capacity of concrete beams before strengthening and after strengthening with FRPs. The results showed an increase in the ductility after strengthening the beams with FRP and that increase of ductility for the concrete strengthened beams with GFRP were better than the strengthened beams with CFRP.

Panchacharam and Belarbi (2002) investigated the torsional behavior of reinforced concrete beams of square cross-section strengthened with GFRP. The major objectives of this research were to study (a) fiber orientation (perpendicular and parallel to the longitudinal axis of the beam), (b) continuous wrap or strips, (c) access to 3 faces or 4 faces of the beam for strengthening, (d) influence of anchors in U-wrapped strengthening schemes, and (e) one ply and two plies orthogonally placed. Figure 2.10 showed the schematic representations of the strengthening schemes.

a) 90 degree complete wrap

Figure 2.10 Schematic representation of strengthening schemes (Panchacharam and Belarbi, 2002)

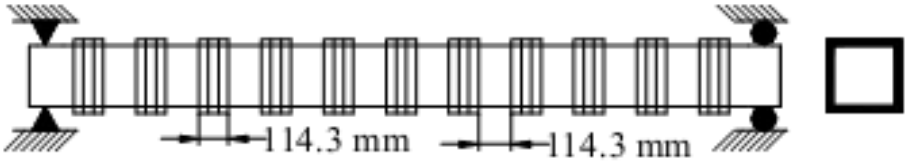

b) 90 degree strips

c) 90 degree U- wrap

d) 90 degree U- wrap with anchors

e) 0 degree, 4 sides

f) 0 degree, 3 sides

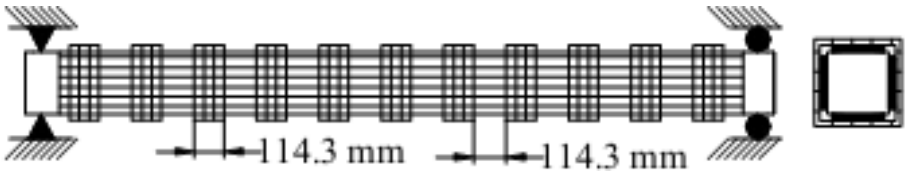

g) 0 degree, 4 sides and 90 degree strips

h) Reference beam

Figure 2.10, continued

The results exhibited significant increase in the cracking and ultimate torsional strength as well as ultimate twist deformations. An increment of about 150% in the ultimate torsional strength was observed for the strengthened beams with complete wraps with fiber orientation at 90º with respect to the longitudinal axis of the beam. When reinforced concrete beams were strengthened with FRP sheets oriented in the longitudinal direction of the beam, where the FRP provided passive prestress forces, significant increase in cracking strength was achieved. When combining FRP sheets in the longitudinal direction of the beam followed by all-around wrapped strips, the experimental results demonstrated that there was a boost in the post-cracking torsional twist and the ultimate strength and ductility of the strengthening beam. In addition, the results showed that similar behavior was observed for strengthening with FRP sheets in the longitudinal direction of the beam on three faces or four faces of the cross-section. The results of U-wrapped strengthening illustrated the least twist capacity due to peeling of FRP sheets along the side of the concrete beam. Anchoring the wraps to the concrete beam improved the twist capacity and failure was mostly due to crushing of the concrete.

Hii and Al-Mahaidi (2006) performed an experimental and numerical study on reinforced concrete beams torsional strengthening with CFRP laminates. They utilized full strips of externally-bonded CFRP for strengthening of solid and box section reinforced concrete beams. The experimental results recorded increase in ultimate

strengths and cracking compared to the control specimens of up to78% and 40%, respectively.

Chalioris (2008) carried out experimental study on torsional strengthening of rectangular and T-shaped beams using CFRP. The strengthened concrete rectangular beams with full wrapping FRP sheets had improved torsional behavior and higher capacity compared to the strengthened concrete rectangular beams with FRP strips. U-jacketed concrete flanged beams reported premature debonding failure and substantial decrease of the potential torsional abilities.

Mohammadizadeh and Fadaee (2009) investigated the torsional behavior of high-strength concrete beams strengthened with CFRP wrap. They tested seven beams; three beams without strengthening and four beams strengthened with CFRP sheets with different configurations including: 1) Full Strip, 2) U-jacket, and 3) Full wrap. This study has reported that the yield torques and the cracking of all strengthened beams with CFRP sheets are greater than the control beams. The results indicated that the increase in magnitude depends on the strengthening configuration and FRP reinforcement ratio. An increase of 55% in the yield torque and 82% in cracking were recorded for the beam strengthened with 2 layers of full wrap CFRP.

2.5 Concluding remarks

This chapter reviews literature related to CFRP strengthening of steel structures. Different types of FRP materials are briefly highlighted. Focus is given on CFRP material, as here application of CFRP in strengthening steel structures for different purposes such as tensile, flexural, shear, repair of fatigue damage, enhancing stability of steel members, and failure modes in CFRP bonded steel system are presented.

The findings from the literature have proven that CFRP strengthening is an effective method in retrofitting and repairing of steel structures. However, literature search has concluded that no studies were found on torsional strengthening of steel structures. Most of the recent studies on torsional strengthening are related to concrete structures. In order to understand the performance of CFRP under torsion, review of torsional strengthening of concrete structures was carried out. It is found that CFRP can also significantly improve the torsion capacity of structural concrete member.

3.0 EXPERIMENTAL PROGRAM

3.1 Introduction

Experimental study is one of the most important methods for investigating the behavior of structural elements. In this study, fifteen square hollow steel sections (SHS) have been tested to study the effects of CFRP layers and strengthening configurations on the behavior of SHS under pure torsion. In this chapter, experimental program, including the properties of the materials, specifications of the specimens, preparation of the beams, torsion test apparatus, and procedure of tests are described in detail. Research flow chart of study is presented in Figure 3.1.

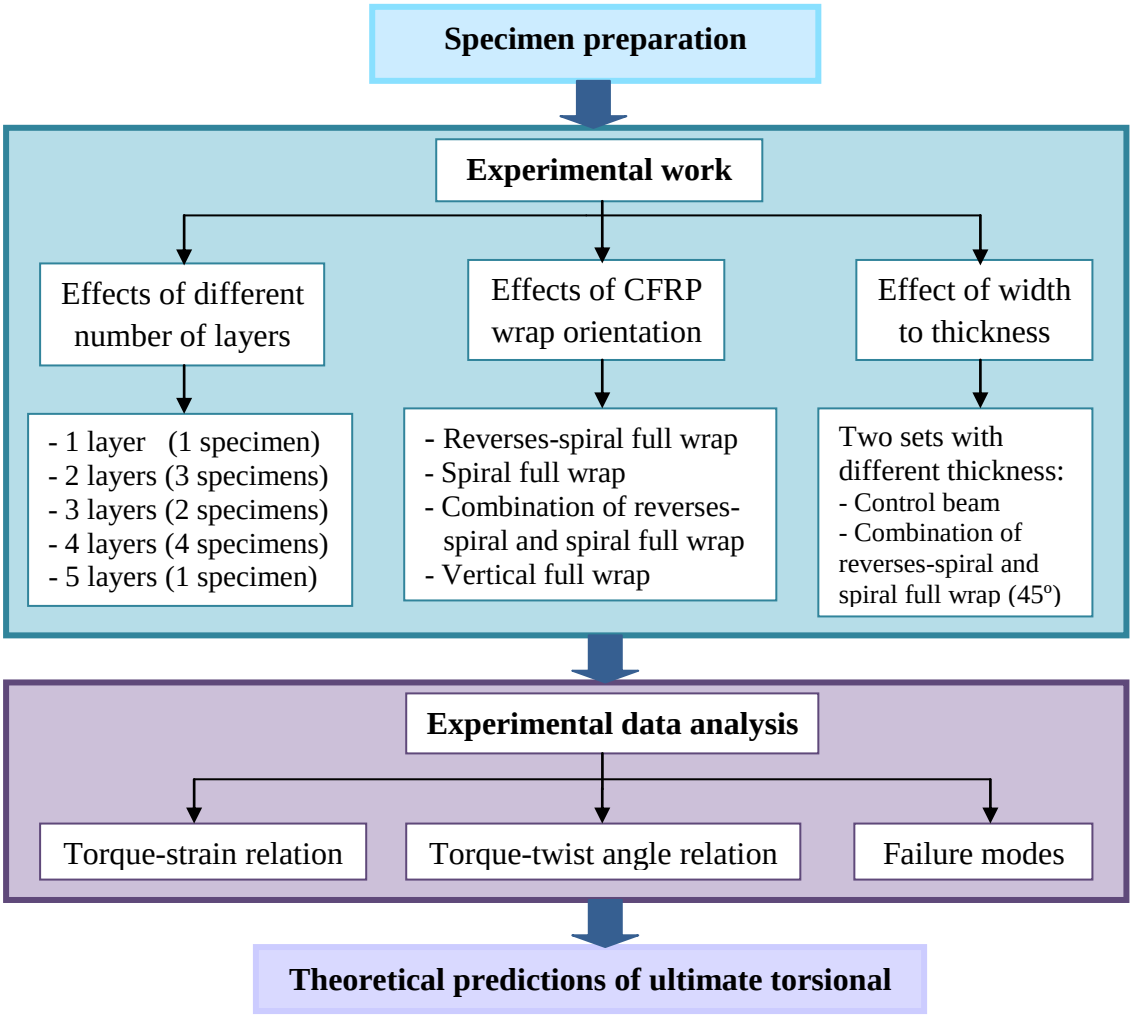

Figure 3.1 Research flow chart

3.2 Materials

The CFRP strengthened square hollow section (SHS) used in this research was a combination of three materials: mild steel (square hollow section), CFRP (torsional reinforcements) and epoxy (adhesive). In the following sections, the properties of these materials are explained in detail.

3.2.1 Steel SHS beams

In this study, mild steel beam sections were utilized. The SHS used in the tests were hot-formed square hollow sections produced in Malaysia. Dimensions of the steel sections are presented in Figure 3.2. The average measured dimensions and material properties of the SHS are given in Table 3.1.

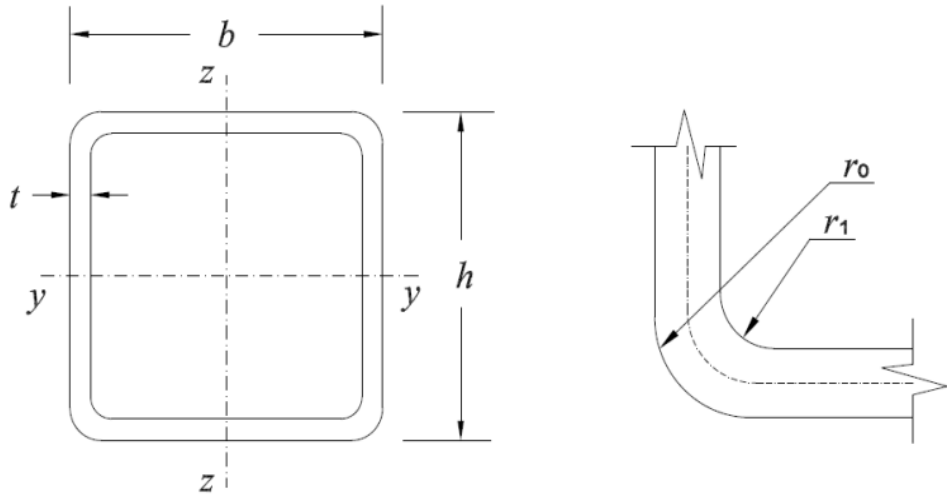

Figure 3.2 Dimensions (cross-section and corner profile)

Table 3.1: Dimensions and properties of the SHS cross-sections (measured)

Section identification no.	Nominal dimensions (h × b × t) (mm)	Average measured dimensions			Length L(mm)	Effective length L_e (mm)	Corner radius (mm)		Stress (N/mm^2)		Elastic modulus (N/mm^2)
		h (mm)	b (mm)	t (mm)			Internal (r_1)	External (r_0)	Yield (F_y)	Ultimate (F_u)	
SHS1	50 × 50 × 3	50.2	50.2	2.70	1400	1160	2.7	4.2	382	431	200000
SHS2	50 × 50 × 4.5	50.09	50.09	4.45	1400	1160	4.45	5.95	382	431	200000

3.2.2 Carbon Fiber Reinforced Polymer (CFRP) Sheet

Fiber reinforced polymer (plastic) (FRP) materials are used for strengthening and rehabilitation of structures. The fibers can be aramid (AFRP), fiberglass (GFRP), or carbon (CFRP). Carbon Fiber Reinforced Polymer (CFRP) is a composite substance with high tensile strength. CFRP is a unidirectional woven carbon fiber fabric for the dry application process; therefore, CFRP is grouped in the orthotropic substance category (Linghoff et al., 2009). CFRP composites are available in two forms; strips (plate) or sheets (wrap). In this study, only CFRP sheets were used. CFRP sheets were produced with different thickness and widths, and were classified based on the elasticity modulus and tensile strength (See section 2.2.1). In this research, the CFRP used was SikaWrap®-200C, supplied by Sika Kimia Sdn.Bhd (Figure 3.3). The properties of this type of CFRP are tabulated in Table 3.2 (Product information, Sika 2012).

Table 3.2: Properties of fibres

CFRP Sheet: SikaWrap®-200C				
Fabric design thickness (mm)	Modulus of elasticity (N/mm^2)	Ultimate tensile strength (N/mm^2)	Ultimate tensile elongation	Thickness (Impregnated with Sikadur®-330) (mm)
0.111	230,000	3,900	1.5%	0.9 per layer

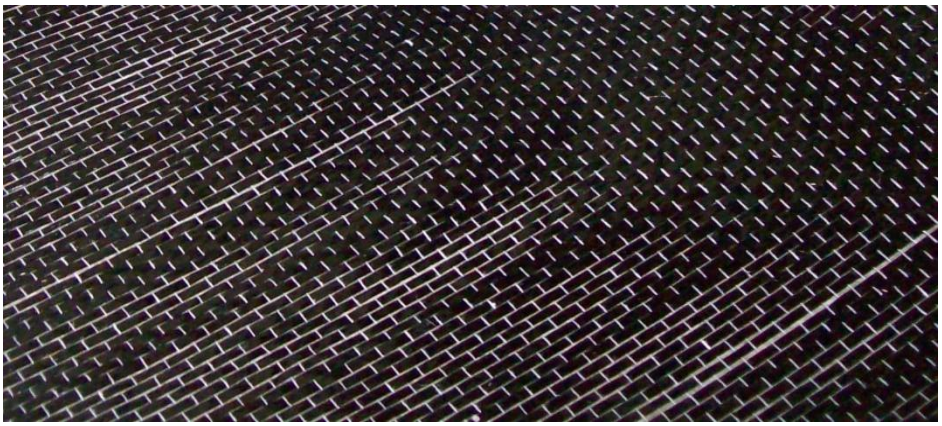

Figure 3.3 CFRP sheet

3.2.3 Adhesive

The structural adhesives used for the installation of CFRP sheets on steel structures should be sufficiently strong to transmit stress between the common surfaces (Schnerch et al., 2005, 2006). The epoxy used in this research was provided by the same supplier. The epoxy used for SikaWrap®-200C is called Sikadur ®-330. The epoxy is a combination of two components; A (resin, white semi-liquid) and B (hardener, grey semi-liquid), mixed in a ratio of 4:1 by weight (Figure 3.4). The properties of the adhesive are given in Table 3.3 (Product information, Sika 2012).

(a) (b)

Figure 3.4 Sikadur ®-330, (a) component A (resin), (b) component B (hardener)

Table 3.3: Properties of adhesive

Adhesive: Sikadur®-330			
Tensile strength (N/mm^2)	Modulus of elasticity (N/mm^2)		Elongation at break %
	Tensile	Flexural	
30	4500	3800	0.9

3.3 Preparation of the specimen

In this study, a total of fifteen SHS (Table 3.4) were prepared in the laboratory of University of Malaya and tested under pure torsion. The length of the beams was 1400 mm while the effective length was approximately 1160 mm (Table 3.1). Firstly, the surface of the steel beam was prepared before applying the CFRP wrap. The surface of the SHS was cleaned of any colour, grease, rust, galvanized coating and impurities. The best technique to remove these contaminations is through sandblasting until a clean and glossy surface is seen (Schnerch et al., 2005, 2007). The steel surfaces were then cleaned with acetone before the adhesive was applied (Figure 3.5).

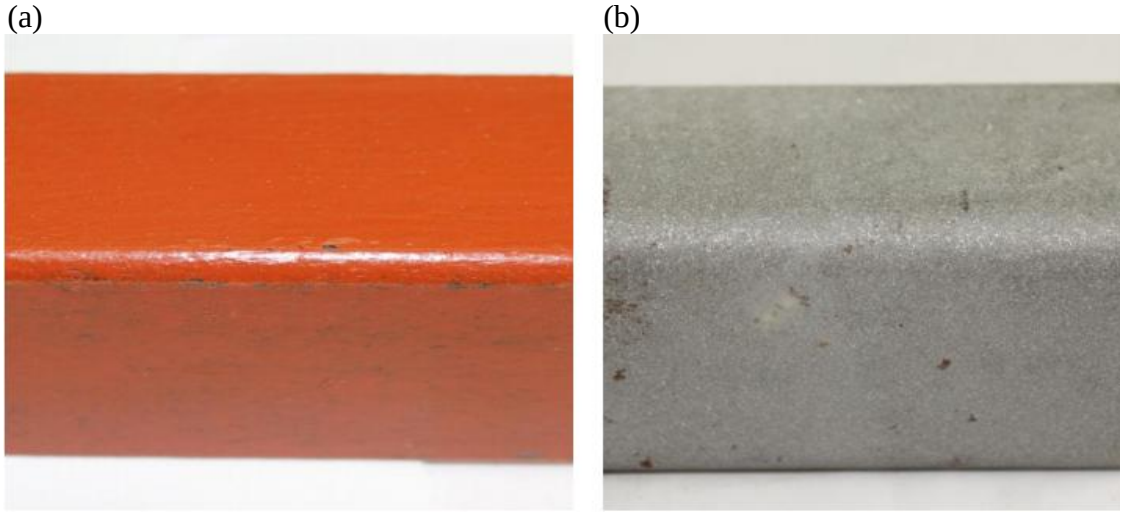

Figure 3.5 Surface preparation, (a) before sandblast, (b) after sandblast

To apply the CFRP sheets on the steel surface, the two components of the epoxy were mixed 4:1 by weight of component A to component B, according to the weight ratio given by the manufacturer (Product Information, Sika 2012). First, each component was mixed thoroughly. Then, component A (resin) was measured and put into a small container. Component B (hardener) was then measured and added to component A (Abdollahi Chahkand et al., 2012). The components were mixed together using a low speed drill (200 rpm) for approximately 3 minutes to create a mixture of light gray (Figure 3.6).

Figure 3.6 Mixing of components A and B (Sikadur ®-330)

The epoxy was applied onto the steel surface using a palette knife (Figure 3.7) and spread with a paintbrush. The CFRP sheet was then applied. To remove air bubbles and excess adhesive, the CFRP sheet roller was used along the direction of the fiber (Figure 3.8). The specimens were kept at room temperature for a week (Zhao et al., 2006).

Figure 3.7 Applying epoxy onto the surface of the SHS

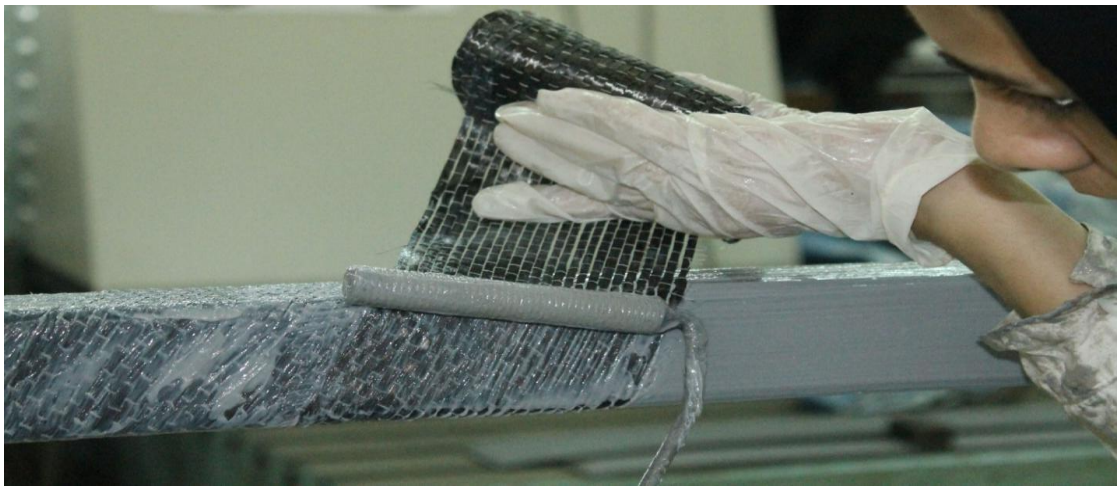

Figure 3.8 Applying CFRP wrap on the surface of the SHS

3.4 Schemes of strengthening

A schematic view of the different types of strengthening configurations and the characteristics of the CFRP wrapping configurations used are shown in Figure 3.9 and Table 3.4, respectively.

The specimens without strengthening schemes are considered as the control beam specimens. They are called SHS1 and SHS2. The rest of the beam specimens were strengthened with CFRP in different configurations. Ten types of strengthening configurations were used in this study for SHS1, and one type of strengthening configuration was used for SHS2. $SHS1_{V90^\circ}$ was wrapped with five layers of CFRP sheets vertically (90º) with respect to the longitudinal axis of the specimen. $SHS1_{R60^\circ}$ was wrapped with one layer of CFRP reverse-spirally (60º) with respect to the longitudinal axis of specimen. $SHS1_{SS60^\circ}$ was wrapped with two layers of CFRP spirally (-60º) with respect to the longitudinal axis of the specimen. $SHS1_{RR60^\circ}$ was wrapped with two layers of CFRP reverse-spirally (60º) with respect to the longitudinal axis of the specimen. $SHS1_{SR60^\circ}$ was a combination of one layer of CFRP sheet spirally wrapped (-60º) and one layer of CFRP sheet reverse-spirally wrapped (60º) with respect to the longitudinal axis of the specimen. $SHS1_{SRS60^\circ}$ was wrapped with three layers of alternating spiral (-60º) and reverse-spiral (60º) arrangement of CFRP with respect to the longitudinal axis of the specimen. $SHS1_{RSR60^\circ}$ was wrapped with three layers of alternating reverse-spiral (60º) and spiral (-60º) arrangement of CFRP with respect to the longitudinal axis of the specimen. $SHS1_{RRRS60^\circ}$ was wrapped with four layers of CFRP that combined three layers of reverse-spiral (60º) and one layer of spiral (-60º) arrangement of CFRP wrap with respect to the longitudinal axis of the specimen. $SHS1_{SRSR60^\circ}$ was wrapped with four layers of alternating spiral (-60º) and reverse-spiral (60º) arrangement of CFRP with respect to the longitudinal axis of the specimen. $SHS1_{SRSR45^\circ}$ and $SHS2_{SRSR45^\circ}$ were wrapped with four layers of alternating spiral (-45º)

and reverse-spiral (45º) arrangement of CFRP with respect to the longitudinal axis of the specimen.

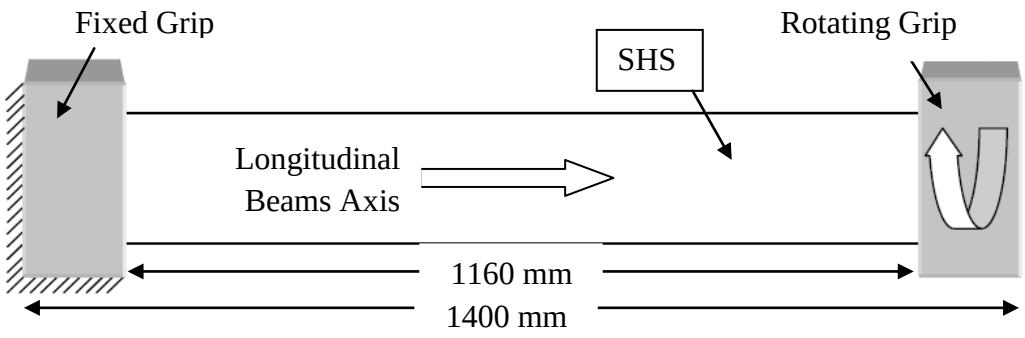

(a) SHS1 & SHS2 : Control beams

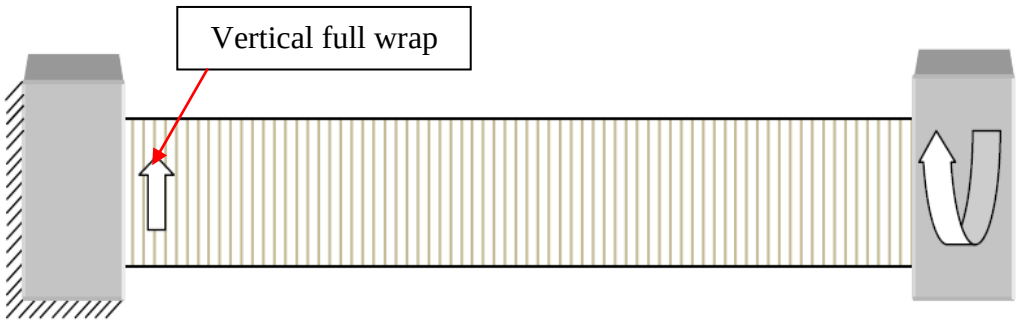

(b) Vertical wrap

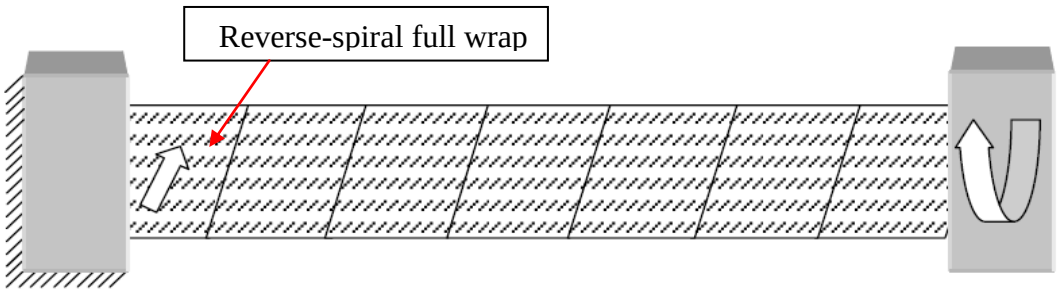

(c) Reverse spiral wrap

Figure 3.9 Types of CFRP strengthening configurations (not to scale)

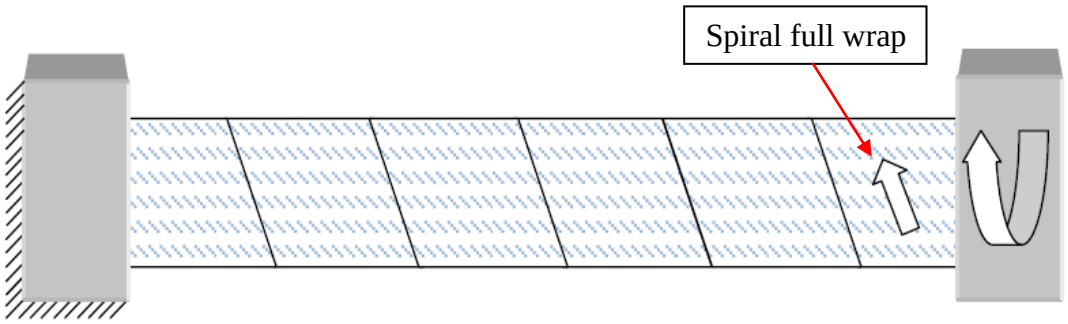

(d) Spiral wrap

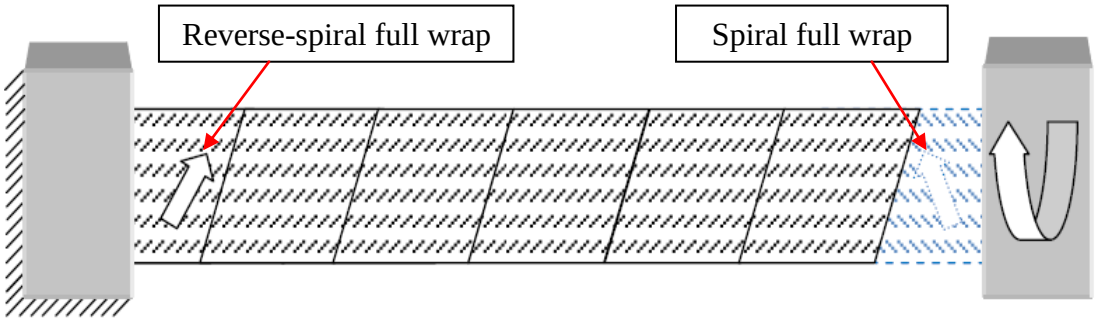

(e) Combination of reverses-spiral and spiral wrap

Figure 3.9, continued

Table 3.4: The characteristics of the specimens

Section identification no.	Angle of CFRP (θ)	Configuration	No. of layers
SHS1	-	Control beam	None
$SHS1_{V90^\circ}$	90º	Vertical full Wrap	5
$SHS1_{R60^\circ}$	60º	Reverse-spiral full wrap	1
$SHS1_{SS60^\circ}$	- 60º	Spiral full wrap	2
$SHS1_{RR60^\circ}$	60º	Reverse-spiral full wrap	2
$SHS1_{SR60^\circ}$	- 60º & 60º	Spiral & reverse-spiral full wrap	2
$SHS1_{SRS60^\circ}$	60º & - 60º	Reverse-spiral & spiral full wrap	3
$SHS1_{RSR60^\circ}$	- 60º & 60º	Spiral & reverse-spiral full wrap	3
$SHS1_{RRRS60^\circ}$	60º & - 60º	Reverse-spiral & spiral full wrap	4
$SHS1_{SRSR60^\circ}$	- 60º & 60º	Spiral & reverse-spiral full wrap	4
$SHS1_{SRSR45^\circ}$	- 45º & 45º	Spiral & reverse-spiral full wrap	4
SHS2	-	Control beam	None
$SHS2_{SRSR45^\circ}$	- 45º & 45º	Spiral & reverse-spiral full wrap	4

3.5 The torsion test apparatus

The torsion test apparatus (Figure 3.10) is used to carry out the torsion test on steel or concrete specimens or other rod specimens. The torsion testing rig used in this study was comprised of a fixed grip and a pivoted rotating grip (counterclockwise) (Figure 3.11). The apparatus was designed to function correctly and safely up to a torque of 10000 Nm. Figure 3.12 shows the grips of the torsion testing apparatus. All tests were controlled and data were collected using computer U60 software which displayed the result in the form of a graph plotting the torsion load versus torsion angle under the specified parameter conditions.

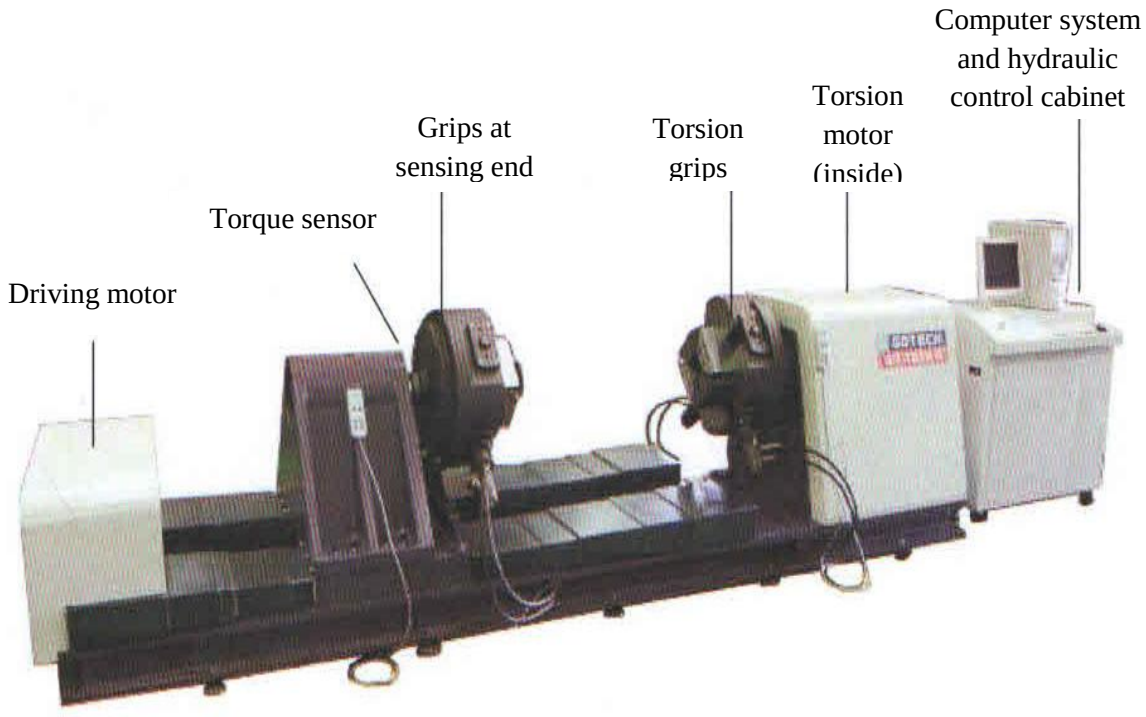

Figure 3.10 The torsion testing apparatus (schematic)

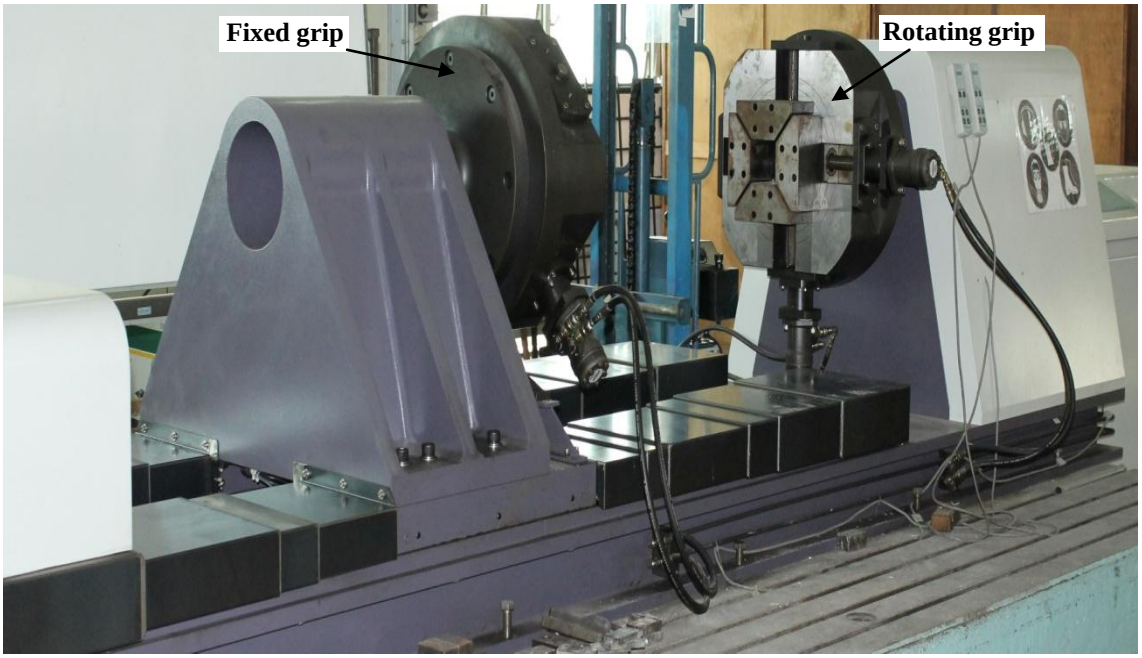

Figure 3.11 The torsion testing apparatus

(a)

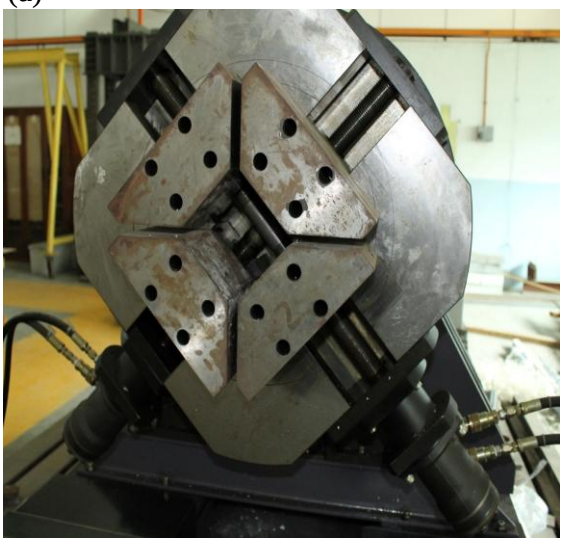

(b)

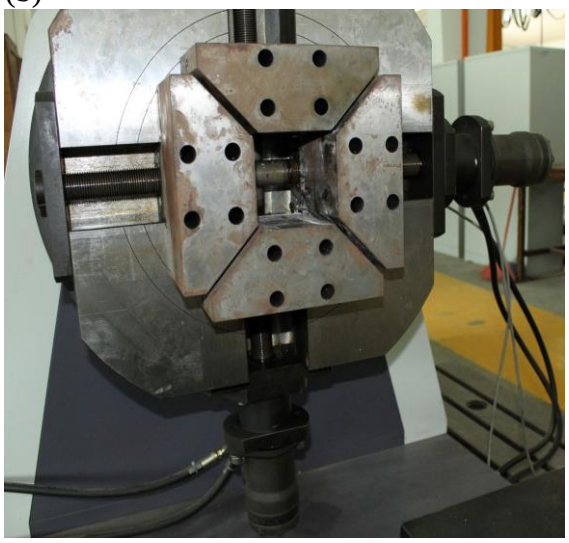

Figure 3.12 Grips of the torsion testing apparatus, (a) Fixed grip, (b) Rotating grip (counterclockwise)

3.6 Instrumentation

3.6.1 Brittle coatings

A thin layer of substance called a brittle coating was applied to the outside surface of the steel section, in order to improve the visibility of the distribution of the torsional stress. The control beam specimens were painted with a lime wash composed of three parts of water to four parts of hydrated lime (Figure 3.13). Then, the dark coloured lines could be seen against the background. When the material yielded, the oxide brittle coatings failed by cracking and flaking (Ridley-Ellis, 2000).

Figure 3.13 Control beams painted with a lime wash

The shear slip lines (also known as Lüder's lines) can be observed in the maximum shear stress direction. Because steel is homogeneous, the information obtained from the brittle coating can help to interpret the data from the strain gauges (Ridley-Ellis et al., 2003). Lüder's lines and yield lines can be seen in Figure 3.14.

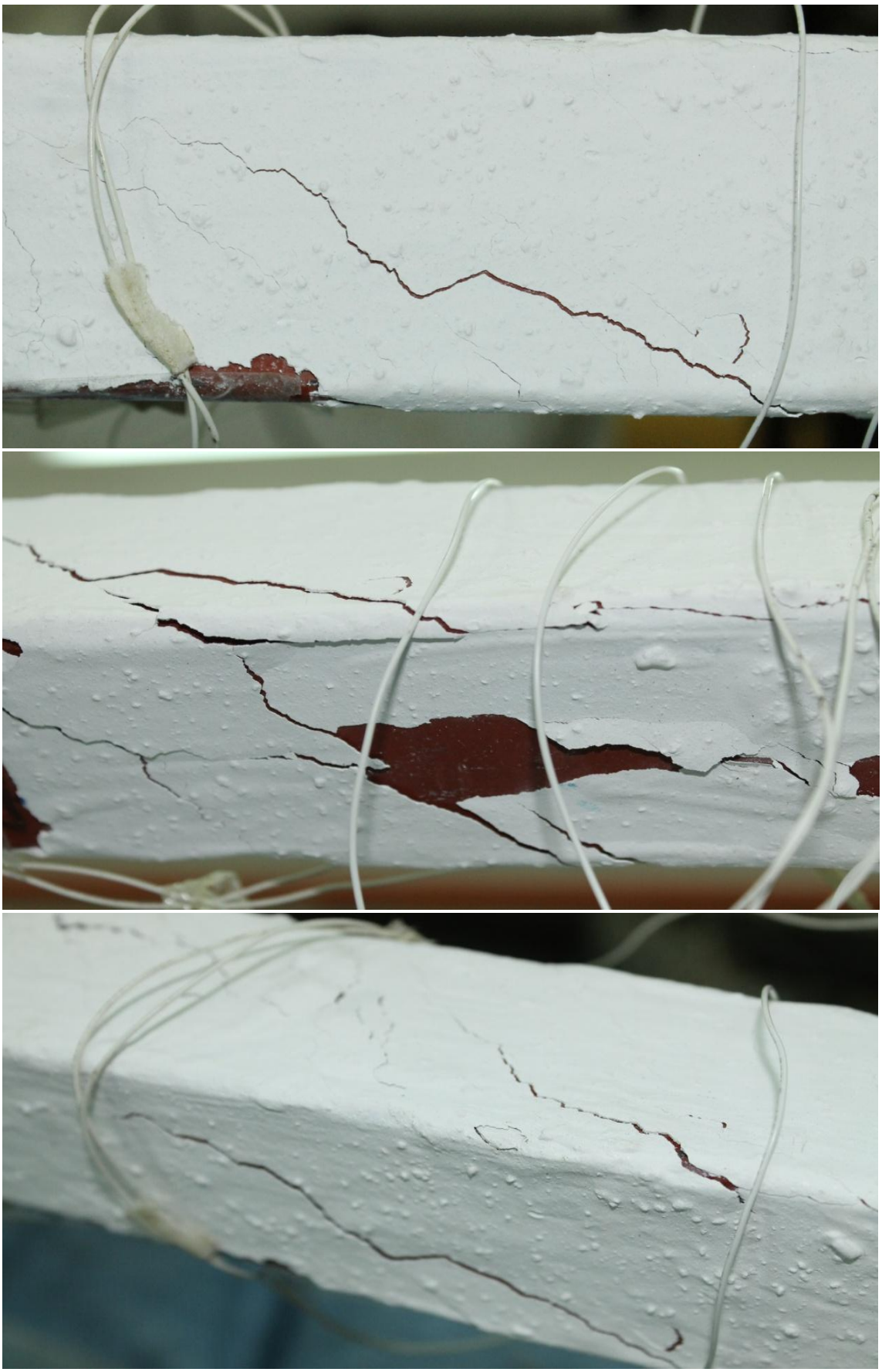

Figure 3.14 Yield lines in a brittle coating

3.6.2 Electrical resistance strain gauges

Strain gauges are installed in special regions of the laboratory test structures to measure strain. The gauge sensitivity is dependent on selection of alloy for the wire of gauge and the gauge configuration (Ridley-Ellis, 2000). There are many different types of strain gauge. Linear gauge is measured strain in single direction. A three-element strain gauge rosette is used at a single location to measure strain in more than one direction (Ridley-Ellis, 2000). Polymer strain gauge for composite materials is installed parallel to the fiber direction of the CFRP to record the distribution of the strain.

In this research, strain gauges manufactured by Kyowa Electronic Instruments were used to measure surface strains. Linear strain gauges (KFG-5-120-C1-11), three-element rosettes (KFG-5-120-D17-11), and polymer strain gauges for composite materials (KFRP-5-120-C1-9L1M2R) with gauge lengths of 5 mm were used to measure the surface strains (Figure 3.15).

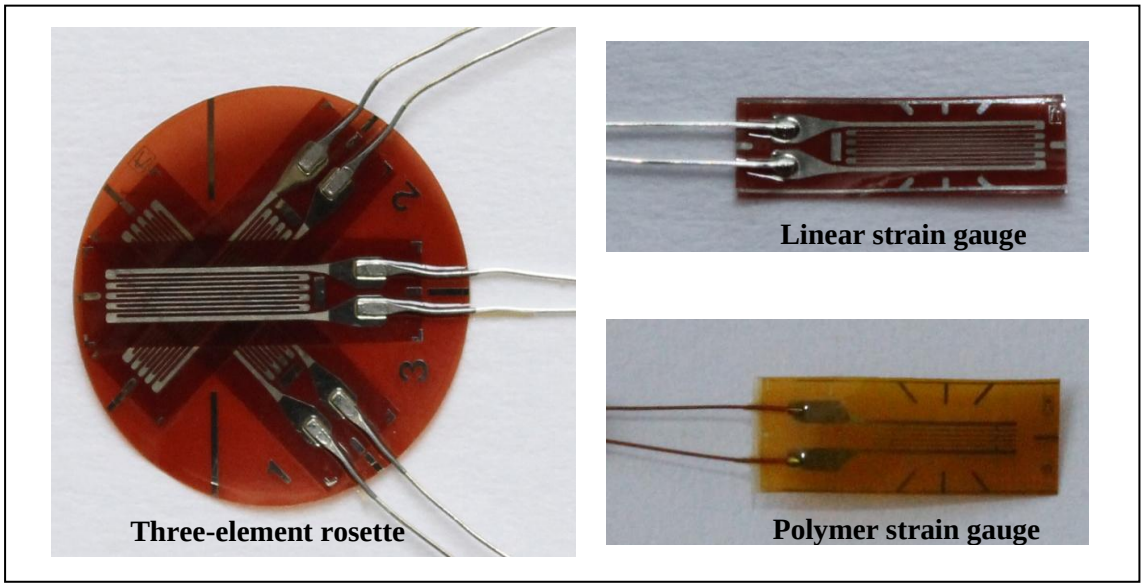

Figure 3.15 Different types of strain gauges used in this study

3.6.2.1 Electrical resistance strain gauges of the control beam (SHS1 and SHS2)

Prior to installation of the strain gauge on the surface of the control beam, the selected surfaces were sandblasted and then smoothened using rough and coarse-grained sandpaper, followed by soft sandpaper. Subsequently, the surfaces were cleaned with acetone. Finally, the strain gauges were installed on the SHS surface using Super Glue.

On side 1 (bottom side), two linear strain gauges and a three-element strain gauge rosette are installed at 0.25, 0.5, and 0.75 of the length of the control beam. The strain gauge arrangement pattern on the control beam at the mid span is shown in Figure 3.16. Locations of the rosettes and linear gauges at 0.25, 0.5, and 0.75 of the beam length are shown in Figure 3.17.

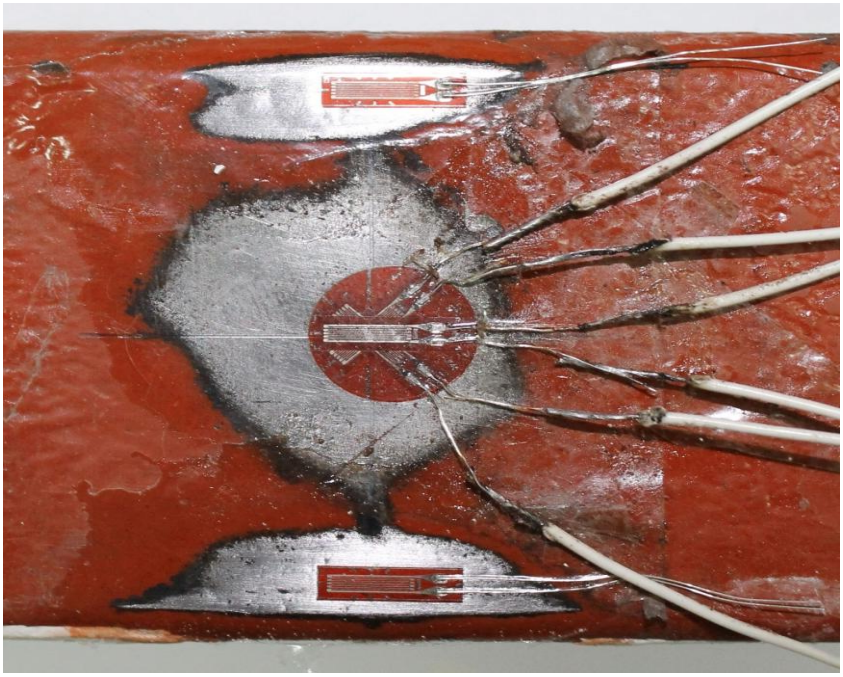

Figure 3.16 Strain gauge arrangement pattern on the control beam on side 1

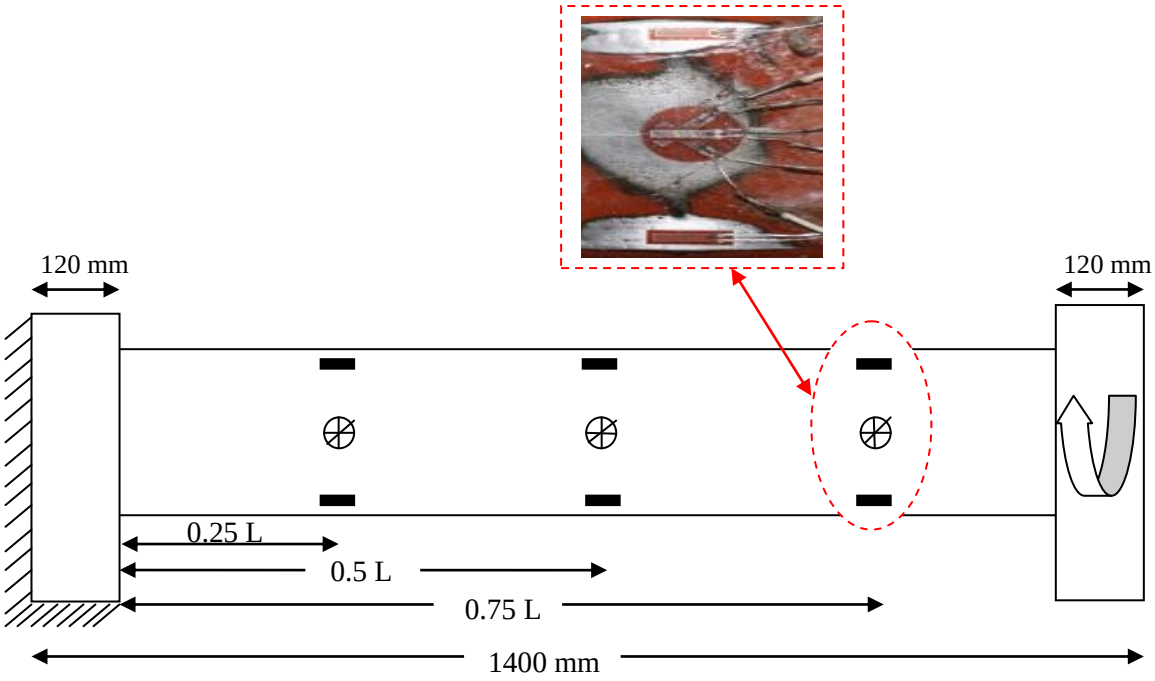

Figure 3.17 Locations of the strain gauges on the control beam at 0.25L, 0.5L, and 0.75L on side 1

On side 2 (left side of fixed grip), three rosette strain gauges were installed at 0.25, 0.5, and 0.75 of the beam length. Locations of the rosette strain gauges are shown in Figure 3.18. On sides 3 (right side of fixed grip) and 4 (top side), rosette strain gauges were installed at the mid span of the control beam (Figure 3.19).

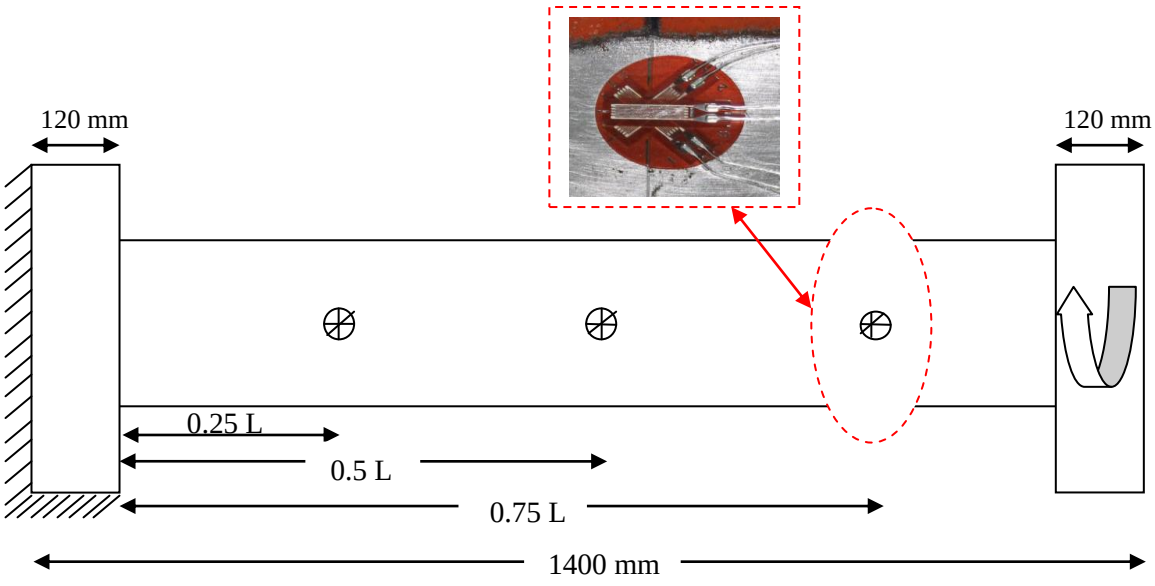

Figure 3.18 Locations of the rosette strain gauges on the control beam at 0.25L, 0.5L, and 0.75L on side 2

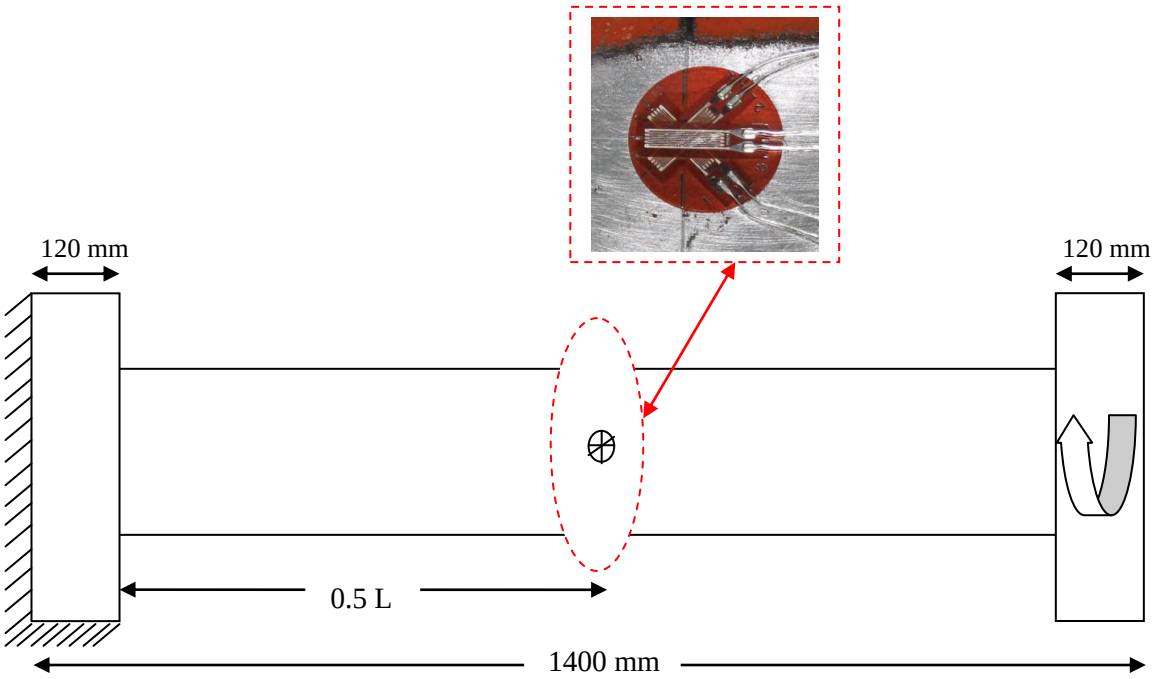

Figure 3.19 Locations of the rosette strain gauge on the control beam at mid span on sides 3 and 4

3.6.2.2 Electrical resistance strain gauges of the strengthened beam specimens

For measuring the strain due to pure torsion on the steel surface of all strengthened beam speecimens, the linear strain gauges were installed at 45° with respect to the longitudinal axis of specimens. A linear strain gauge with gauge length of 5 mm was installed to measure strain on side 1, at mid span (Figure 3.20). The strain gauge wires passing through the CFRP sheet is shown in Figure 3.21. On sides 1 and 2, polymer strain gauges were installed at 0.25, 0.5, and 0.75 of the beam length parallel to the fiber direction of the CFRP to record the distribution of the strain. The locations of the polymer strain gauges for specimen $SHS1_{V90^\circ}$ are shown in Figure 3.22.

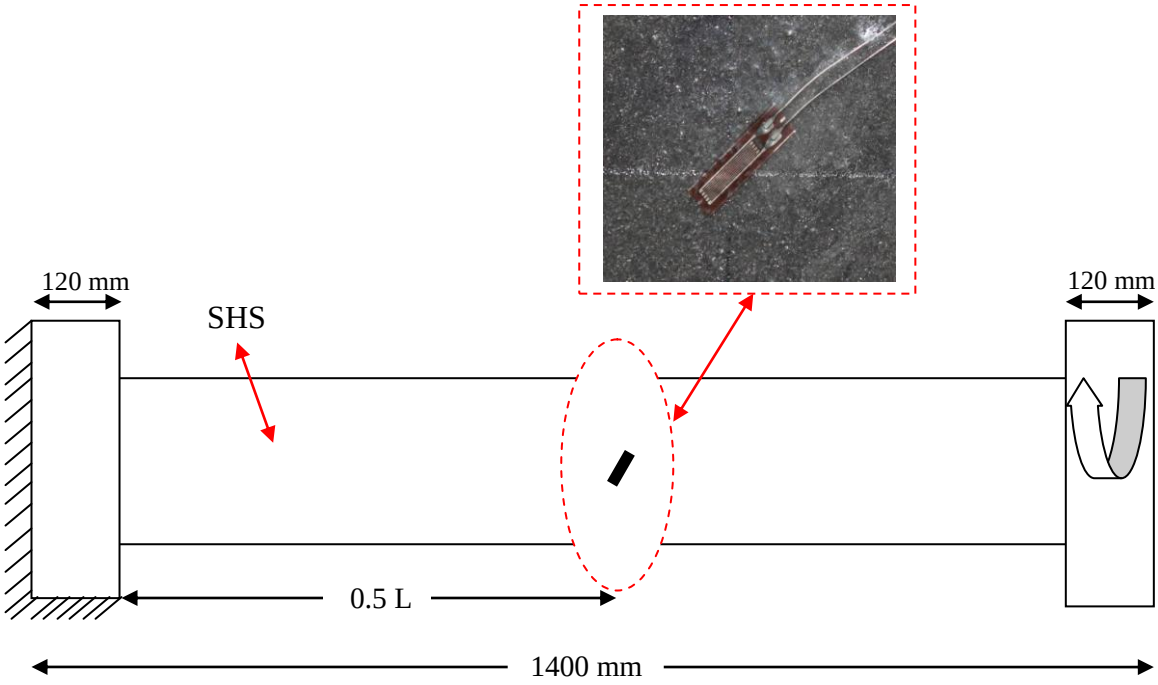

Figure 3.20 Location of the linear strain gauge on the steel surface at mid span on side 1

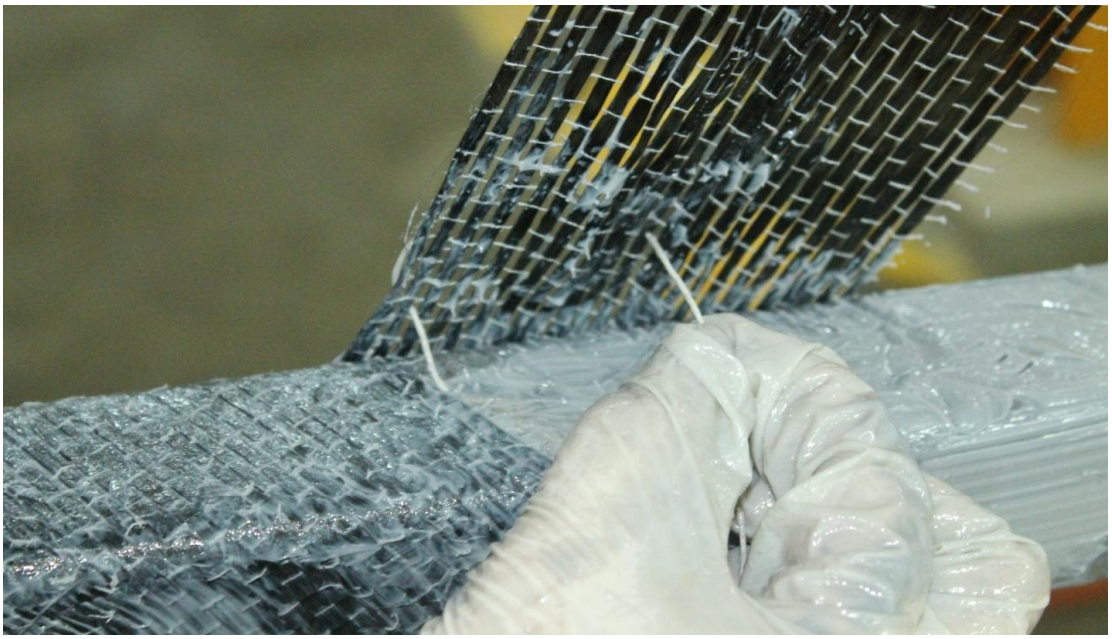

Figure 3.21 Strain gauge wires passing through the CFRP sheet

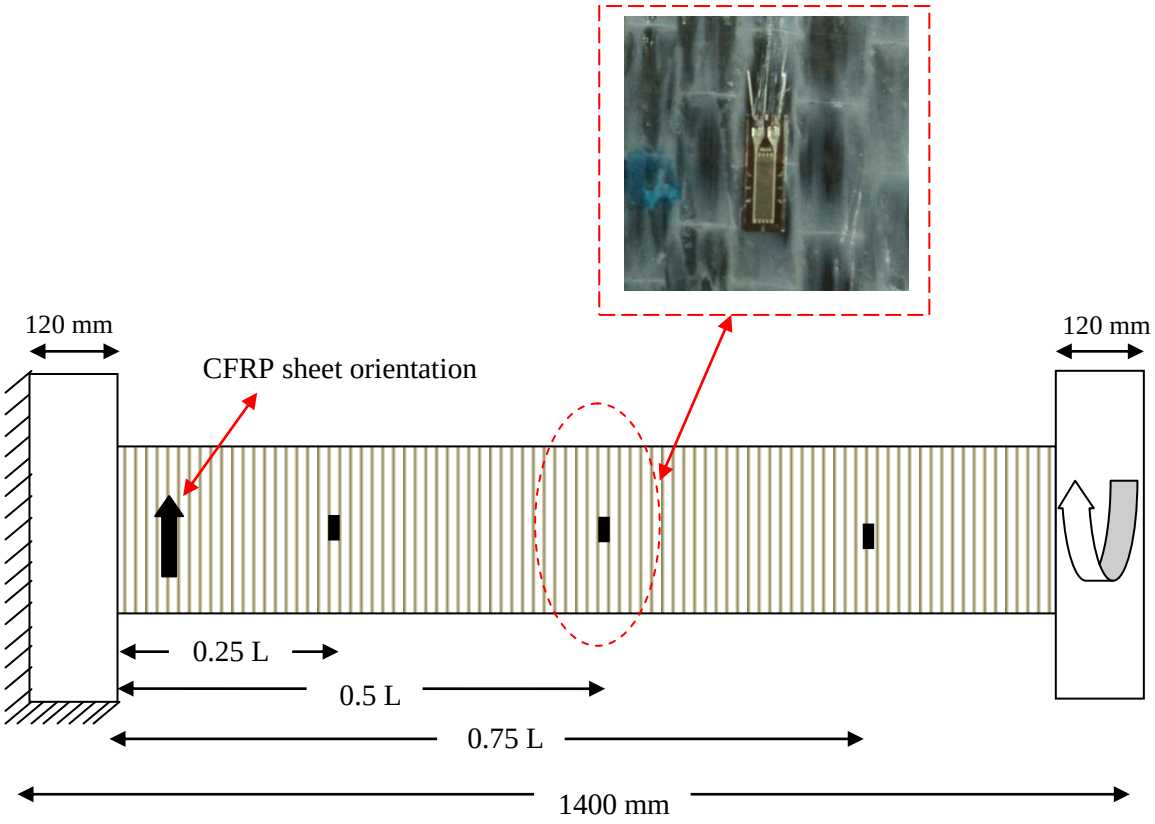

Figure 3.22 Locations of the polymer strain gauges on the CFRP sheet at 0.25L, 0.5L, and 0.75L (Vertical full wrap)

For spirally wrapped or reverse-spirally wrapped specimens, polymer strain gauges were installed parallel to the fiber direction of the CFRP sheet at 0.25, 0.5, and 0.75 of the beam length to record the distribution and measure the strain on sides 1 and 2. The locations of the polymer strain gauges for the specimens with spiral full wrap and reverse-spiral full wrap are shown in Figure 3.23 and Figure 3.24, respectively.

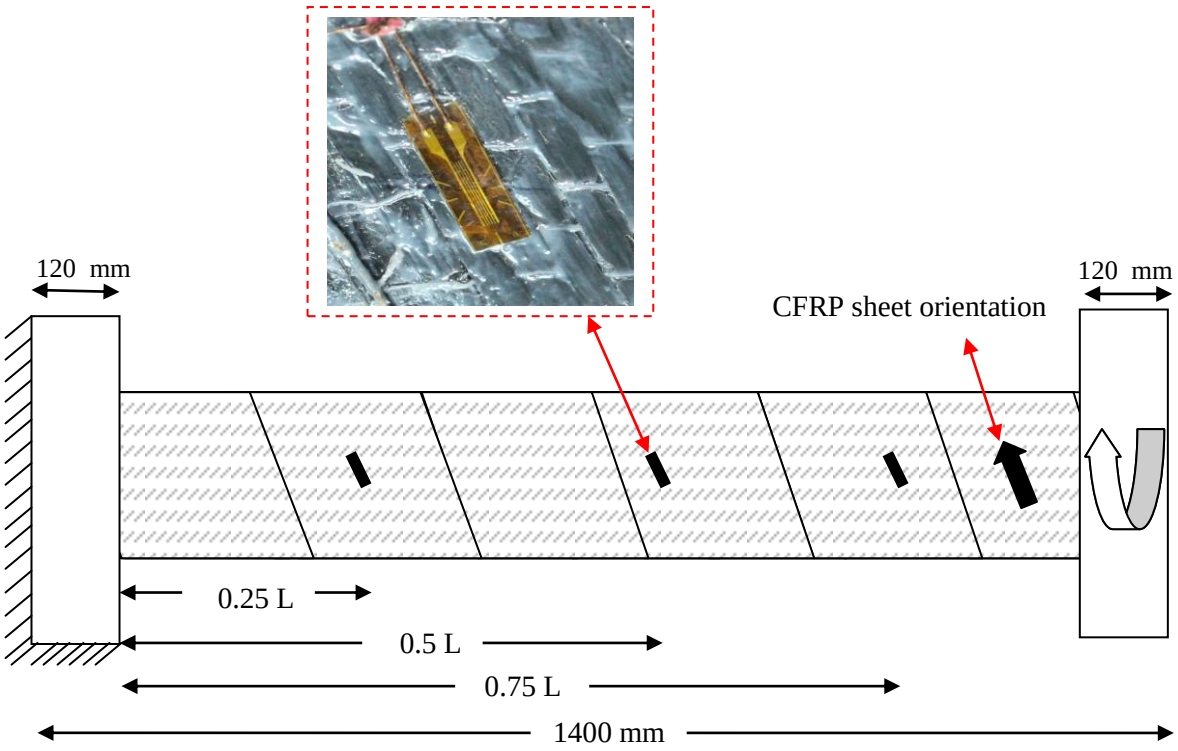

Figure 3.23 Locations of the polymer strain gauges on the CFRP sheet at 0.25L, 0.5L, and 0.75L (Spiral full wrap)

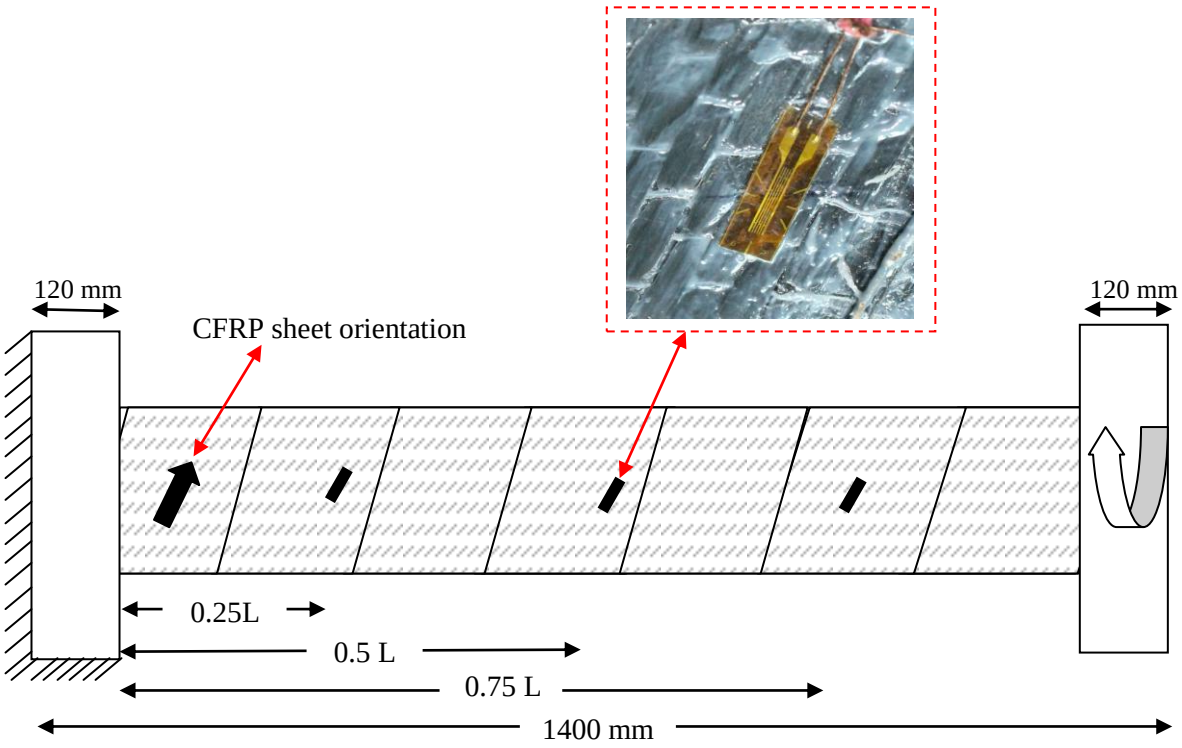

Figure 3.24 Locations of the polymer strain gauges on the CFRP sheet at 0.25L, 0.5L, and 0.75L (Reverse-spiral full wrap)

In addition, to accurately measure the strain due to pure torsion on the steel surface for specimens $SHS1_{SRSR60^\circ}$, $SHS1_{SRSR45^o}$, and $SHS2_{SRSR45^o}$, a three-element strain gauge rosette was installed on the bottom of the steel surface (side 1) at mid span. On the left side of fixed grip (side 2), the linear strain gauge (45˚ with respect to the longitudinal axis of the beam) was installed to measure the strain on the steel surface at mid span. The strain gauge arrangement pattern on the steel surface of specimens $SHS1_{SRSR60^\circ}$, $SHS1_{SRSR45^o}$, and $SHS2_{SRSR45^o}$ are shown in Figure 3.25.

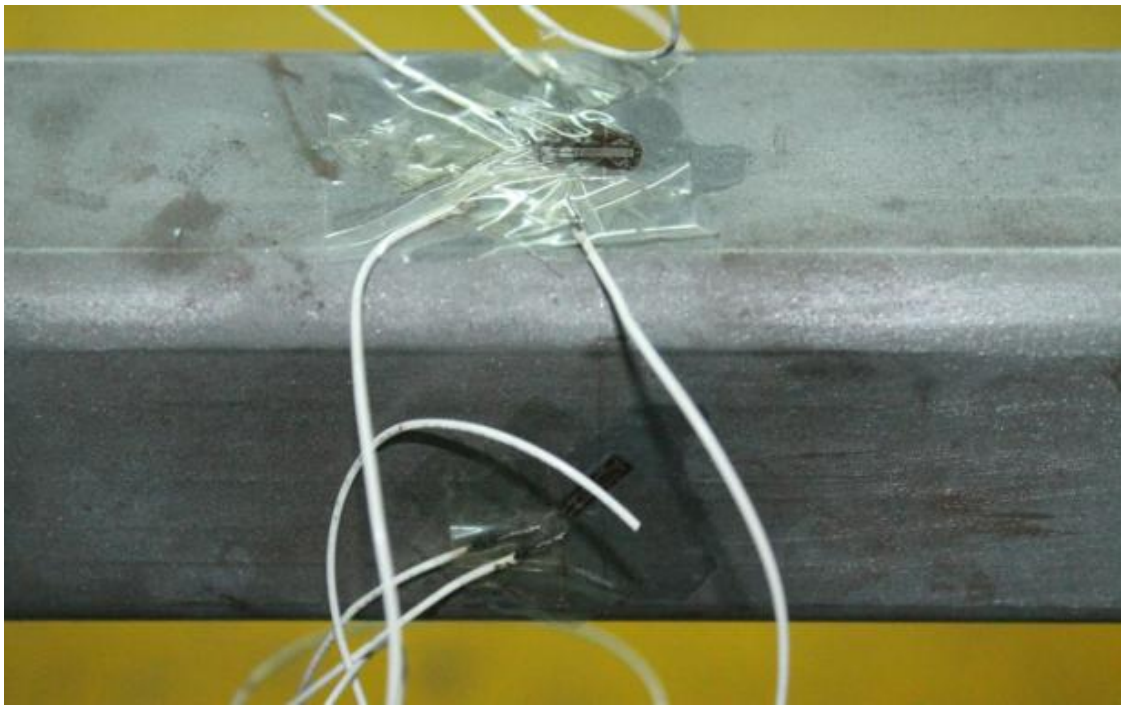

Figure 3.25 Strain gauge arrangement pattern on the steel surface of strengthened beam specimens $SHS1_{SRSR60^\circ}$, $SHS1_{SRSR45^o}$, and $SHS2_{SRSR45^o}$

For specimens $SHS1_{SRSR60^\circ}$, $SHS1_{SRSR45^o}$, and $SHS2_{SRSR45^o}$, polymer strain gauges were installed on sides 1 and 2 at 0.25, 0.5, and 0.75 of the beam length to measure the strain on the CFRP wrap (Figure 3.26).

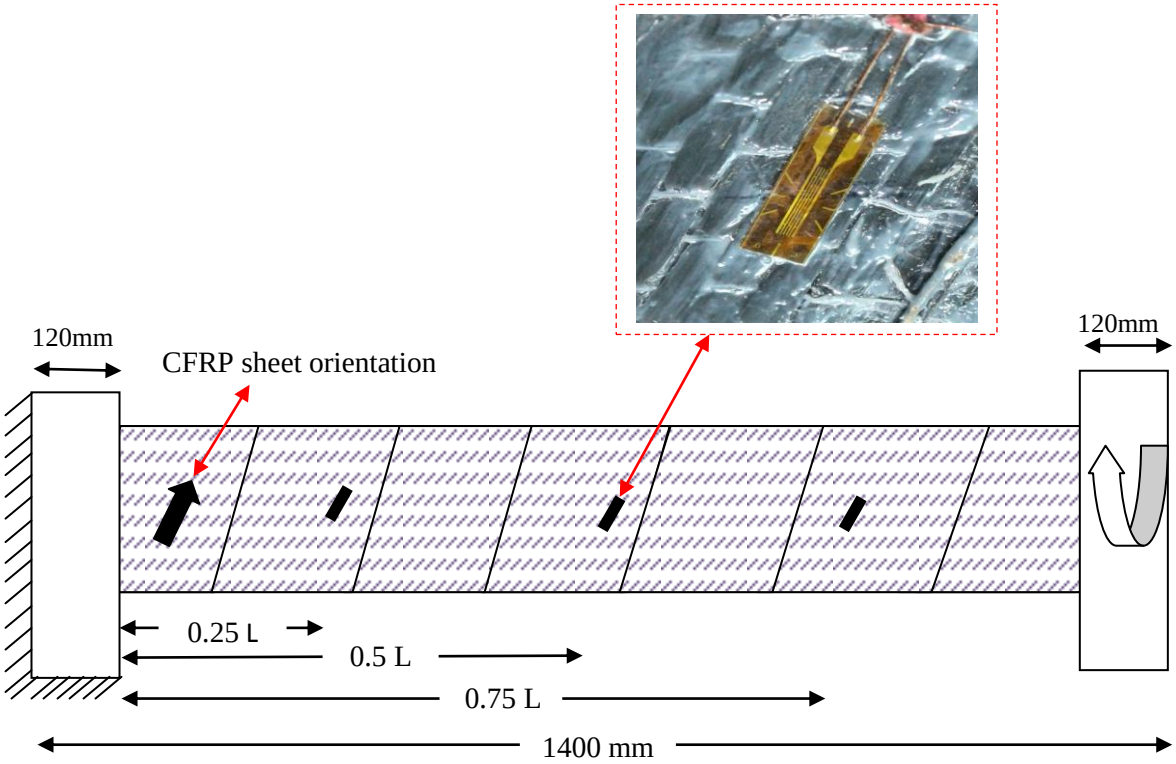

Figure 3.26 Locations of the polymer strain gauges on the CFRP sheet at 0.25L, 0.5L, and 0.75L for specimens $SHS1_{SRSR60^{\circ}}$, $SHS1_{SRSR45^{\circ}}$, and $SHS2_{SRSR45^{\circ}}$

4.0 RESULTS AND DISCUSSION

4.1 Introduction

This chapter presents the experimental results and discussion of the behavior of the torque- rotation curves, strain gauge readings, failure modes and torsional capacity prediction of CFRP strengthened SHS compared with the experimental results. Finally, the findings of the experimental investigations are summarised.

4.2 Torque- rotation curves

For all torque- rotation curves, three different zones can be seen on each curve. The first zone represents the torsional stiffness of the un-yielded specimen, the second zone represents the stiffness of the yielded specimen and the last zone corresponds to the damaged cross-section with yielded torsional steel and ruptured CFRP sheets. The torque-twist curves for all specimens are linear with a constant slope until yielding. After yielding, the torsional stiffness decrease significantly while affected by volumetric ratio and orientation angle of CFRP sheets. In all torque- rotation curves, the difference observed in the initial stiffness of the control specimen compared to the strengthened specimens can be attributed to an imperfect grip of the testing machine. The author believes that such difference does not substantially affect the result of the torsional strengthening of the specimens.

4.2.1 Comparison between vertical and reverse-spiral wrap

$SHS1_{V90^o}$ was strengthened with five unidirectional layers of CFRP. Although 5 layers of CFRP sheets were utilized in this specimen, this strengthening configuration was found to be not efficient. This is due to each of the layer being vertically wrapped at 90º

with respect to the longitudinal axis, which resulted in the angle of orientation of the fibers being different from the direction of the shear stresses. $SHS1_{R60^o}$ was wrapped with one layer of CFRP reverse-spiral (60º) with respect to the longitudinal axis of the specimen, where fiber direction is along the shear direction. The experimental results of $SHS1_{V90^o}$ and $SHS1_{R60^o}$ is shown in Table 4.1.

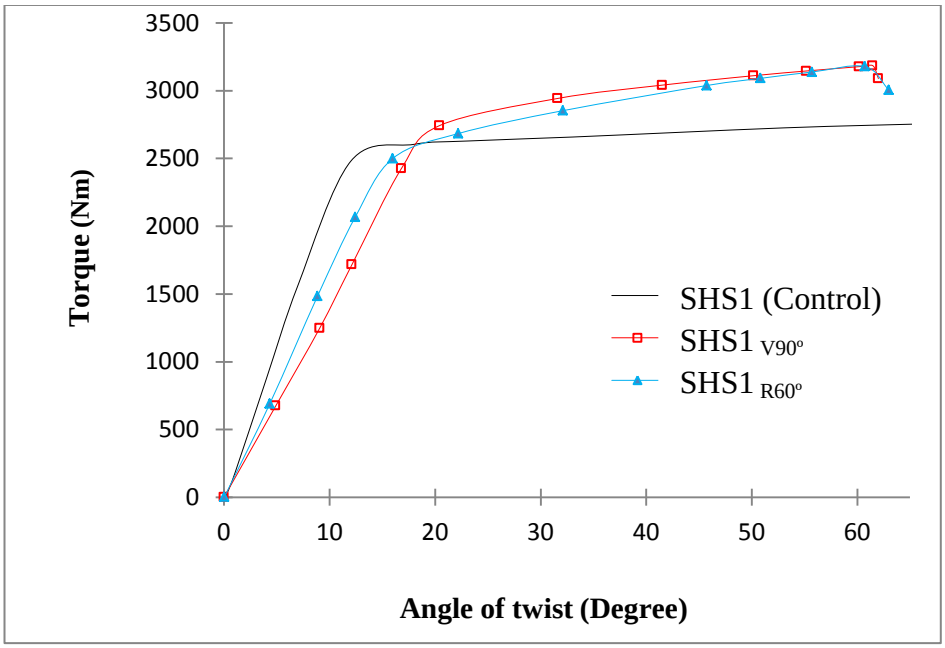

Figure 4.1 Torque-twist curves for $SHS1_{V90^o}$ and $SHS1_{R60^o}$

Table 4.1: Experimental results of $SHS1_{V90^o}$ and $SHS1_{R60^o}$

Section identification no.	No. of layers	Elastic torsional capacity (Nm)	Increasing torsional capacity %	Ultimate torsional capacity (Nm)	Increasing torsional capacity %
SHS 1	-	2637	-	2774	-
$SHS1_{V90^o}$	5	2800	6.18	3186	14.85
$SHS1_{R60^o}$	1	2684	1.78	3179	14.60

4.2.2 Effect of two layers of CFRP

Figure 4.2 and Table 4.2 present the experimental results of $SHS1_{SS60^o}$, $SHS1_{RR60^o}$, and $SHS1_{SR60^o}$ (2 layers of CFRP sheets) strengthened using different fiber configurations.

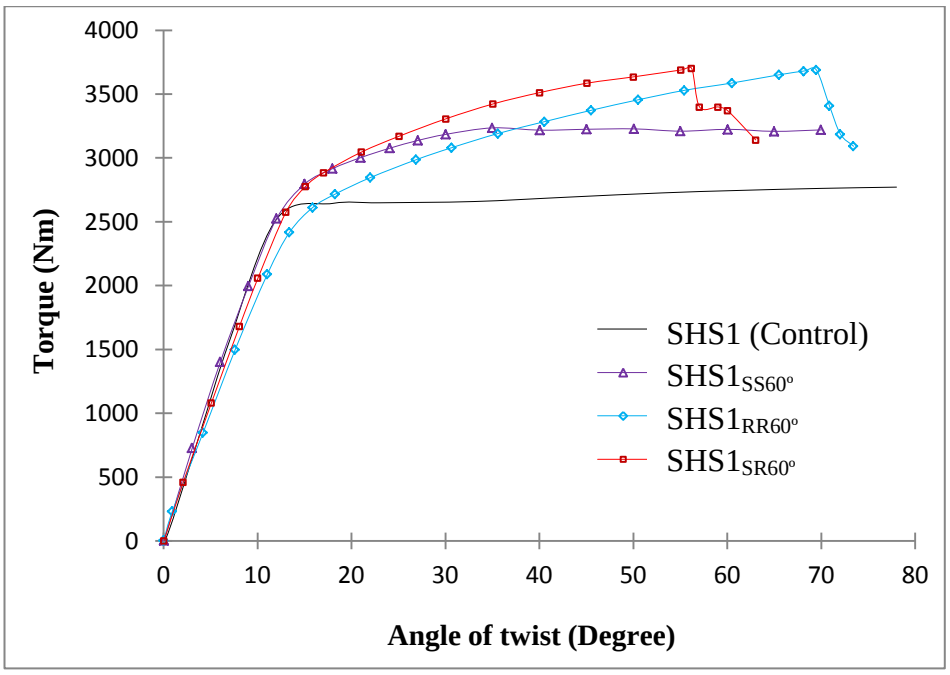

Figure 4.2 Torque-twist curves for $SHS1_{SS60^\circ}$, $SHS1_{RR60^\circ}$, and $SHS1_{SR60^\circ}$

Table 4.2: Experimental results of $SHS1_{SS60^o}$, $SHS1_{RR60^o}$, and $SHS1_{SR60^o}$

Section identification no.	No. of layers	Elastic torsional capacity (Nm)	Increasing torsional capacity %	Ultimate torsional capacity (Nm)	Increasing torsional capacity %
SHS 1	-	2637	-	2774	-
$SHS1_{SS60^o}$	2	2796	6.02	3235	16.61
$SHS1_{RR60^o}$	2	2690	2.00	3689	32.98
$SHS1_{SR60^o}$	2	2805	6.37	3701	33.41

It can be observed in Figure 4.2 and Table 4.2 that strengthened specimens $SHS1_{RR60^o}$ and $SHS1_{SR60^o}$ provided much higher ultimate torque and were more ductile compared to specimen $SHS1_{SS60^o}$. The reason of deficiency of strengthened specimen $SHS1_{SS60^o}$ in comparison with specimens $SHS1_{RR60^o}$ and $SHS1_{SR60^o}$ is that the orientation angle of fibers was in the spiral direction. In addition, strengthened specimens $SHS1_{SS60^o}$ and $SHS1_{SR60^o}$ had a higher elastic torque (initial torsional stiffness of un-yielded specimens) compared to specimen $SHS1_{RR60^o}$. It can be concluded that the best orientation angle for torsional strengthening of steel structures is a combination of spiral and reverse-spiral CFRP wraps ($SHS1_{SR60^o}$). For specimen $SHS1_{SR60^o}$, the gain in elastic and ultimate

torsional capacity was 6.37% and 33.41%, respectively, compared to the control specimen (SHS1).

4.2.3 Effect of three layers of CFRP

Table 4.3 and Figure 4.3 present the experimental results of $SHS1_{SRS60^o}$ and $SHS1_{RSR60^o}$ (3 layers of CFRP sheets) strengthened using different orientations. It can be observed in Table 4.3 and Figure 4.3 that strengthened specimen $SHS1_{RSR60^o}$ had higher ultimate torque and was more ductile compared to specimen $SHS1_{SRS60^o}$. However, strengthened specimen $SHS1_{SRS60^o}$ had a higher elastic torque compared to specimen $SHS1_{RSR60^o}$. $SHS1_{SRS60^o}$ had earlier rupture of the CFRP sheets compared to $SHS1_{RSR60^o}$. In general, if the orientation angle of fibers is in the spiral direction, the elastic torque can be increased and cause premature failure of the CFRP sheet. If the orientation angle of fibers is in the reverse-spiral direction, the ultimate torque and ductility increases.

Table 4.3: Experimental results of $SHS1_{SRS60^o}$ and $SHS1_{RSR60^o}$

Section identification no.	No. of layers	Elastic torsional capacity (Nm)	Increasing torsional capacity %	Ultimate torsional capacity (Nm)	Increasing torsional capacity %
SHS 1	-	2637	-	2774	-
$SHS1_{SRS60^o}$	3	3066	16.26	3919	41
$SHS1_{RSR60^o}$	3	2818	6.86	4054	46

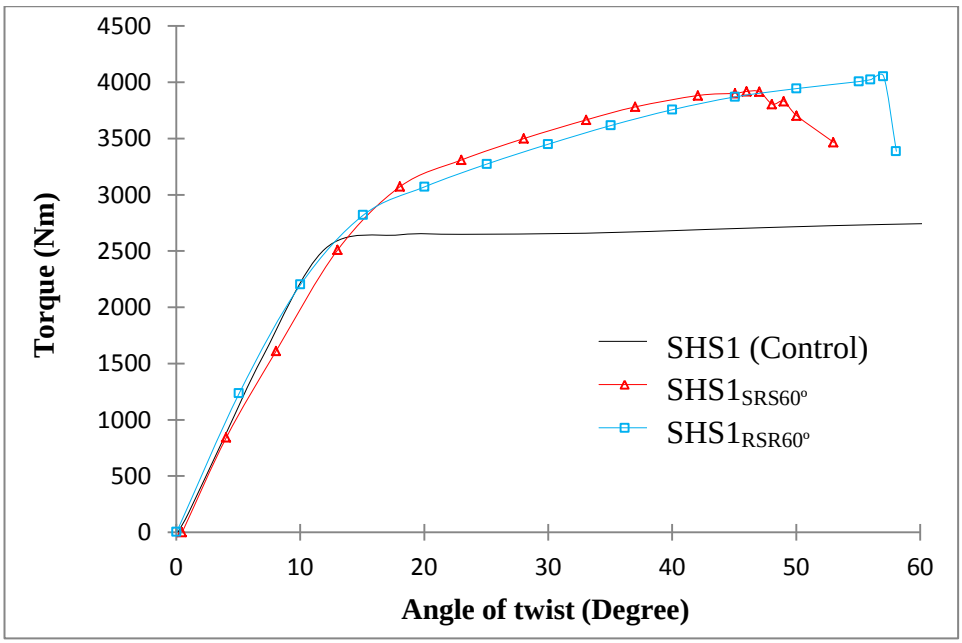

Figure 4.3 Torque-twist curves of $SHS1_{SRS60^\circ}$ and $SHS1_{RSR60^\circ}$

4.2.4 Effect of four layers of CFRP and different angle orientation

To observe the significant strength of the CFRP reinforcing system using 4 layers CFRP, four specimens were studied. Each specimen was a SHS wrapped with a predetermined configuration of fiber reinforced polymer as the reinforcing system which is described in section 3.4. The four specimens were labeled as SHS1 (control beam), $SHS1_{RRRS60^o}$, $SHS1_{SRSR60^o}$, and $SHS1_{SRSR45^\circ}$. The values of the twist angle versus the applied torque are presented in Table 4.4.

Table 4.4: Experimental results of $SHS1_{RRRS60^o}$, $SHS1_{SRSR60^o}$, and $SHS1_{SRSR45^\circ}$

Section identification no.	No. of layers	Elastic torsional capacity (Nm)	Increasing torsional capacity %	Ultimate torsional capacity (Nm)	Increasing torsional capacity %
SHS 1	-	2637	-	2774	-
$SHS1_{RRRS60^o}$	4	2959	12.2	4442	60.12
$SHS1_{SRSR60^o}$	4	3122	18.4	4462	60.85
$SHS1_{SRSR45^\circ}$	4	3192	21.04	5051	82.08

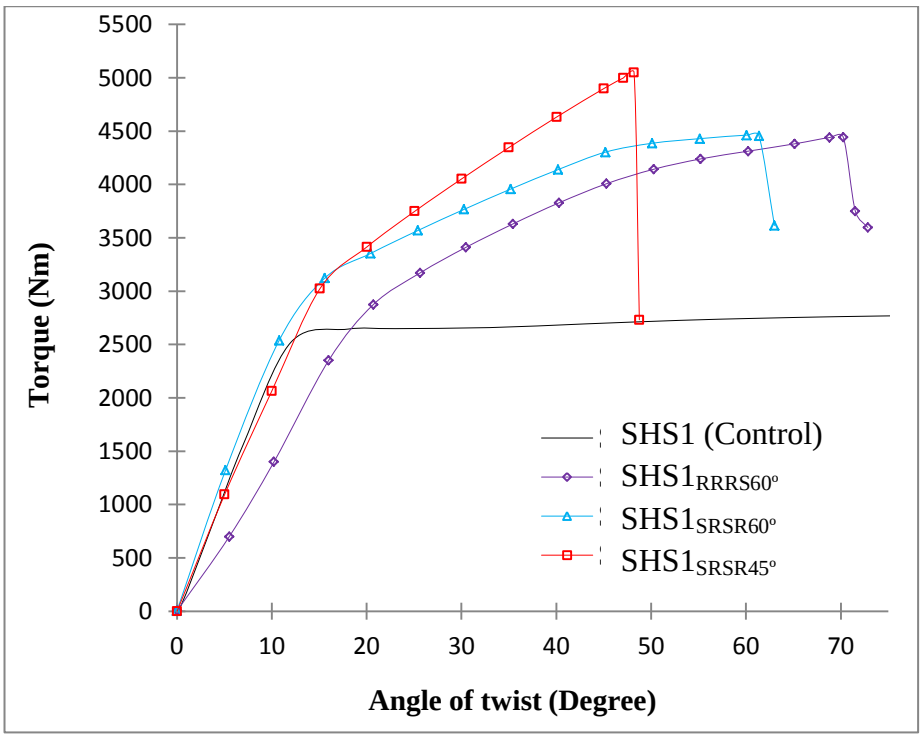

Figure 4.4 Torque-twist curves for $SHS1_{RRRS60^\circ}$, $SHS1_{SRSR60^\circ}$, and $SHS1_{SRSR45^\circ}$

From experimental results presented in Table 4.4 and Figure 4.4, although specimens $SHS1_{SRSR60^o}$ and $SHS1_{RRRS60^o}$ have equal number of layers of CFRP sheets but the elastic region of $SHS1_{SRSR60^o}$ is more than that of $SHS1_{RRRS60^o}$. This is due to specimen $SHS1_{SRSR60^o}$ having more number of layers of CFRP wrapped in the configuration of spiral direction compared with $SHS1_{RRRS60^o}$. It can also be observed in Table 4.4 and Figure 4.4 that strengthened specimen $SHS1_{SRSR45^\circ}$ had a higher elastic and ultimate torque compared to specimens $SHS1_{RRRS60^o}$ and $SHS1_{SRSR60^o}$. This is due to the utilization of CFRP sheet at an angle of 45º with respect to the longitudinal axis of the specimen. As introduced by Otto Mohr in 1882, Mohr's Circle illustrates principal stresses and stress transformations via a graphical format (Figure 4.5). As shown in Figure 4.5, the maximum shear stress is shown in blue, and the two principal stresses are demonstrated in red. The shear stress equals the maximum shear stress when the stress element is rotated 45° away from the principal directions, and when the stress element is aligned with the principal directions, the normal stresses equal the principal stresses (Ferdinand et al., 2006).

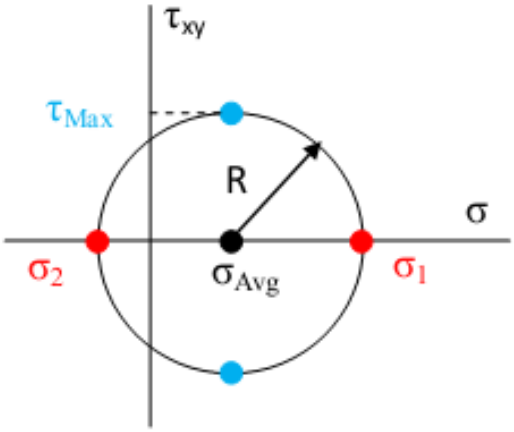

Figure 4.5 Mohr's circle (Ferdinand et al., 2006)

In addition, control specimens were coated with a lime wash which is a primitive form of brittle coating so that the dark colored lines show up against the white background when cracks appear (Figure 4.6). Accordingly, cracks appeared at approximately -45º with respect to the longitudinal axis of the specimens, which is also the direction of the principal stresses. In this study, for the spiral wrapped specimens, the crack was parallel to the CFRP orientation whereas for the reverse-spiral wrapped specimens, the crack was perpendicular to the CFRP orientation (Figure 4.6).

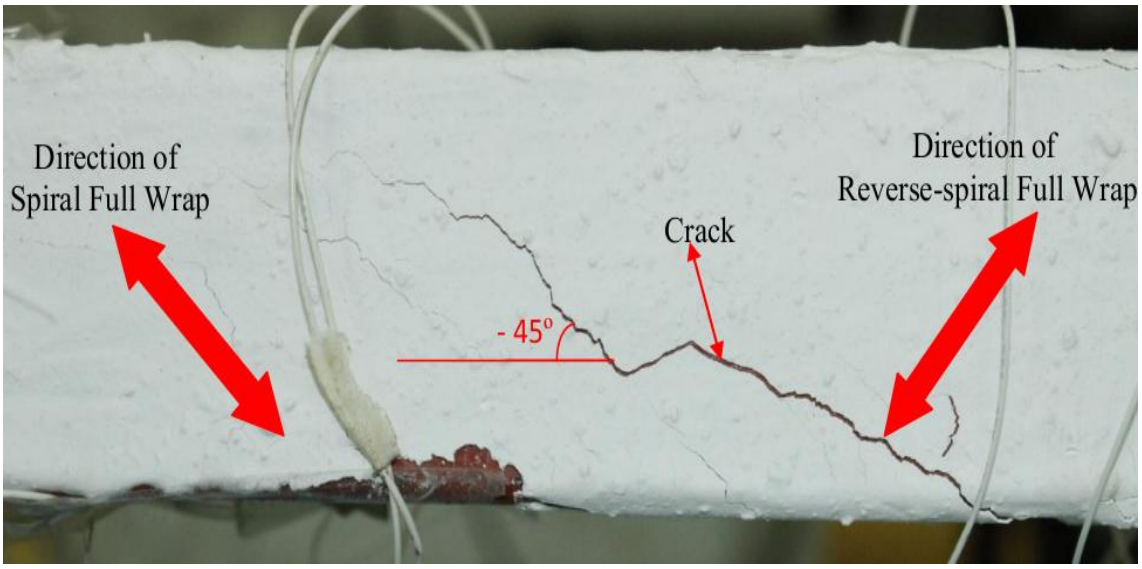

Figure 4.6 Cracks in the brittle coating due to pure torsion on the control beam

Therefore, from experimental results presented in this section, it can be seen that the best torsional strengthening of the SHS section was with four layers of alternating spiral (-45º) and reverse-spiral (45º) wrapping arrangement of CFRP with respect to the longitudinal axis of the specimen ($SHS1_{SRSR45^\circ}$).

4.2.5 Effect of different thickness

To investigate the effect of width to thickness (b/t) ratio of the SHS beam sections under pure torsion, two sets with different thickness i.e. 2.7 and 4.45 mm were considered. Each set consisted of two specimens with the same thickness including; 1) control beam specimen (SHS1 and SHS2), and 2) strengthened beam specimen with four layers of alternating spiral (-45º) and reverse-spiral (45º) arrangement of CFRP ($SHS1_{SRSR45^\circ}$ and $SHS2_{SRSR45^\circ}$). The values of twist angle versus the applied torque of these specimens are presented in Table 4.5.

Table 4.5: Experimental results of $SHS1_{SRSR45^\circ}$ and $SHS2_{SRSR45^\circ}$

Section identification no.	No. of layers	Elastic torsional capacity (Nm)	Increasing torsional capacity %	Ultimate torsional capacity (Nm)	Increasing torsional capacity %
SHS1	-	2637	-	2774	-
$SHS1_{SRSR45^\circ}$	4	3192	21.04	5051	82.08
SHS2	-	4102	-	4390	-
$SHS2_{SRSR45^\circ}$	4	5048	23.06	7127	62.35

For specimens $SHS1_{SRSR45^\circ}$ and $SHS2_{SRSR45^\circ}$, the gains in elastic torsional capacity were 21.04 and 23.06 % compared to control specimens SHS1 and SHS2, respectively. The gains in ultimate torsional capacity for specimens $SHS1_{SRSR45^\circ}$ and $SHS2_{SRSR45^\circ}$ were 82.05 and 62.35% compared to control specimens SHS1 and SHS2, respectively (Table 4.5). By qualitative study of Figure 4.7, it can be seen that with regards to the increase in thickness for thicker sections of both the control beam (SHS2) and strengthened beam ($SHS2_{SRSR45^\circ}$), significant increase of elastic and load bearing capacity were

achieved compared with the thinner sections (SHS1 and $SHS1_{SRSR45^o}$). From limited experimental results, it was shown that CFRP strengthening of torsional member was more effective on a beam with larger b/t ratio, where a 82% and 62% gain in ultimate torsional capacity was obtained for b/t ratio of (50/2.7) and (50/4.45), respectively. Zhao and Al-Mahaidi (2009) investigated on web buckling of lightsteel beams strengthened with CFRP subjected to end-bearing forces. Their results showed that the CFRP strengthening significantly increases the web buckling capacity especially for those with large web depth-to-thickness ratio.

In Figure 4.7, the difference observed in the initial stiffness of the specimens can be that such difference does not substantially affect the result of the torsional strengthening of the specimens.

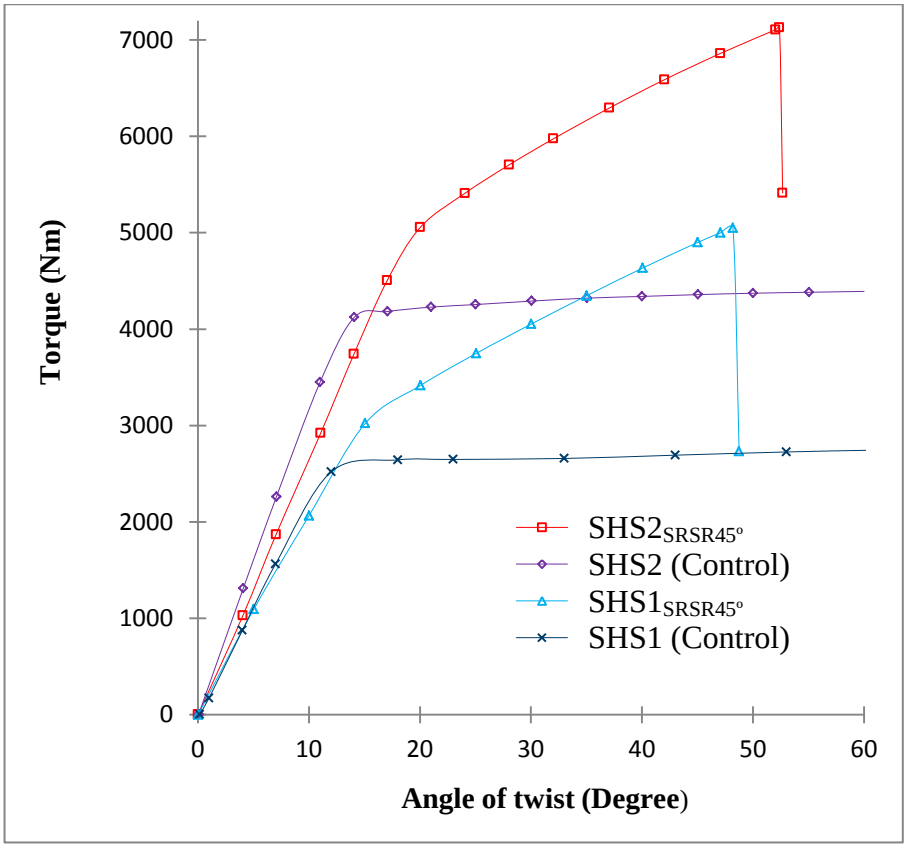

Figure 4.7 Torque-twist curves for $SHS1_{SRSR45^\circ}$ and $SHS2_{SRSR45^\circ}$

4.3 Strain gauge readings

4.3.1 Strain in control beam

The strains were monitored using the rosette strain gauge mounted on the surface of the steel control beam specimen at the middle of the specimen length. Figure 4.8 and Figure 4.9 show the torque-strain curves and arrangement of strain gauges for control beams SHS1 and SHS2, respectively. The curves in Figure 4.8 were plotted based on the strain in strain gauges no. 1, 2, 3, 4 and 5 of SHS1. The yield and ultimate torques for SHS1 were 2643 Nm and 2782 Nm, respectively (Figure 4.8a). The curves in Figure 4.9 were plotted based on the strain in strain gauges no. 1, 2, and 3 of SHS2. The yield and ultimate torques for SHS2 were 4102 Nm and 4391 Nm, respectively (Figure 4.9a). It can be observed in Figure 4.8 that the values of strains corresponding to strain gauges no. 3, 4 and 5 were close to zero for SHS1. For SHS2, the value of strain in strain gauge no. 3 was close to zero (Figure 4.9). These values can be attributed to pure shear stresses. When a beam is subjected to a pure torsional moment, normal stresses are negligible in the longitudinal and transverse directions of the beam. The shear stress can be the principal stress at ±45º with respect to the longitudinal axis of the beam. Figure 4.8 and Figure 4.9 show strain gauges no. 1 and 2 at ±45º with respect to the longitudinal axis of the control beam (for other torque-strain curves refer to Appendix A). Figure 4.10 shows specimen SHS2 (control beam) during the test.

(a) (b)

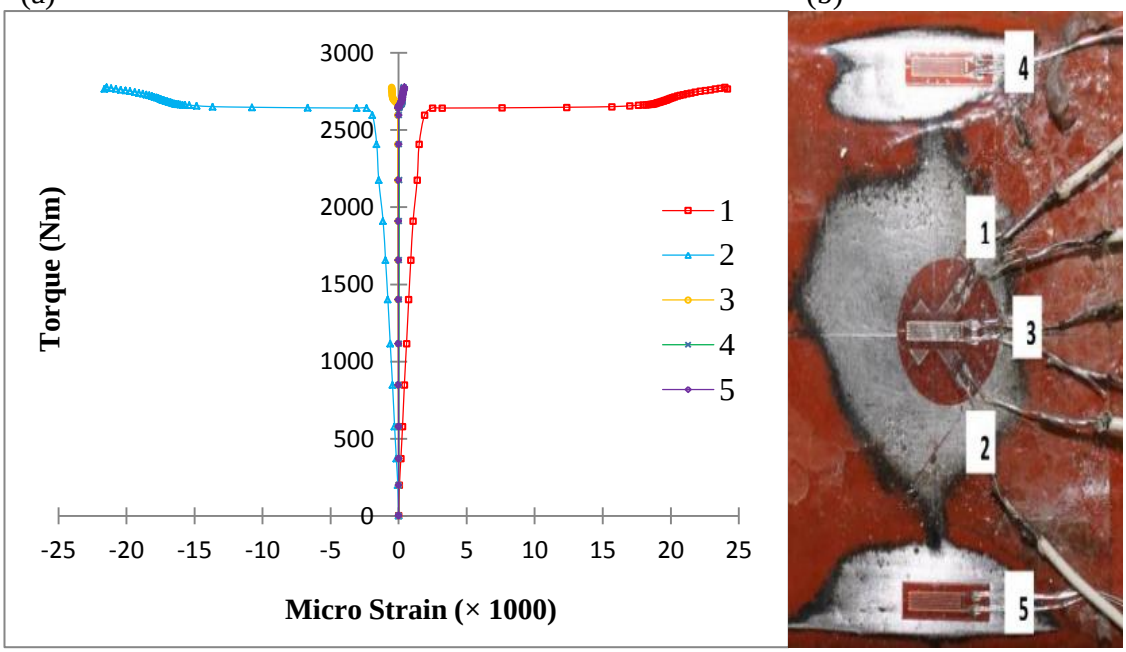

Figure 4.8 (a) The torque-strain curves of SHS 1, (b) Strain gauge arrangement on control beam SHS 1 at mid span

(a) (b)

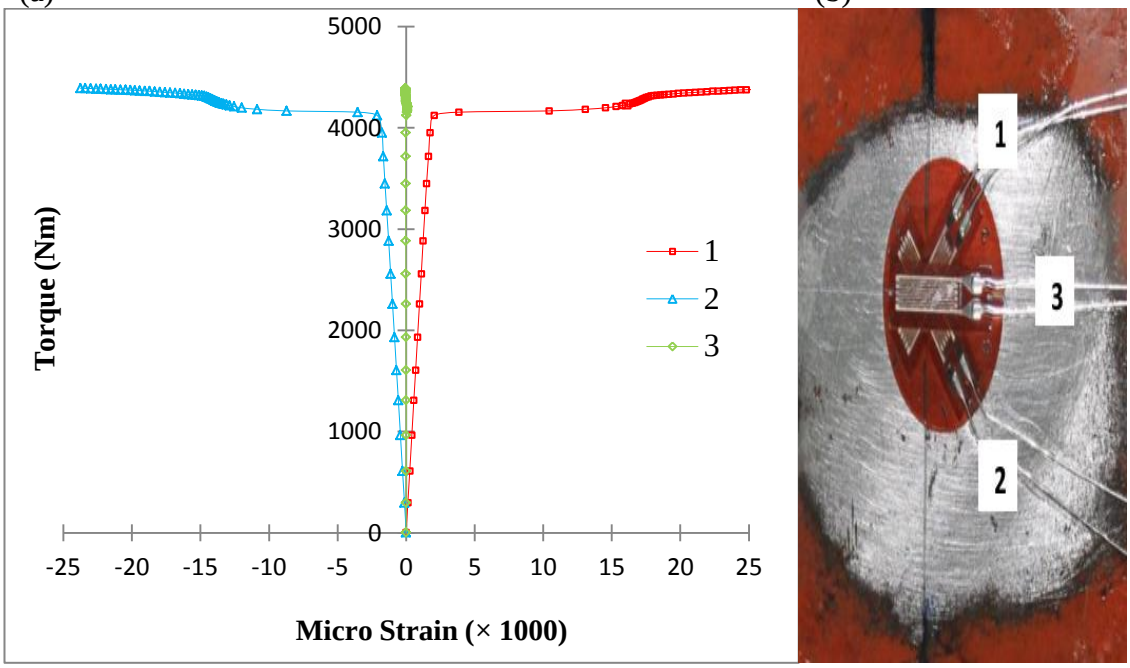

Figure 4.9 (a) The torque-strain curves of SHS 2, (b) Strain gauge arrangement on control beam SHS 2 at mid span

Figure 4.10 The SHS2 during testing

4.3.2 Strain in the strengthened beam specimens

4.3.2.1 Vertical and reverse-spiral wrap

In this study, specimen $SHS1_{V90^o}$ was configured with five layers of CFRP which was unidirectional vertically wrapped (90º) with respect to the longitudinal axis, and $SHS1_{R60^o}$ was wrapped with one layer of CFRP reverse-spiral (60º) with respect to the longitudinal axis of the specimen. Figure 4.11 shows the experimental results of $SHS1_{V90^o}$ and $SHS1_{R60^o}$ in terms of the torque versus strain of CFRP sheets. The strain levels of strengthened specimen $SHS1_{V90^o}$ was 1636 με while the strain levels of $SHS1_{R60^o}$ was 7670 με. The reason for the deficiency of strengthened specimen $SHS1_{V90^o}$ is that the orientation angle of fibers was not in the direction of the shear stresses.

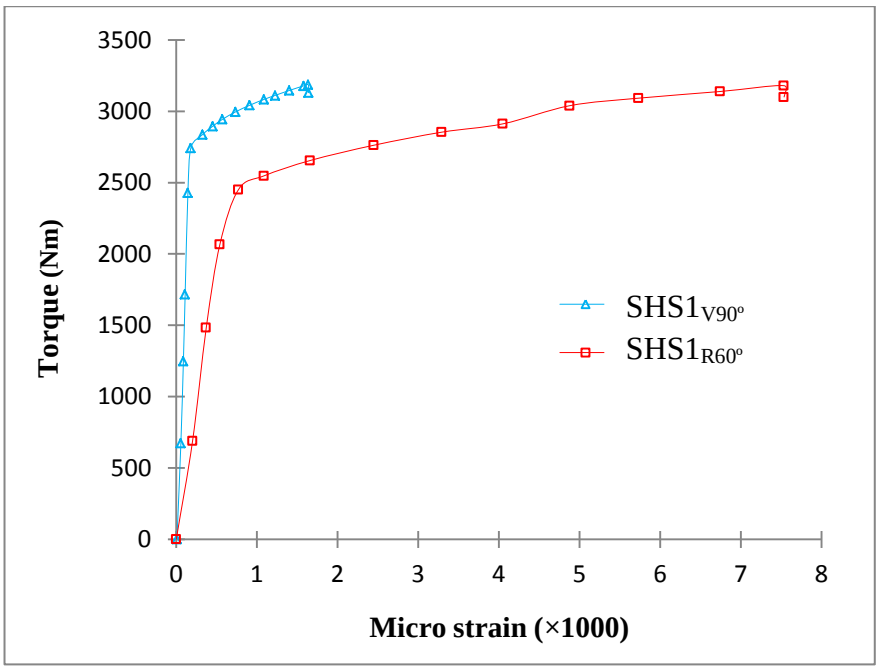

Figure 4.11 Strain values on CFRP for strengthened beams $SHS1_{V90^{o}}$ and $SHS1_{R60^{o}}$ at mid span

4.3.2.2 Two layers of CFRP

In Figure 4.12, typical torque-strain curves for the specimens strengthened using 2 layers of CFRP sheets with different strengthening configurations were plotted. By qualitative study of Figure 4.12, it can be seen that for a given torque, strain levels of strengthened specimen $SHS1_{SR60^{\circ}}$ was more than those of specimens $SHS1_{RR60^{\circ}}$ and $SHS1_{SS60^{\circ}}$ (for other torque-strain curves refer to Appendix A). It can be observed in Figure 4.12 that the combination of 1 layer spiral and 1 layer reverse-spiral ($SHS1_{SR60^{\circ}}$) wrapping with respect to the longitudinal axis of specimen ($SHS1_{SR60^{\circ}}$) guaranteed that the material is efficiently employed.

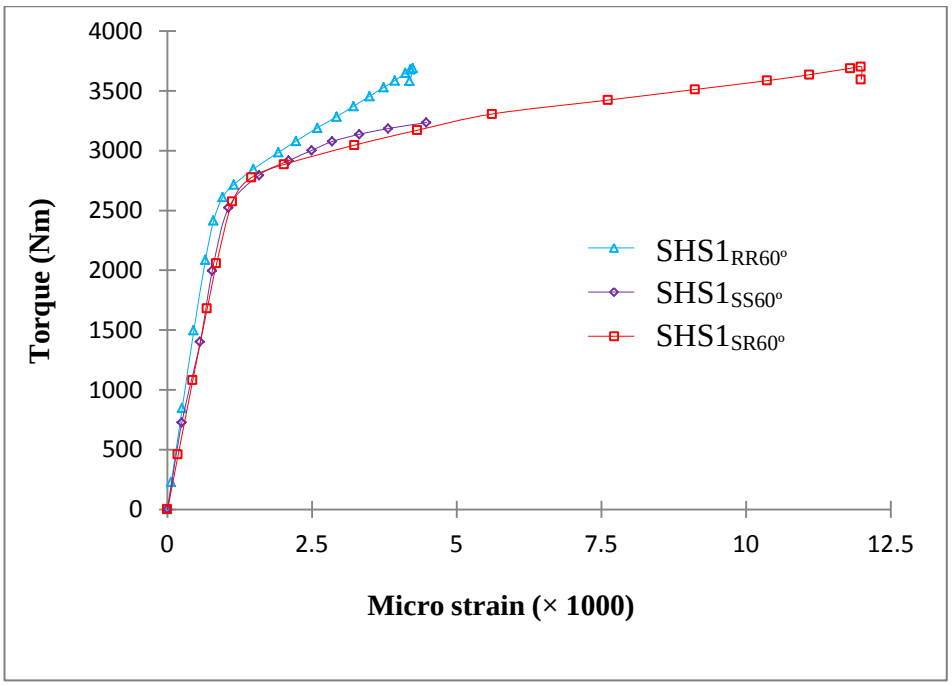

Figure 4.12 Strain values on CFRP for strengthened beams $SHS1_{SR60^o}$, $SHS1_{RR60^o}$, and $SHS1_{SS60^o}$ at mid span

4.3.2.3 Three layers of CFRP

In Figure 4.13, typical torque-strain curves for specimens $SHS1_{SRS60^o}$ and $SHS1_{RSR60^o}$ were plotted. It can be seen that for a given torque, strain levels of strengthened specimen $SHS1_{RSR60^o}$ was more than that of specimen $SHS1_{SRS60^o}$. The reason for the deficiency of strengthened specimen $SHS1_{SRS60^o}$ in comparison with specimen $SHS1_{RSR60^o}$ is that the orientation angle of the fibers was almost in the spiral direction and this resulted in premature failure (for other torque-strain curves refer to Appendix A).

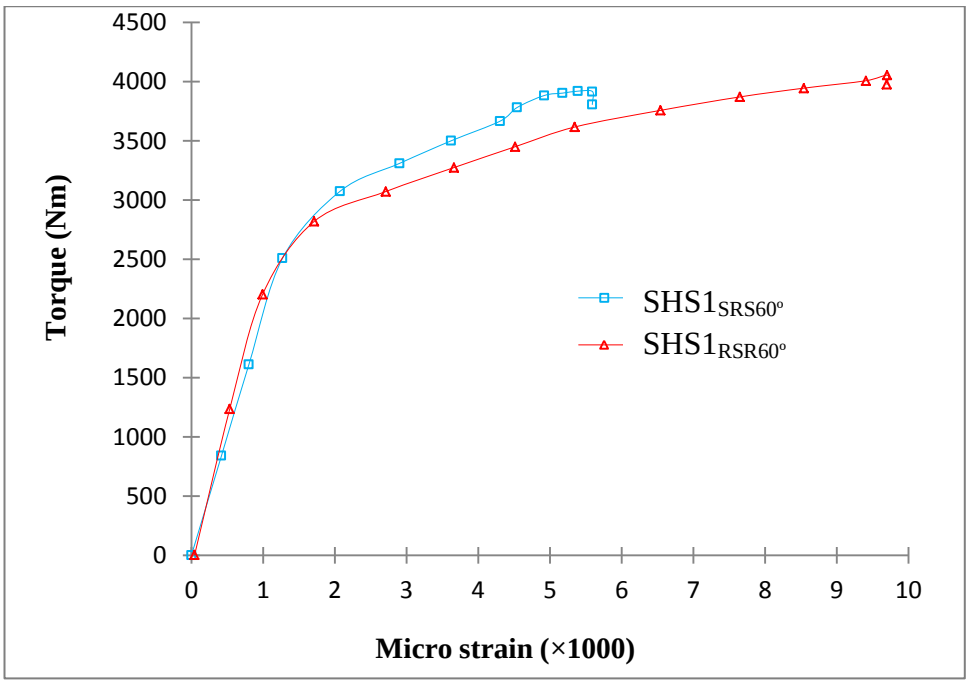

Figure 4.13 Strain values on CFRP for strengthened beams $SHS1_{RSR60º}$ and $SHS1_{SRS60º}$ at mid span

4.3.2.4 Four layers of CFRP

Figure 4.14 indicates the typical torque-strain curves of CFRP at mid span for specimens $SHS1_{RRRS60º}$, $SHS1_{SRSR60º}$, $SHS1_{SRSR45^{\circ}}$ and $SHS2_{SRSR45^{\circ}}$. In Figure 4.14, the difference observed in the initial stiffness of the specimens can be attributed to a less-than- perfect fixed condition achieved in the setup. The author believes that such difference does not substantially affect the result of the torsional strengthening of the specimens. By qualitative study of Figure 4.14, it can be seen that by increasing the torque, the strain on the steel and CFRP was increased too, especially at higher torque levels after yielding. Lenwari et al. (2006), Al-Emrani et al. (2005), and Buyukozturk et al. (2004) also made similar observations. Comparison of specimens $SHS1_{SRSR60º}$ and $SHS1_{SRSR45^{\circ}}$ showed that the 45˚ angle orientation of fibers gave higher ultimate capacity. It can be observed in Figure 4.14 that specimens $SHS1_{SRSR45^{\circ}}$ and $SHS2_{SRSR45^{\circ}}$ which were wrapped with four layers of alternating spiral (-45º) and reverse-spiral (45º) arrangement of CFRP with respect to the longitudinal axis of the SHS section showed

that the fibers guarantee that the material is efficiently employed. In addition, with regards to increase in thickness, for a thicker section ($SHS2_{SRSR45^o}$), significant increase of elastic (primary stiffness) and torsional moment bearing capacity were achieved compared to thinner sections ($SHS1_{RRRS60^o}$, $SHS1_{SRSR60^o}$, and$SHS1_{SRSR45^\circ}$).

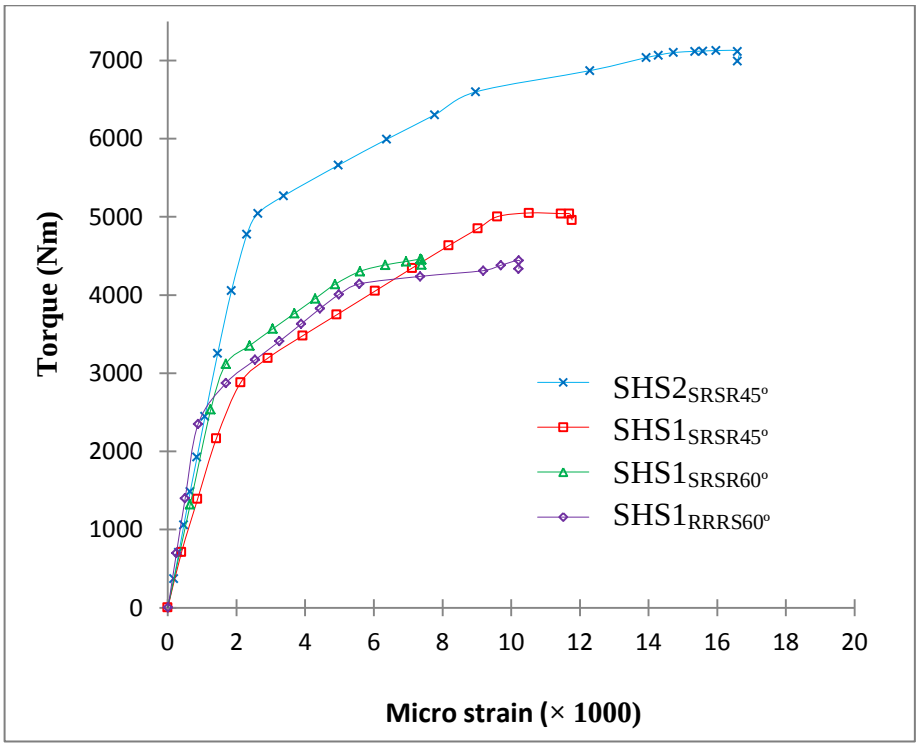

Figure 4.14 Strain values on the CFRP at mid span for the $SHS1_{RRRS60^o}$, $SHS1_{SRSR60^o}$, $SHS1_{SRSR45^\circ}$ and $SHS2_{SRSR45^\circ}$

Figure 4.15 indicates the typical torque-strain curves at mid span for $SHS1_{SRSR60^o}$. It can be seen that for a given torque, the strain levels on the steel surface was more than the strain levels on the CFRP. At max torque (4462 Nm), the strain levels on the steel surface at mid-span was 34164με and the strain levels on the CFRP at mid-span for side 1 and side 2 were 7423 and 10044με, respectively.

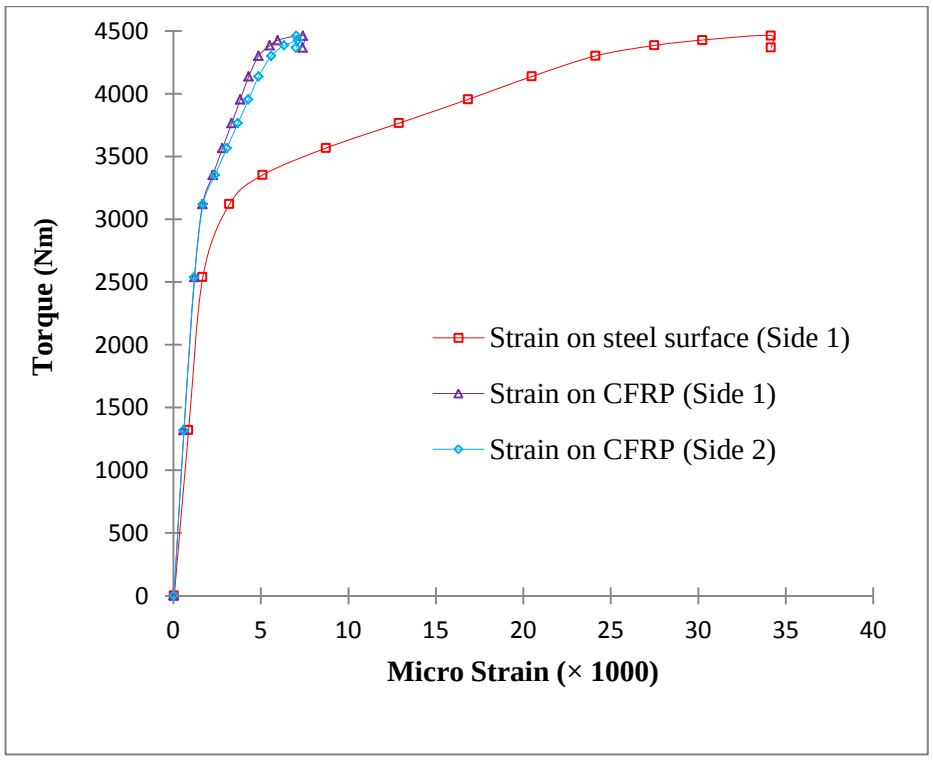

Figure 4.15 Strain values on the steel surface and on the CFRP at mid-span for strengthened beam $SHS1_{SRSR60^o}$

Figure 4.16 shows the typical torque-strain curves at mid span for $SHS1_{SRSR45^\circ}$. At max torque (5051 Nm), the strain levels of the steel surface at mid-span for side 1 and side 2 were 7010 and 7228με, respectively, whereas the strain levels of the CFRP at mid-span for side 1 and side 2 were 8531 and 11453με, respectively. From Figure 4.16, it can be observed that for $SHS1_{SRSR45^\circ}$, the level of strain on the steel and CFRP are close to each other compared to $SHS1_{SRSR60^\circ}$ (Figure 4.15).

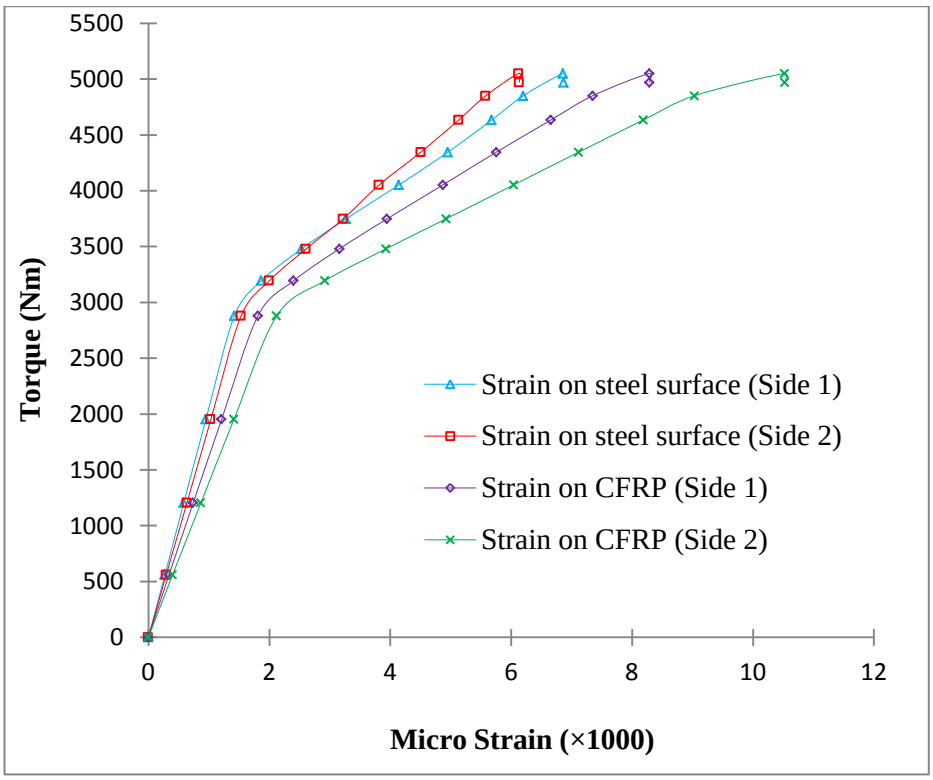

Figure 4.16 Strain values on the steel surface and on the CFRP at mid-span for strengthened beam $SHS1_{SRSR45^{\circ}}$

Figure 4.17 shows the typical torque-strain curves at mid span for specimen $SHS2_{SRSR45^{\circ}}$. At max torque (7127 Nm), the strain levels of the steel surface at mid-span for side 1 and side 2 were 10273 and 18723 με, respectively, whereas the strain levels of the CFRP at mid-span for side 1 and side 2 were 8670 and 16597με, respectively. In Figure 4.17, it can be observed that for specimen $SHS2_{SRSR45^{\circ}}$, the level of strain on the steel and CFRP are close to each other, as with specimen $SHS1_{SRSR45^{\circ}}$ (Figure 4.16).

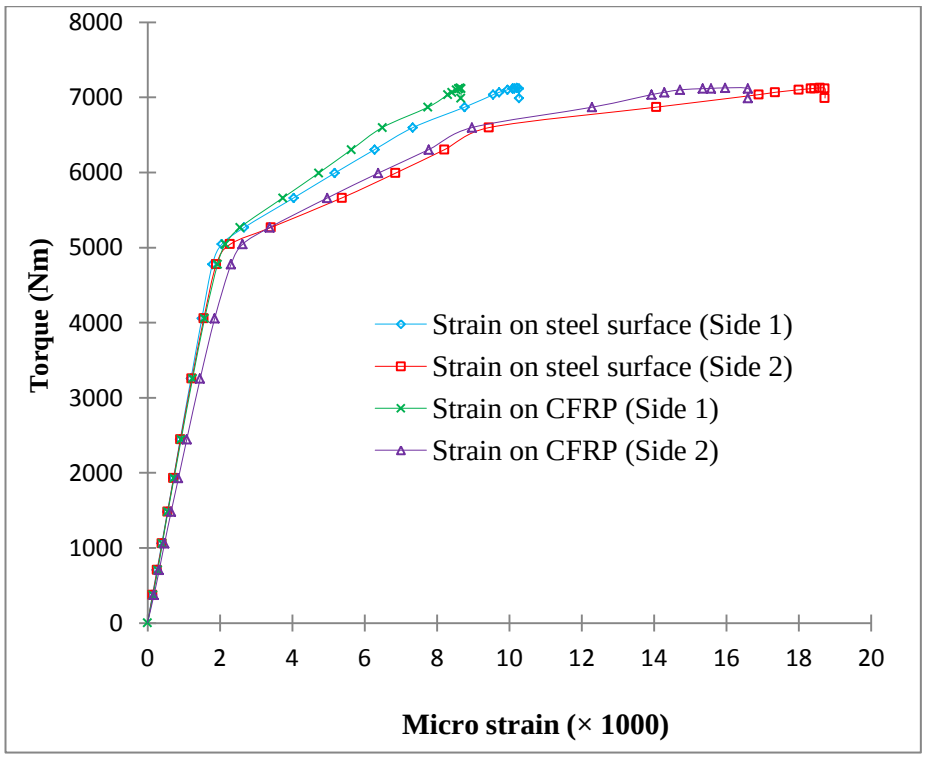

Figure 4.17 Strain values on the steel surface and on the CFRP at mid-span for strengthened beam $SHS2_{SRSR45^{\circ}}$

4.4 Failure modes

In general, failure modes for CFRP sheet strengthened specimens under torque are rupture, debonding, splitting, and delamination. Rupture occurs when the CFRP cracks in the transverse of the CFRP direction (Figure 4.18a). Debonding occurs when both the CFRP and adhesive separate from the steel surface (Figure 4.18b) while splitting occurs when the CFRP cracks parallel to the CFRP direction (Figure 4.18c). Delamination (Figure 4.18d) occurs when the CFRP separate into individual layers in the longitudinal direction (Narmashiri et al., 2012).

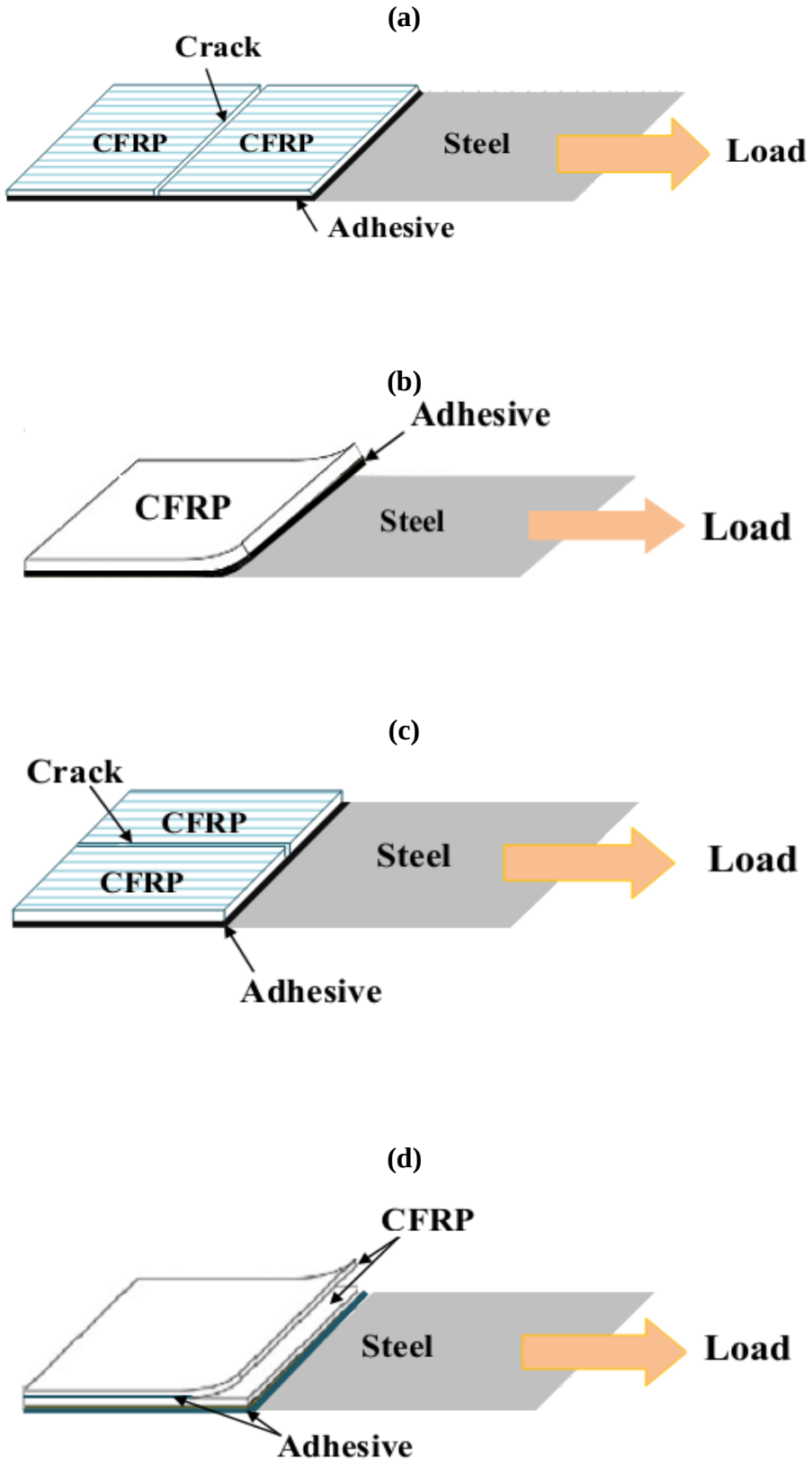

Figure 4.18 CFRP failure modes (a) rupture, (b) debonding, (c) splitting, and (d) delamination (Narmashiri et al., 2012)

4.4.1 Failure modes of vertical and reverse-spiral wrap

Due to the CFRP cracks parallel to the CFRP direction, splitting failure mode was observed for specimen $SHS1_{V90^o}$ (Figure 4.19). For specimen $SHS1_{R60^\circ}$, CFRP rupture and debonding occurred in the direction of the reverse-spiral wrap (Figure 4.20).

Figure 4.19 CFRP splitting failure mode of $SHS1_{V90^o}$

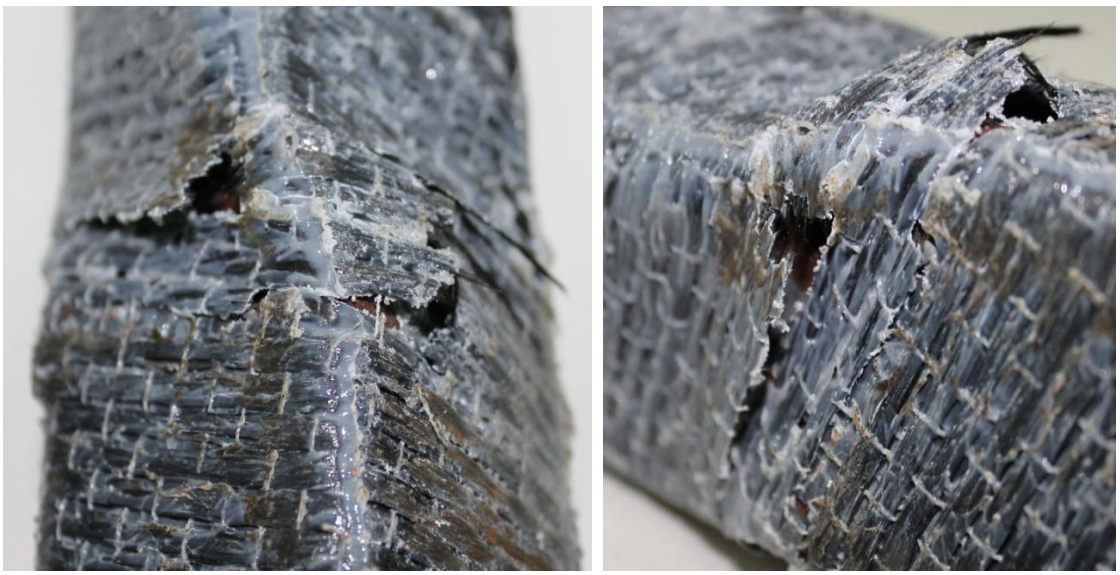

Figure 4.20 CFRP rupture and debonding failure modes of $SHS1_{R60^\circ}$

4.4.2 Failure modes of two layers of CFRP

Interestingly, in specimen $SHS1_{SS60^o}$ cracks developed on three sides in the direction of the longitudinal axis of the specimen (Figure 4.21). Splitting of the CFRP occurred at the mid-span.

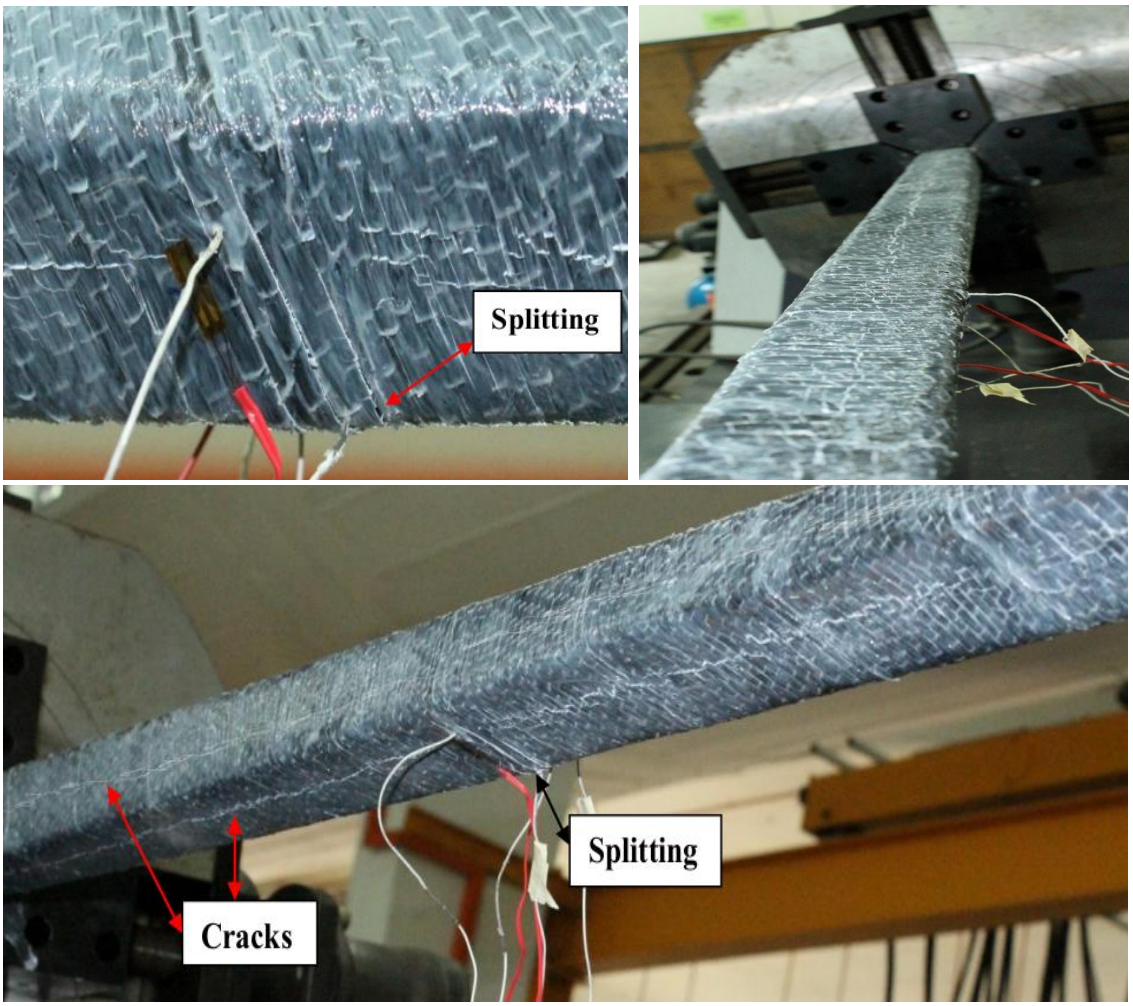

Figure 4.21CFRP splitting failure mode of $SHS1_{SS60^o}$

For specimens $SHS1_{RR60^o}$ and $SHS1_{SR60^o}$, CFRP rupture and debonding occurred in the direction of the reverse-spiral wrap (Figure 4.22 and Figure 4.23). For $SHS1_{RR60^o}$, the failure occurred close to the rotate grip. For $SHS1_{SR60^o}$, the failure occurred at mid span where the strain gauge wires were installed on the steel surface passing through the CFRP sheet.

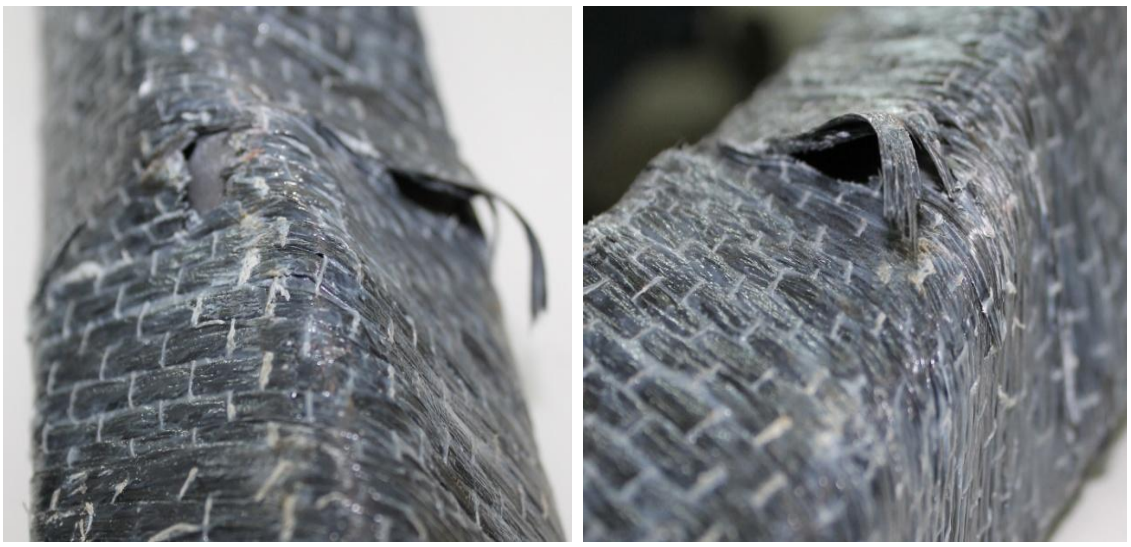

Figure 4.22 CFRP rupture and debonding failure modes of $SHS1_{RR60^o}$

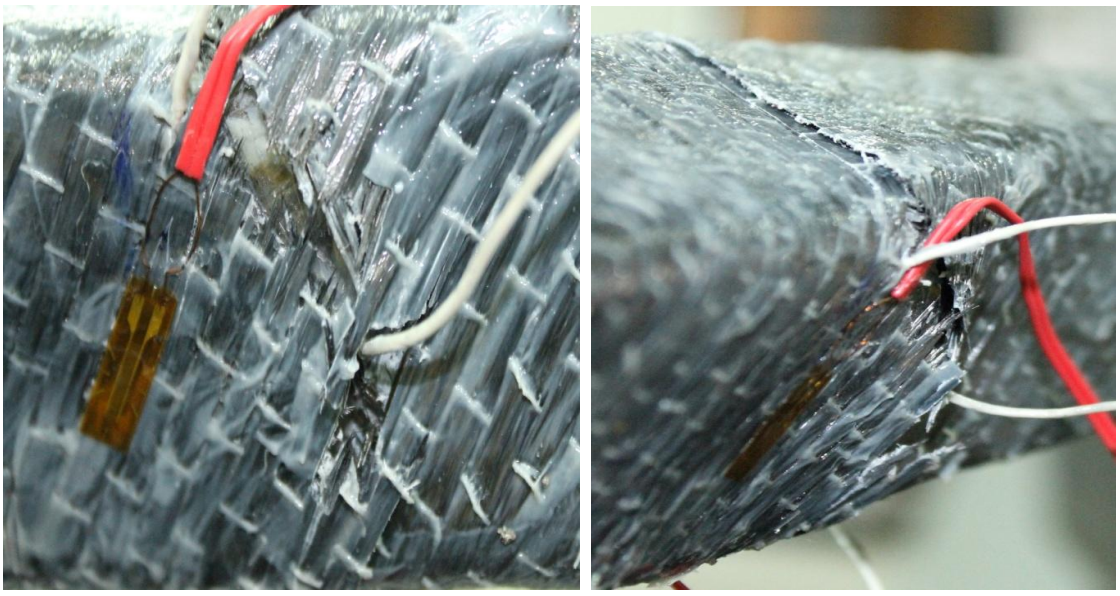

Figure 4.23 CFRP rupture and debonding failure modes of $SHS1_{SR60^o}$

4.4.3 Failure modes of three layers of CFRP

For $SHS1_{SRS60^o}$ and $SHS1_{RSR60^o}$, the failure occurred at mid span. In specimen $SHS1_{SRS60^o}$, splitting of the CFRP occurred in the CFRP direction (Figure 4.24). It can be observed that the failure modes of $SHS1_{SRS60^o}$ and $SHS1_{SS60^o}$ were similar. It is interesting to note that when the orientation angle of fibers was in the direction of spiral wrap, splitting failure occurred.

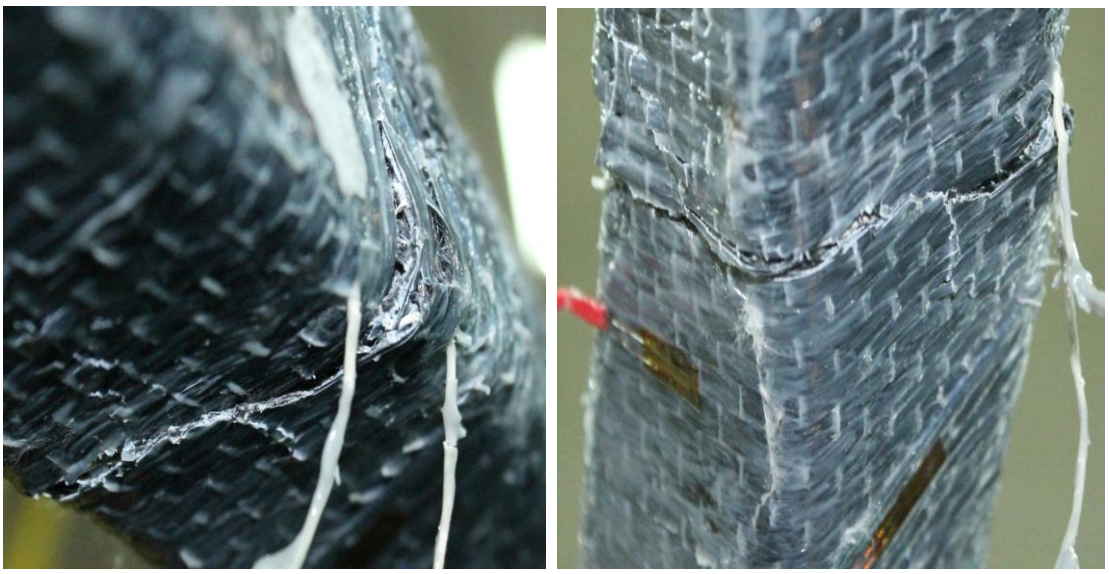

Figure 4.24 CFRP splitting failure mode of $SHS1_{SRS60^o}$

For specimen $SHS1_{RSR60^o}$, CFRP rupture and debonding occurred in the direction of the reverse-spiral wrap (Figure 4.25). It can be seen that the failure modes of $SHS1_{RSR60^o}$ and $SHS1_{RR60^o}$ were similar. In general, when the orientation angle of fibers is in the direction of the reverse-spiral wrap, CFRP rupture and debonding occurred.

Figure 4.25 CFRP rupture and debonding failure mode of $SHS1_{RSR60^o}$

4.4.4 Failure modes of four layers of CFRP

For $SHS1_{RRRS60^o}$ (Figure 4.26), $SHS1_{SRSR60^o}$ (Figure 4.27), $SHS1_{SRSR45^\circ}$ (Figure 4.28) and $SHS2_{SRSR45^\circ}$ (Figure 4.29), CFRP rupture and debonding occurred in the direction of the reverse-spiral wrap.

Figure 4.26 CFRP rupture and debonding failure mode of $SHS1_{RRRS60^o}$

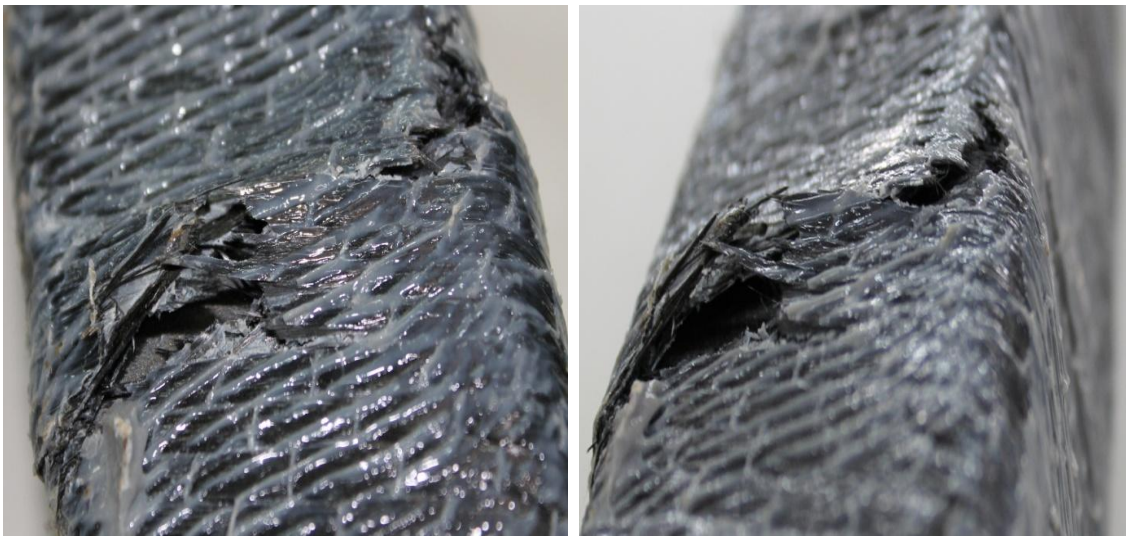

Figure 4.27 CFRP rupture and debonding failure mode of $SHS1_{RSRS60^o}$

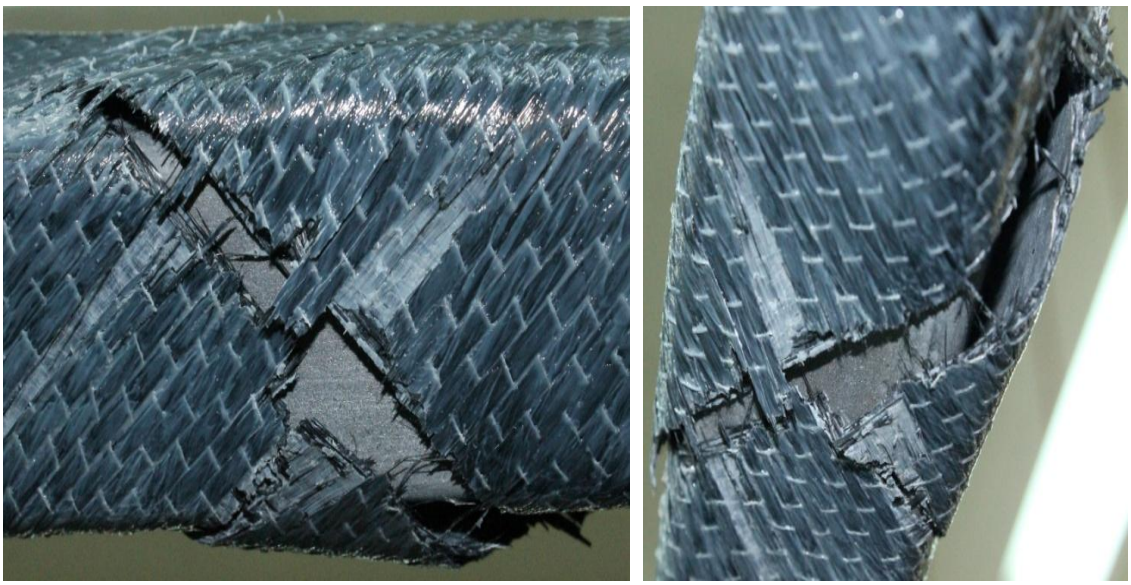

Figure 4.28 CFRP rupture and debonding failure mode of $SHS1_{SRSR45^{\circ}}$

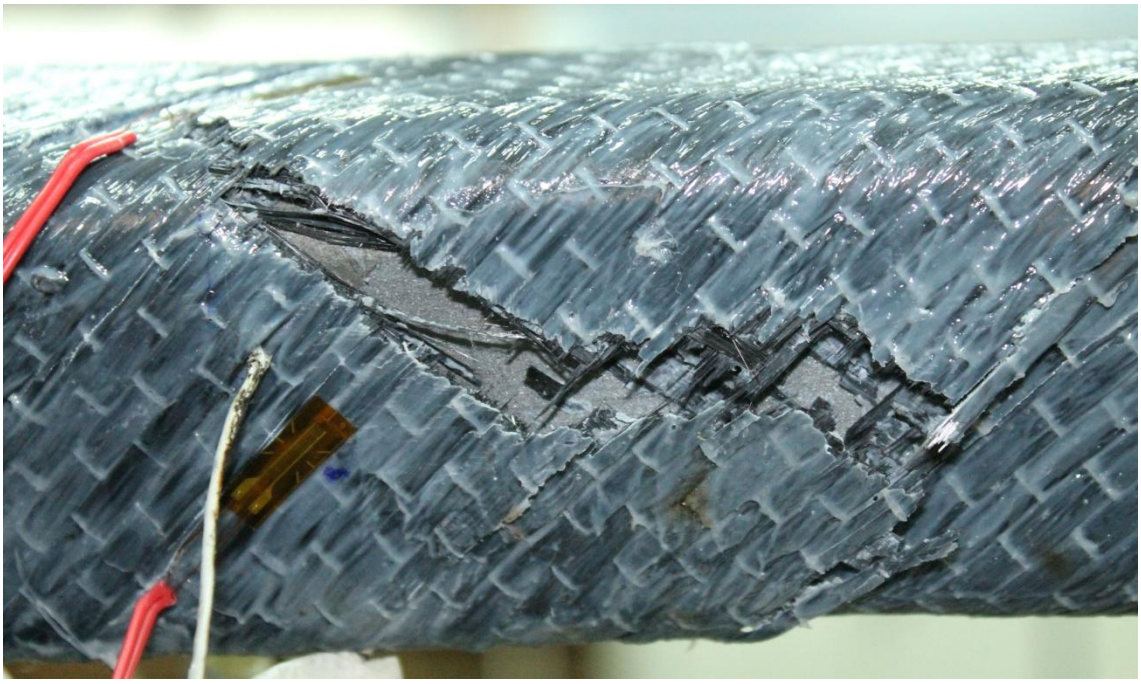

Figure 4.29 CFRP rupture and debonding failure mode of $SHS2_{SRSR45^{\circ}}$

By comparing the failure modes of different types of strengthening schemes, it can be seen that the orientation angle of the fiber had significant effect on torsional behavior. Interestingly, by utilizing CFRP at a 45˚ angle in the direction of the principal tensile stresses, the failure mode which was brittle failure can be clearly seen at an angle of 45˚ with respect to the longitudinal axis of the beam. However, if the angle of the fiber was at 60º, the angle of rupture of the fiber was scattered and the fiber behaved in a more

ductile manner. (for other figures of failure modes of CFRP sheet strengthened specimens refer to Appendix B).

4.5 Torsional capacity prediction of CFRP strengthened SHS

Following extensive experimental work on different CFRP configurations and number of layers, theoretical predictions of ultimate torsional capacity of strengthened steel hollow sections are proposed. The basis of calculation was based on the classical torsion formula. Modified geometrical properties of CFRP strengthened steel sections were formulated (Abdollahi Chahkand et al., 2013). The plastic torsional capacity (T_{pl}) for a box section can be determined by taking into account the flow of uniform plastic shear around the cross-section, given as

$$T_{pl} = 2tA_h \tau_y \quad (4.1)$$

Where t is the thickness of the SHS, τ is the shear stress which is equal to $0.6f_y$ and f_y is the yield stress of the SHS. A_h is the enclosed area (Figure 4.30a) which is given by

$$A_h = (b - 2r_{ext})(h - t) + 2(h - 2r_{ext})r_m + \pi r_m^2 \quad (4.2)$$

Where r_{ext} is the external corner radius, r_{int} is the internal corner radius and r_m is the mid-corner radius given by

$$r_m = (r_{ext} + r_{int})/2 \quad (4.3)$$

When CFRP is applied, the proposed method considers equivalent thickness approach. The CFRP thickness can be equivalent to steel thickness as given by

$$t_{es} = (E_{CFRP}/E_{steel})nt_{fiber} \quad (4.4)$$

Where E_{CFRP} is the Young's modulus of CFRP and E_{steel} is the Young's modulus of the steel, n is the number of layers and t_{fiber} is the thickness of the fiber. Figure 4.30b shows

the dimensions of the equivalent SHS with CFRP, then the equivalent dimensions become

$$b_{eq} = b + 2t_{es} \quad (4.5)$$

$$h_{eq} = h + 2t_{es} \quad (4.6)$$

$$t_{eq} = t + t_{es} \quad (4.7)$$

$$r_{ext,eq} = r_{ext} + t_{es} \quad (4.8)$$

$$r_{m,eq} = (r_{ext,eq} + r_{int})/2 \quad (4.9)$$

$$A_{h,eq} = (b - 2r_{ext})(h_{eq} - t_{eq}) + 2(h - 2r_{ext})r_{m,eq} + \pi r_{m,eq}^2 \quad (4.10)$$

(a)

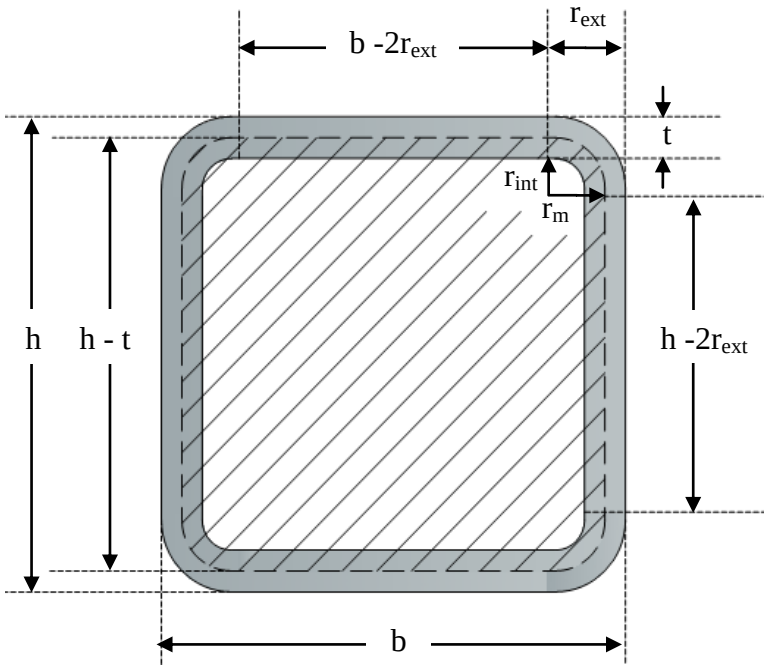

Figure 4.30 Dimensions to calculate the enclosed area, (a) SHS without CFRP, (b) SHS with CFRP

(b)

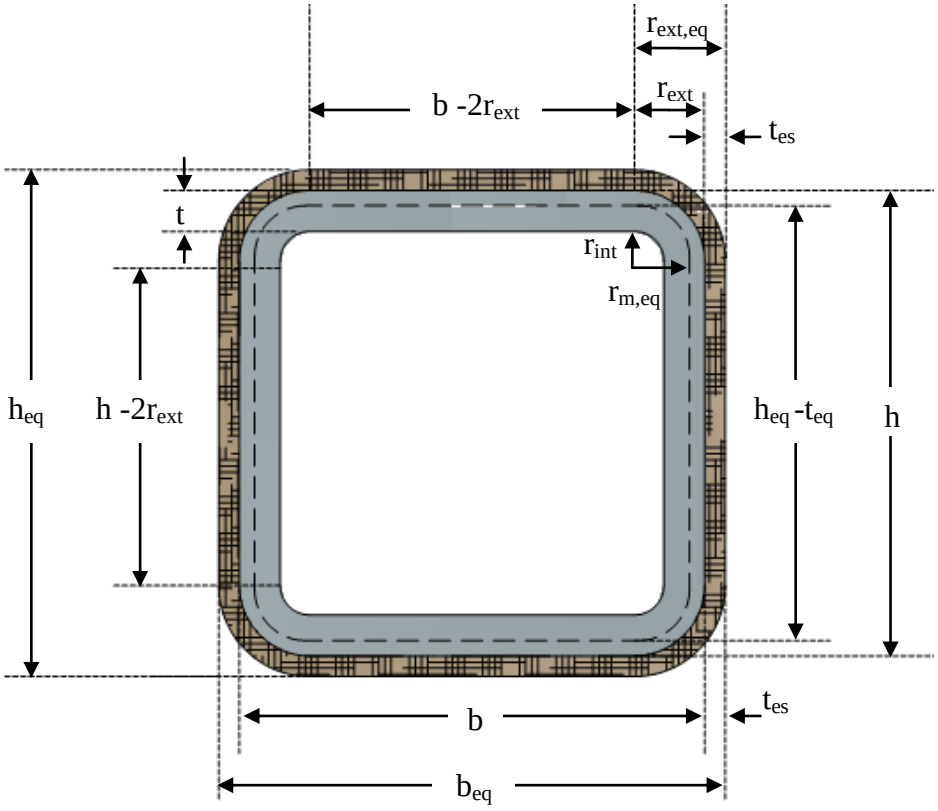

Figure 4.30, continued

Then, the torsional capacity, T_{pl} can be calculated by using Eq. 4.1, where t is replaced by t_{eq} (Eq. 4.7) and A_h is replaced by $A_{h,eq}$ (Eq. 4.10). The value τ should be increased because of the strain hardening. The extreme case will be $0.6f_u$ where f_u is the ultimate tensile strength of steel SHS. Thus torsional capacity of the strengthened beam with CFRP is given by

$$T_{pl,eq} = 2\, t_{eq}\, A_{h,eq}\, 0.6F_u \qquad (4.11)$$

The calculated torsional capacity for all the strengthened beams, where fiber direction was along the shear direction is presented in Table 4.6. It should be noted that the strengthening scheme using vertical fibres alone was found not efficient. Therefore no predictions are included in the thesis for this strengthening scheme. Comparison

between the experimental values and theoretical prediction shows that the values are in good agreement.

Table 4.6: Comparison of ultimate capacity of proposed method with test results

Section identification no.	Angle of CFRP	No. of layers	Experimental torsional capacity (Nm)	Proposed method for torsional capacity (Nm)	Experimental torsional capacity/ Proposed method
SHS1	-	None	2774	2766	1.00
$SHS1_{R60^{\circ}}$	- 60º	1	3179	3394	0.93
$SHS1_{SS60^{o}}$	- 60º	2	3235	3571	0.90
$SHS1_{RR60^{o}}$	60º	2	3689	3571	1.03
$SHS1_{SR60^{o}}$	- 60º & 60º	2	3701	3571	1.03
$SHS1_{SRS60^{o}}$	60º & - 60º	3	3919	3744	1.04
$SHS1_{RSR60^{o}}$	- 60º & 60º	3	4054	3744	1.08
$SHS1_{RRRS60^{o}}$	60º & - 60º	4	4442	3920	1.13
$SHS1_{SRSR60^{o}}$	- 60º & 60º	4	4462	3920	1.14
$SHS1_{SRSR45^{o}}$	- 45º & 45º	4	5051	3920	1.28
SHS2	-	None	4390	4387	1.00
$SHS2_{SRSR45^{o}}$	- 45º & 45º	4	7127	5824	1.22

5.0 CONCLUSIONS

5.1 General

The purpose of this study was to fill the knowledge gap on the behavior of CFRP strengthened hollow structural member under pure torsion. In particular, this research presented several key findings relating to reinforcing systems for SHS to withstand torsional moment using novel wrapping configurations of CFRP sheets. The behavior of pure torsion strengthening on SHS using CFRP was investigated. The effect of strengthening of SHS using different number of layers of CFRP wrap was compared. The best configuration of CFRP orientation was selected by comparing different configurations including vertical, spiral, reverse-spiral and a combination of spiral wrapping and reverse-spiral wrapping. Another goal of this study was to investigate the effect of b/t ratio of steel section on pure torsion strengthening using CFRP wrap. Theoretical predictions of ultimate torsional capacities of CFRP strengthened steel hollow sections were proposed. The findings of this thesis were summarized. Recommendations for future works are highlighted here.

5.2 Torsional strengthening of steel hollow section

This study aimed to develop a reinforcing system that is relatively simple and can be applied on existing superstructures. To investigate the effects of different number of layers and orientations of CFRP sheets, twelve beams were examined. Two specimens without strengthening were designated as the control beam specimens. Ten beam specimens were strengthened with different number of layers and orientations of CFRP including: 1) Five layers of vertical (90˚) full wrap, 2) One layer of reverse-spiral (60˚) full wrap, 3) Two layers of spiral (-60˚) full wrap, 4) Two layers of reverse-spiral (60˚) full wrap, 5) Two layers of alternating spiral (-60˚) and reverse-spiral (60˚) full wrap, 6)

Three layers of alternating spiral (-60˚) and reverse-spiral (60˚) full wrap, 7) Three layers of alternating reverse-spiral (60˚) and spiral (-60˚) full wrap, 8) Four layers that included a combination of three layers of reverse-spiral (60º) and one layer of spiral (-60º) full wrap, 9) Four layers of alternating spiral (-60˚) and reverse-spiral (60˚) full wrap, 10) Four layers of alternating spiral (-45˚) and reverse-spiral (45˚) full wrap. The aim was to determine the effects of the number of CFRP layers and strengthening configurations on the torsional behavior of SHS.

The main objective of this thesis was to investigate the abilities of the CFRP strengthening schemes in delaying or preventing structural failure of the hollow structural member under pure torsion. The elastic and ultimate torques of all the strengthened steel specimens were greater than that of the control specimens. The increase in magnitude depended on the CFRP strengthening configuration.

When the orientation of the fibers was in the spiral direction, the yield torque and initial stiffness were slightly higher compared to reverse-spiral direction. The ultimate torques and ductility were higher when the orientation of the fibers was in reverse-spiral.

The best strengthening scheme was obtained for specimen $SHS1_{SRSR45^o}$, where the beam was wrapped with four layers of alternating spiral (-45º) and reverse-spiral (45º) arrangement of CFRP with respect to the longitudinal axis of the specimen. For this specimen ($SHS1_{SRSR45^o}$), the elastic torsional capacity was 3192 N.m, which was a 21% increase compared to the control beam (2637 N.m) while the ultimate torsional capacity was 5051(N.m). A significant increment of more than 82% was achieved on the ultimate torsional capacity of this specimen.

In general, it was observed that the failure mode of specimens strengthened with the orientation of fiber in the spiral direction was splitting. On the other hand, the failure

modes of specimens strengthened with the orientation of fiber in the reverse-spiral direction were rupture and debonding.

By comparing failure modes of specimens strengthened with the orientation of fiber at 60º and 45º ($SHS1_{SRSR60º}$ and $SHS1_{SRSR45°}$, respectively), it can be seen that the fiber angle orientation had significant effect on the torsional behavior. Interestingly, by utilizing CFRP at a 45˚ angle in the direction of the principal tensile stresses, the failure modes were clearly seen in the angle of 45˚ to the longitudinal beam axis and brittle failure occurred. However, if the fiber orientation was at 60º, the angle of rupture of the fiber was scattered and the fiber behaved in a more ductile manner.

To investigate the effect of b/t ratio of the SHS on pure torsion, two sets with different thickness i.e. 2.7 and 4.45 mm were considered. Each set had two specimens with the same thickness including; 1) control beam specimen (SHS1 and SHS2), and 2) strengthened beam specimen with four layers of alternating spiral (-45º) and reverse-spiral (45º) arrangement of CFRP ($SHS1_{SRSR45°}$ and $SHS2_{SRSR45°}$). From limited experimental results, CFRP strengthening of the torsional member was more effective on a beam with larger b/t ratio, where a 82% and 62% gain in ultimate torsional capacity was obtained for b/t ratio of (50/2.7) and (50/4.45), respectively.

In addition, theoretical predictions of ultimate torsional capacity of strengthened square hollow steel section beams were proposed based on the classical torsion theory with modified geometric properties of the strengthened specimens. By comparing the experimental results and the calculated values using the simplified expression, it was found that the values are in good agreement.

5.3 Recommendations for future work

The following recommendations can be considered for future study.

a) To evaluate the load-deformation responses of torsional loaded square hollow steel section by using CFRP strip (plate).

b) To study the effect of using full-covering and partial-covering of CFRP wrap on torsional behavior of square hollow steel section.

c) To study the effects of various thickness and types of CFRP wraps to calculate the CFRP effective thickness of different CFRP types for torsional strengthening of square hollow steel section.

d) To study the effect of concrete- filled thin-walled square hollow steel section under pure torsion strengthening with CFRP wrap.

e) To study the effect of concrete- filled thin-walled square hollow steel section under pure torsion strengthening with CFRP strip (plate).

f) To model and analyse the torsional behavior of strengthened square hollow steel section using CFRP wrap with finite element analysis for wider verification.

REFERENCES

Abdollahi Chahkand, N., Zamin Jumaat, M., Ramli Sulong, N. H., Zhao, X. L., & Mohammadizadeh, M. R. (2013). Experimental and theoretical investigation on torsional behaviour of CFRP strengthened square hollow steel section. *Thin-Walled Structures*, 68, pp. 135-140.

Abdollahi Chahkand, N., Zamin Jumaat, M., Ramli Sulong, N. H., Mohammadizadeh, M. R., Asadi, A., & Mojarrad, M. (2012). Experimental investigation on torsional behavior of CFRP strengthened square hollow steel section, *Forensic Engineering 2012:Gateway to a Better Tomorrow Proceedings of the 6th Congress on Forensic Engineering* (ASCE 2013), San Francisco, CA. pp 1101-1110.

Al-Emrani, M., Linghoff, D., & Kliger, R. (2005). *Bonding strength and fracture mechanisms in composite steel-CFRP elements*. Paper presented at the international symposium on bond behavior of FRP in structures (BBFS 2005).

Al-Mahaidi, R., & Hii, A. K. Y. (2007). Bond behaviour of CFRP reinforcement for torsional strengthening of solid and box-section RC beams. *Composites: Part B*, 38, pp. 720–731.

Al-Zubaidy, H., Al-Mahaidi, R., & Zhao, X. L. (2012). Experimental investigation of bond characteristics between CFRP fabrics and steel plate joints under impact tensile loads. *Composite Structures*, 94(2), pp. 510-518.

Ameli, M., Ronagh, H. R., & Dux, P. F. (2007). Behaviour of FRP strengthened reinforced concrete beams under torsion. *Journal of Composite for Construction*, 11(2), pp. 192-200.

Bambach, M. R., Jama, H. H., & Elchalakani, M. (2009a). Axial capacity and design of thin-walled steel SHS strengthened with CFRP. *Thin-Walled Structures*, 47(10), pp. 1112-21.

Bambach, M. R., Elchlakani, M., & Zhao, X. L. (2009b). Composite steel CFRP SHS tubes under axial impact. *Composite Structures*, 87(3), pp. 282-292.

Buyukozturk, O., Gunes, O., & Karaca, E. (2004). Progress on understanding debonding problems in reinforced concrete and steel members strengthened using FRP composites. *Construction and Building Materials*, 18, pp. 9–19.

Chalioris, C. E. (2008). Torsional strengthening of rectangular and flanged beams using Carbon fibre-reinforced-polymers – Experimental study. *Construction and Building Materials*, 22, pp. 21–29.

Deng, J., Lee, M. M. K., & Li, S. (2011). Flexural strength of steel–concrete composite beams reinforced with a prestressed CFRP plate. *Construction and Building Materials*, 25, pp. 379–384.

El-Tawil, S., Ekiz, E., Goel, S., & Chao, S. H. (2011). Retraining local and global buckling behavior of steel plastic hinges using CFRP. *Journal of Constructional Steel Research*, 67(3), pp. 261-269.

Fawzia, S., Zhao, X. L., & Al-Mahaidi, R. (2006). Bond-slip model for CFRP sheets bonded to steel plate. *In: Third international conference on FRP composites in civil engineering.*

Fang, I. K. & Shiau, J. K. (2004). Torsional behaviour of normal- and high-strength concrete beams. *ACI Structural Journal*, 101(3), pp. 304-13.

Ferdinand, P., Russell, E., & John, T. (2006). *Mechanics of materials*, McGraw-Hill.

Fernando, D., Yu, T., Teng, J. G., & Zhao, X. L. (2009). CFRP strengthening of rectangular steel tubes subjected to end bearing loads: Effect of adhesive properties and finite element modeling. *Thin-Walled Structures*, 47, pp. 1020 –1028.

FIB. Externally bonded FRP reinforcement for RC structures, (2001). *FIB Bulletin 14*, *FIB – International Federation for Structural Concrete*, Lausanne, pp. 59-68.

Ghobarah, A., Ghorbel, M. N., & Chidiac, S. E. (2002). Upgrading torsional resistance of reinforced concrete beams using fiber-reinforced polymer. *Journal Composite Construction*, 6(4), pp. 257–63.

Gosbell, T., & Meggs, R. (2002). West Gate bridge approach spans FRP strengthening Melbourne, Australia. *In: IABSE symposium Melbourne*, Melbourne.

Haedir, J., & Zhao, X. L. (2011). Design of short CFRP-reinforced steel tubular columns. *Journal of Constructional Steel Research*, 67(3), pp. 497-509.

Haedir, J., Zhao, X. L., Bambach, M. R., & Grzebieta, R. H. (2010). Analysis of CFRP externally-reinforced steel CHS tubular beams. *Composite Structures*, 92(12), pp. 2992-3001.

Hii, A. K. Y., & Al-Mahaidi, R. (2005). Torsional strengthening of solid and box-section RC beams using CFRP composites. *In: Composites in construction 2005 – third international conference*, Lyon, France.

Hii, A. K. Y., & Al-Mahaidi, R. (2006). An experimental and numerical investigation on torsional strengthening of solid and box-section RC beams using CFRP laminates. *Composite Structures*, 75, pp. 213–221.

Harries, K. A., Peck, A. J., & Abraham, E. J. (2009). Enhancing stability of structural steel sections using FRP. *Thin-Walled Structures*, 47(10), pp. 1092-1101.

Jiao, H., & Zhao, X. L. (2004). CFRP strengthened butt-welded very high strength (VHS) circular steel tubes. *Thin-Walled Structures*, 42, pp. 963–978.

Kima, Y. J., & Harries, K. A. (2011). Fatigue behavior of damaged steel beams repaired with CFRP strips. *Engineering Structures*, 33(5), pp. 1491-1502.

Kopeliovich, D. Carbon Fiber Reinforced Polymer Composites, http://www.substech.com.

Koutchoukali, N., & Belarbi, A. (2001). Torsion of high-strength reinforced concrete beams and minimum reinforcement requirements. *ACI Structural Journal*, 98(4), pp. 462-69.

Lam, C. C. (2008). Repair of cracked steel structures by FRP patching. *Doctor of Philosophy Thesis*, University of Alberta.

Lanier, B., Schnerch, D., & Rizkalla, S. (2009). Behavior of steel monopoles strengthened with high-modulus CFRP materials. *Thin-Walled Structures*, 47(10), pp. 1037-47.

Lenwari, A., Thepchatri, T., & Albrecht, P. (2006). Debonding strength of steel beams strengthened with CFRP plate. *Journal of composites for construction*, 10(1), pp. 69-78.

Linghoff, D., Haghani, R., & Al-Emrani, M. (2009). Carbon-fibre composites for strengthening steel structures. *Thin-walled structures*, 47, pp. 1048-1058.

Liu, H. B., Zhao, X. L., Al-Mahaidi, R. (2006). The effect of fatigue loading on bond strength of CFRP bonded steel plate joints. *Proceedings of the International Symposium on Bond Behaviour of FRP in Structures*, Hong Kong, China.

Liu, H., Xiao, Z., Zhao, X. L., & Al-Mahaidi, R. (2009). Prediction of fatigue life for CFRP-strengthened steel plates. *Thin-Walled Structures*, 47(10), pp. 1069-77.

Mertz, D., & Gillespie, J. (1996). Rehabilitation of steel bridge girders through the application of advanced composite material. *NCHRP 93-ID11Transportation Research Board*, Washington, D.C., 1-20.

Mohammadizadeh, M. R. & Fadaee, M. J. (2009). Torsional behaviour of high-strength concrete beams strengthened using CFRP sheets; an experimental and analytical Study. *International Journal of Science and Technology*, 16(4), pp. 321-330.

Narmashiri, K., Zamin Jumaat, M., & Ramli Sulong, N. H. (2012). Failure analysis and structural behaviour of CFRP strengthened steel I-beams. *Construction and Building Materials*, 30, pp. 1–9.

Panchacharam, S. & Belarbi, A. (2002). Torsional behaviour of reinforced concrete beams strengthened with FRP composites. *First FIB Congress*, Osaka, Japan, October 13-19.

Photiou, N. K., Hollaway, L. C., & Chryssanthopoulos, M. K. (2006). Strengthening of an artificially degraded steel beam utilising a carbon/glass composite system. *Construction and Building Materials*, 20, pp. 11–21.

Product Information, Edition5/2012, Sika Kimia Sdn. Bhd. Sika (Singapore) Pte. Ltd. Sika 2012.

QuakeWrap (2008). Retrieved October 23, 2008, from Quake Wrap: www.quakewrap.com.

Ridley-Ellis, D. J. (2000). Rectangular hollow sections with circular web openings; fundamental behaviour in torsion, bending and shear, *PhD Thesis*, The University of Nottingham.

Ridley-Ellis, D. J., Owen, J. S., & Davies, G. (2003). Torsional behaviour of rectangular hollow sections. *Journal of Constructional Steel* Research, 59, pp. 641–663.

Ronagh, H. R., & Dux, P. F. (2003). Full-scale torsion testing of concrete beams strengthened with CFRP. *In: Proceedings of the First International Conference on the Performance of Construction Materials in the New Millenium*, February, Cairo, pp. 735-743.

Salom, P. R., Gergely, J. & Young, D. T. (2004). Torsional strengthening of spandrel beams with fibre- reinforced polymer laminates. *Journal of Composite for Construction*, 8(2), pp. 157-162.

Schnerch, D. (2005). Strengthening of steel structures with high modulus carbon fiber reinforced polymer (CFRP) materials, Doctor of Philosophy Thesis, North Carolina State University, Raleigh, North Carolina.

Schnerch, D., Dawood, M., Rizkalla, S., Sumner, E., & Stanford, K. (2006). Bond behavior of CFRP strengthened steel structures. *Advances in Structural Engineering*, 9(6), 805-817.

Schnerch, D., Dawood, M., Rizkalla, S., & Sumner, E. (2007). Proposed design guidelines for strengthening of steel bridges with FRP materials. *Construction and Building Materials*, 21, 1001-1010.

Sen, R., & Liby, L. (1994). Repair of steel composite bridge sections using carbon fiber reinforced plastic laminates. FDOT-510616, Florida Dept. of Transportation, Tallahassee, Fla.

Tavakkolizadeh, M., & Saadatmanesh, H. (2003a). Strengthening of steel-concrete composite girders using carbon fiber reinforced polymers sheets. *Journal of Structural Engineering*, ASCE, 129(1), pp. 30–40.

Tavakkolizadeh, M., & Saadatmanesh, H. (2003b). Fatigue strength of steel girders strengthened with carbon fiber reinforced polymer patch. *Journal of Structural Engineering*, ASCE, 129(2), pp. 186–96.

Zhang, J. W., Lu, Z. T. & Zhu, H. (2001). Experimental study on the behaviour of RC torsional members externally bonded with CFRP. *In: FRP Composites in Civil Engineering*, 1, pp. 713-22.

Zhao, X. L., Fernando, D., & Al-Mahaidi, R. (2006). CFRP strengthened RHS subjected to transverse end bearing force. *Engineering Structures*, 28(11), pp. 1555–65.

Zhao, X. L., & Zhang, L. (2007). State of the art review on FRP strengthened steel structures. *Engineering Structures*, 29(8), pp. 1808-1823.

Zhao, X. L., & Al-Mahaidi, R. (2009). Web buckling of lightsteel beams strengthened with CFRP subjected to end-bearing forces. *Thin-Walled Structures*, 47, pp. 1029-1036.

APPENDIX A

In this appendix, the figures of strain along the CFRP sheets for different specimens are presented.

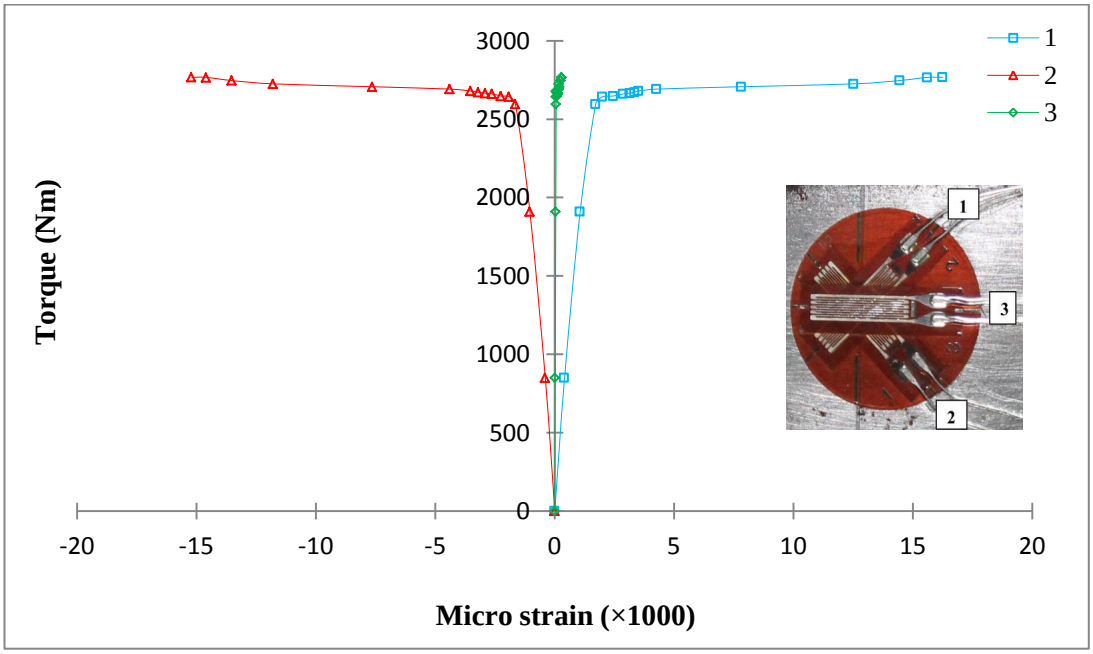

Figure A.1 The torque-strain curves of SHS1 (at 0.25 of length, side 1)

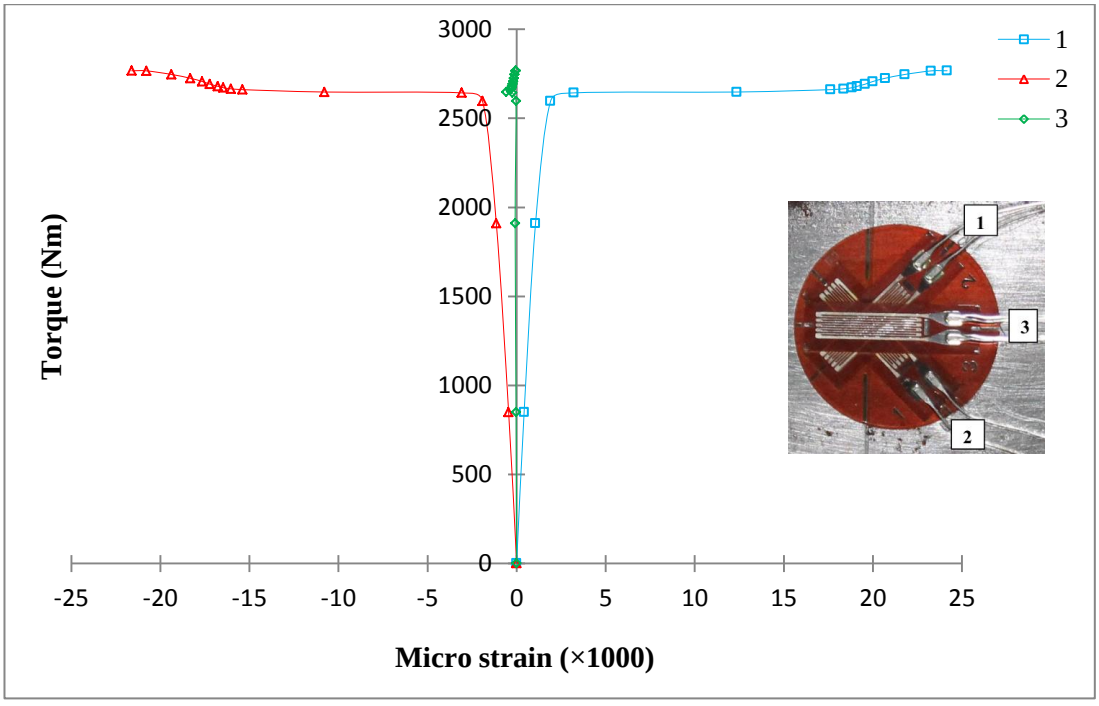

Figure A.2 The torque-strain curves of SHS1 (at 0.5 of length, side 1)

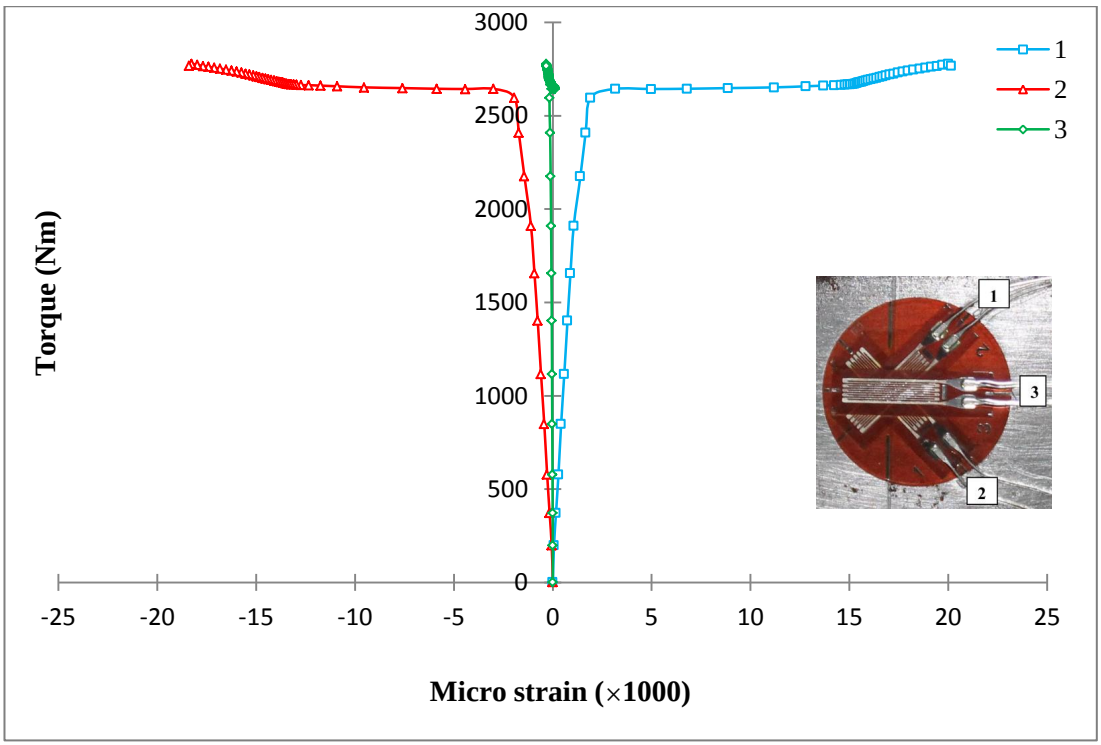

Figure A.3 The torque-strain curves of SHS1 (at 0.75 of length, side 1)

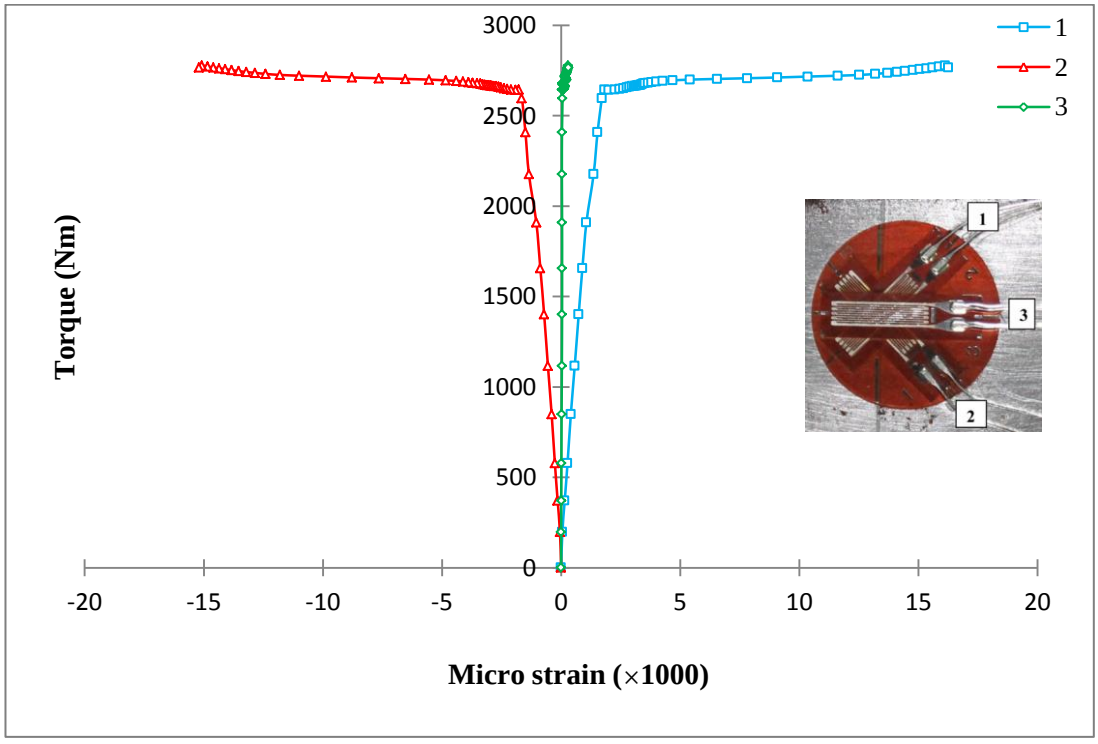

Figure A.4 The torque-strain curves of SHS1 (at 0.25 of length, side 2)

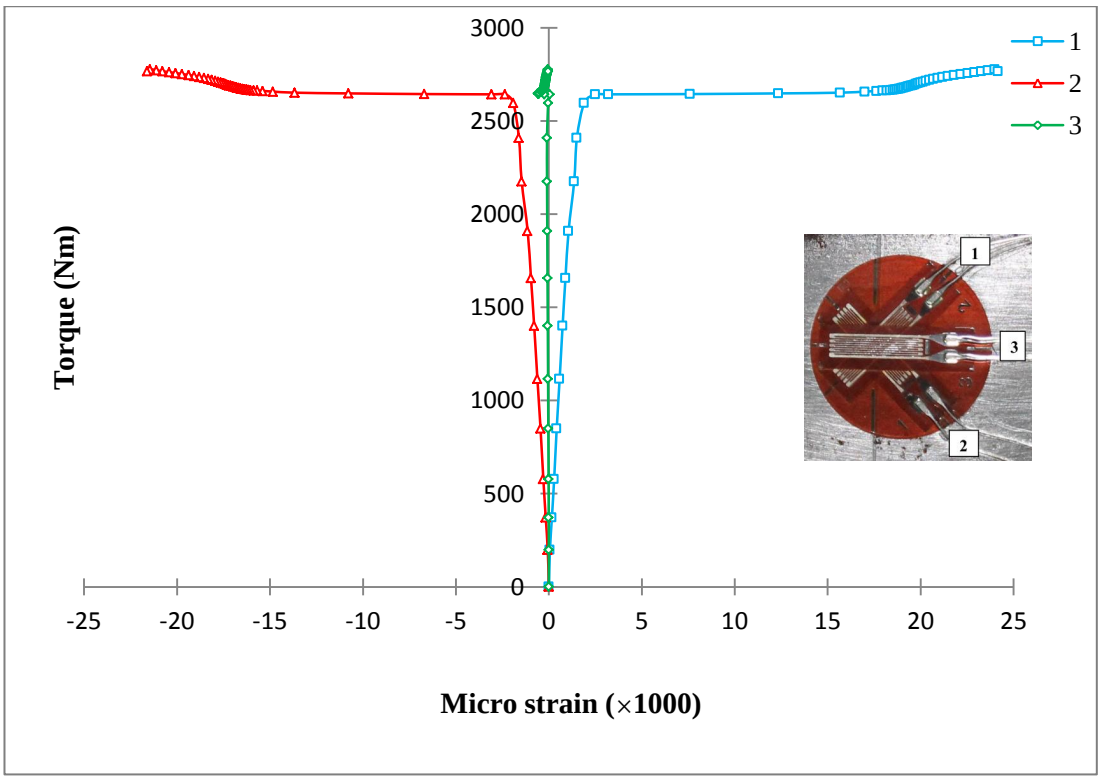

Figure A.5 The torque-strain curves of SHS1 (at 0.5 of length, side 2)

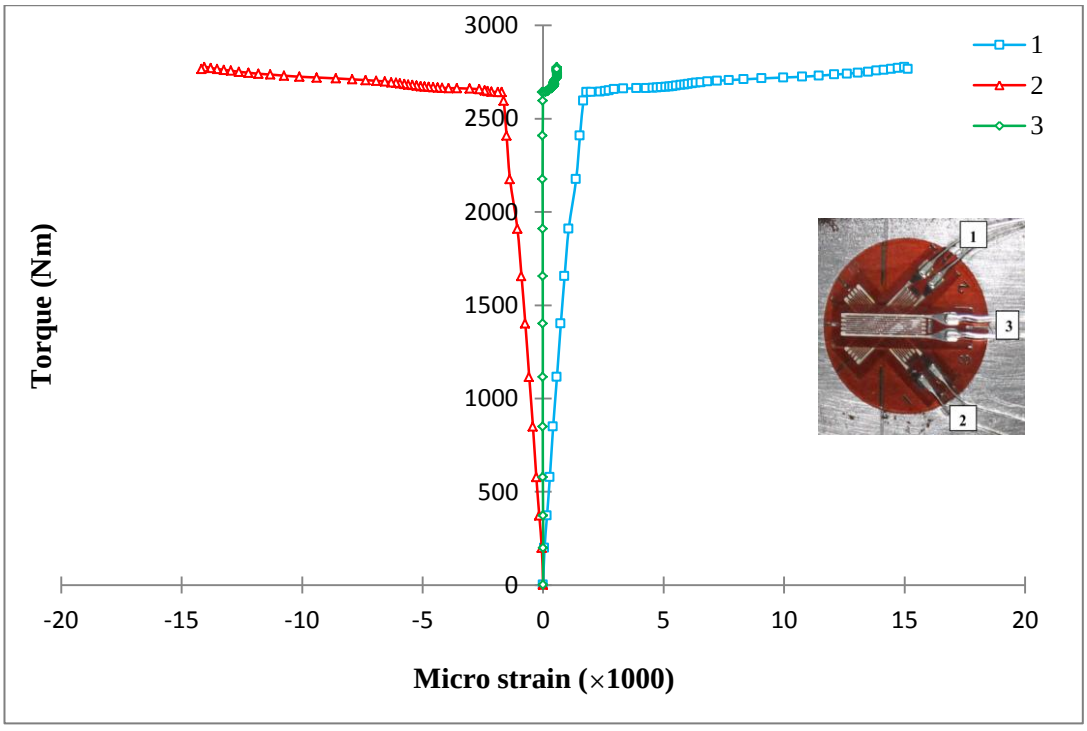

Figure A.6 The torque-strain curves of SHS1 (at 0.75 of length, side 2)

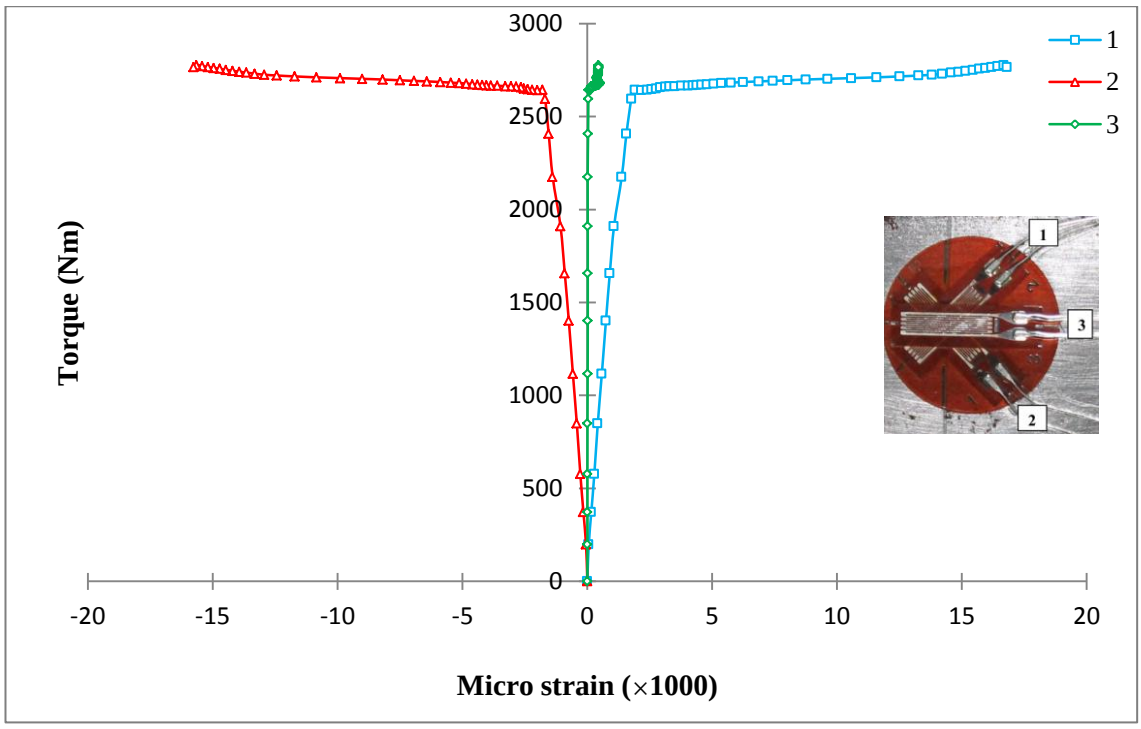

Figure A.7 The torque-strain curves of SHS1 (at 0.5 of length, side 3)

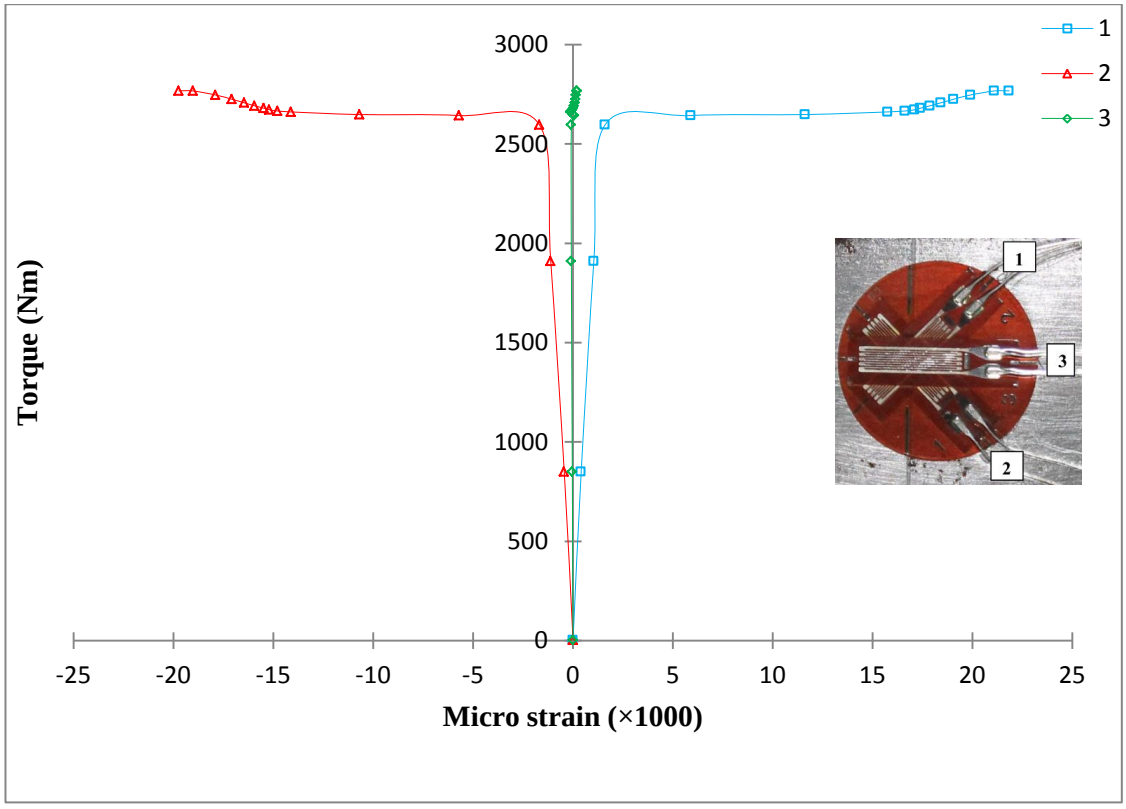

Figure A.8 The torque-strain curves of SHS1 (at 0.5 of length, side 4)

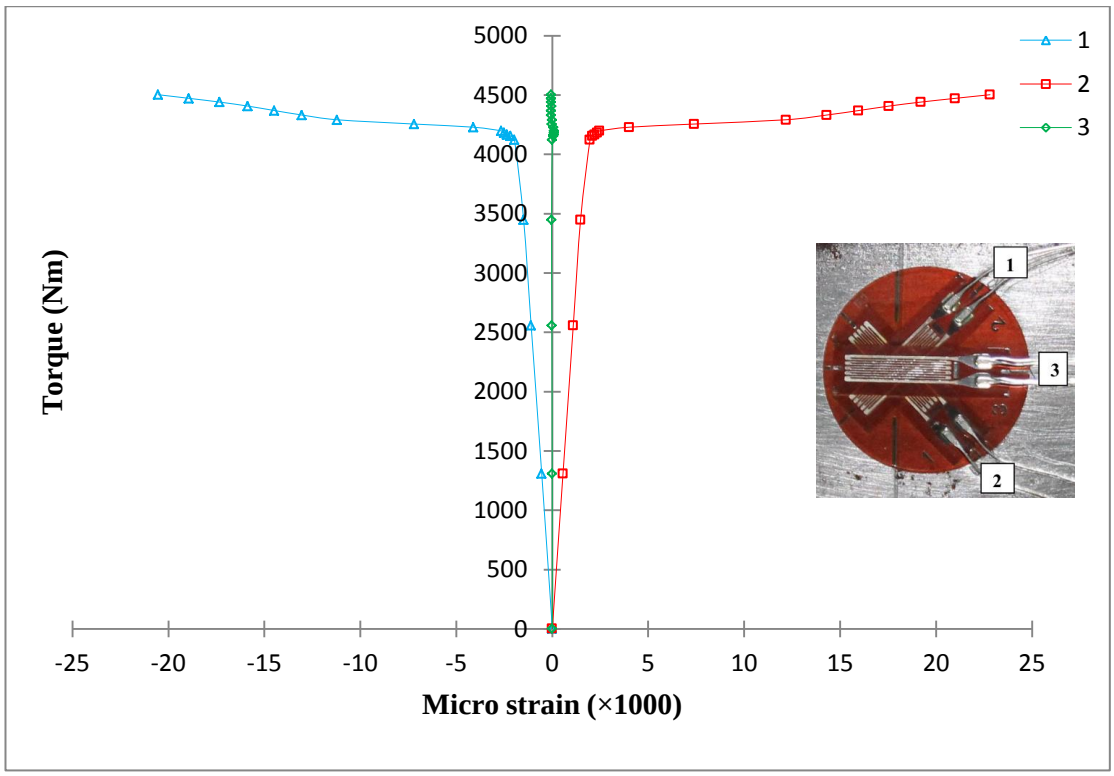

Figure A.9 The torque-strain curves of SHS2 (at 0.5 of length, side1)

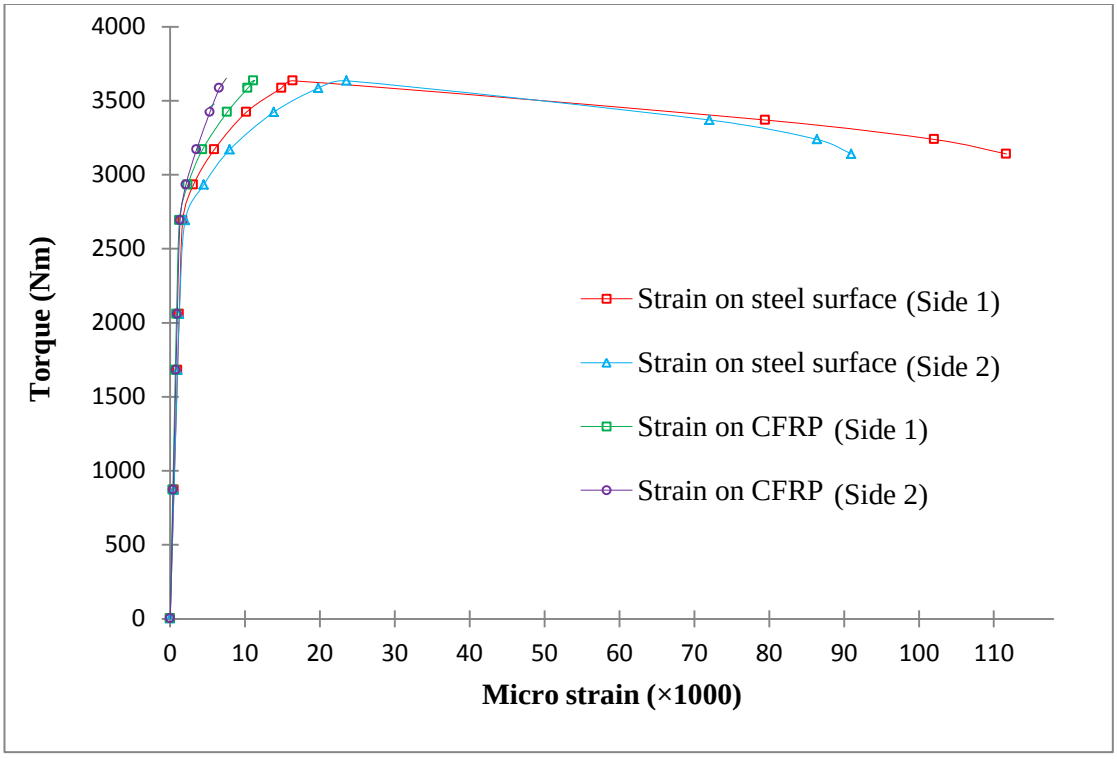

Figure A.10 Strain values on the steel surface and on the CFRP at mid-span for strengthened beam $SHS1_{SR60^{\circ}}$

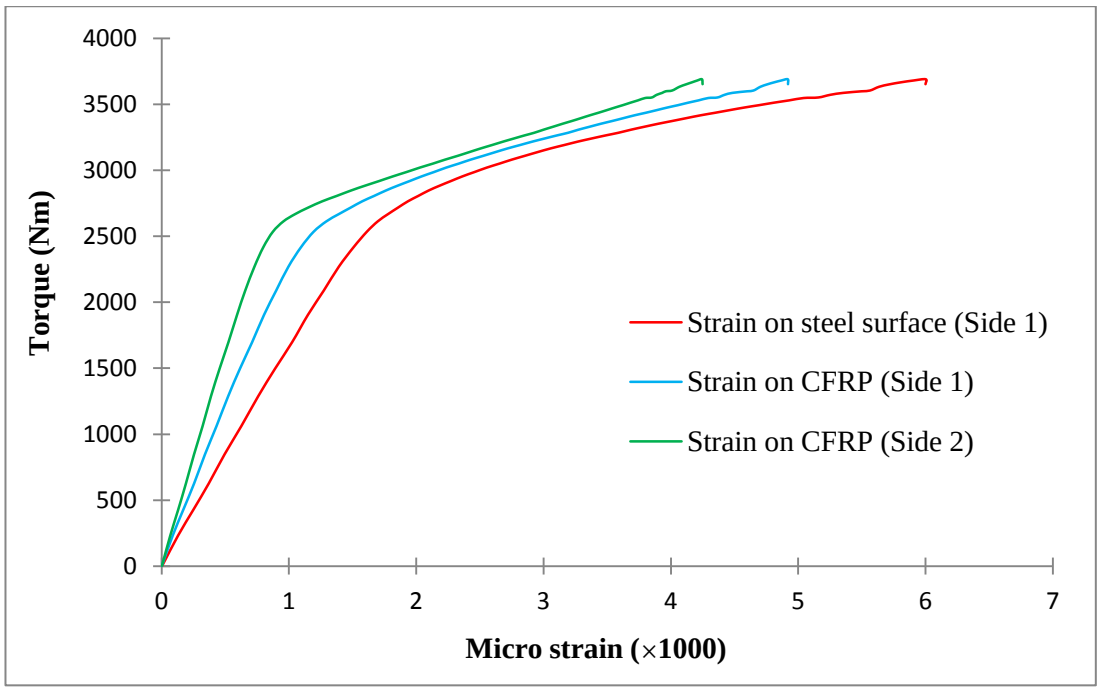

Figure A.11 Strain values on the steel surface and on the CFRP at mid-span for strengthened beam $SHS1_{RR60^{\circ}}$

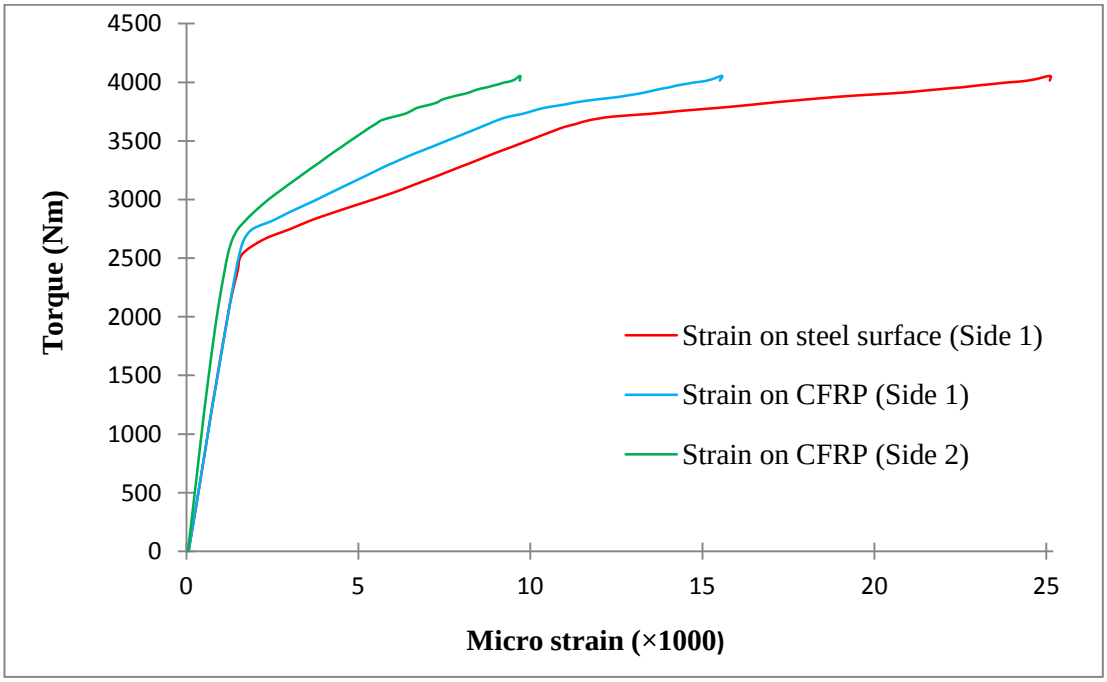

Figure A.12 Strain values on the steel surface and on the CFRP at mid-span for strengthened beam $SHS1_{RSR60^{\circ}}$

APPENDIX B

In this appendix, figures of failure modes for CFRP sheet strengthened specimens are presented.

Figure B.1 CFRP splitting failure mode of $SHS1_{V90^o}$

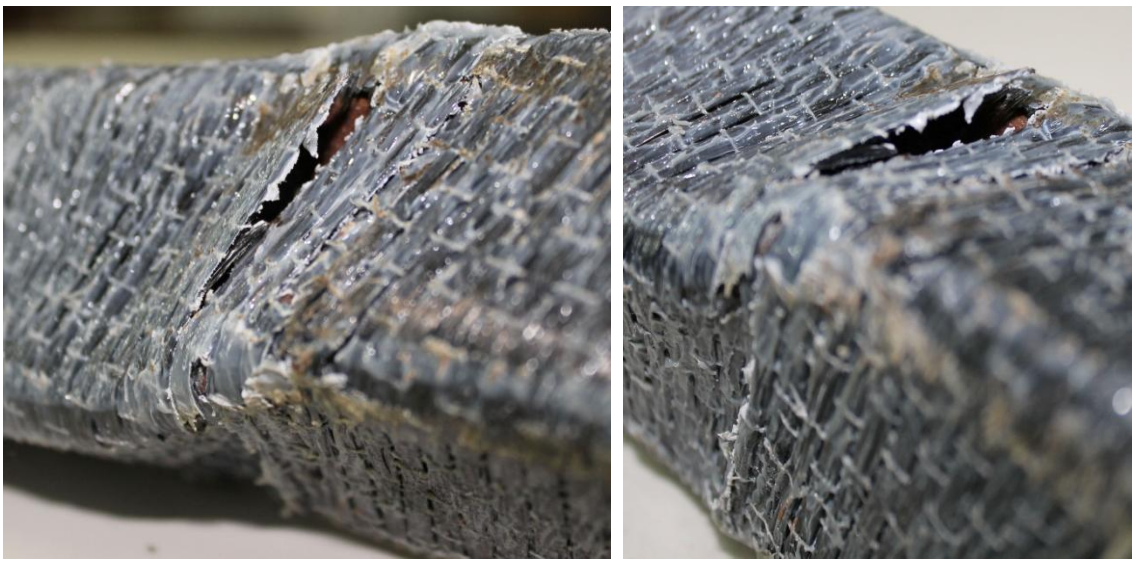

Figure B.2 CFRP rupture and debonding failure modes of $SHS1_{R60^\circ}$

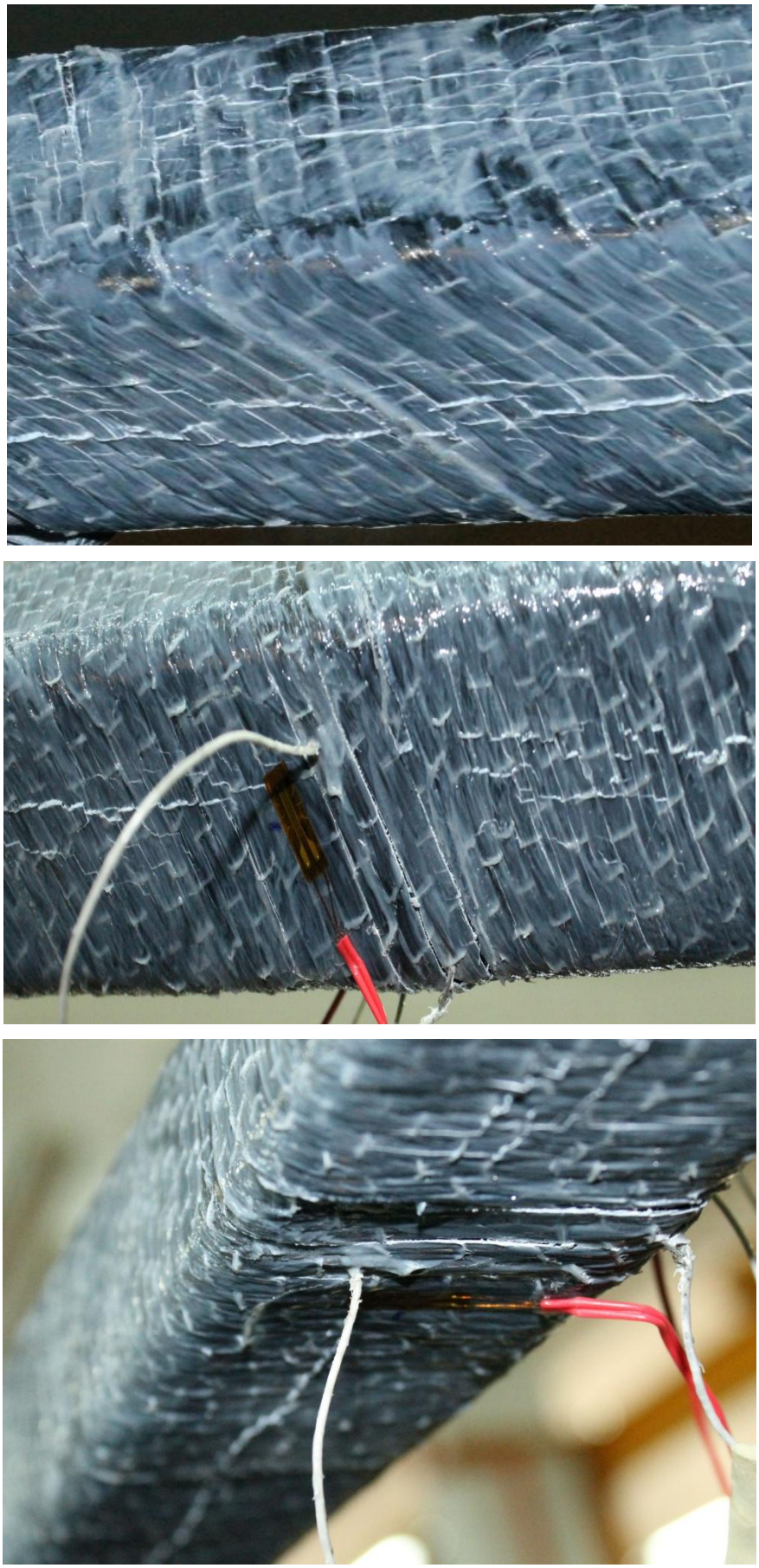

Figure B.3 CFRP splitting failure mode of $SHS1_{SS60^o}$

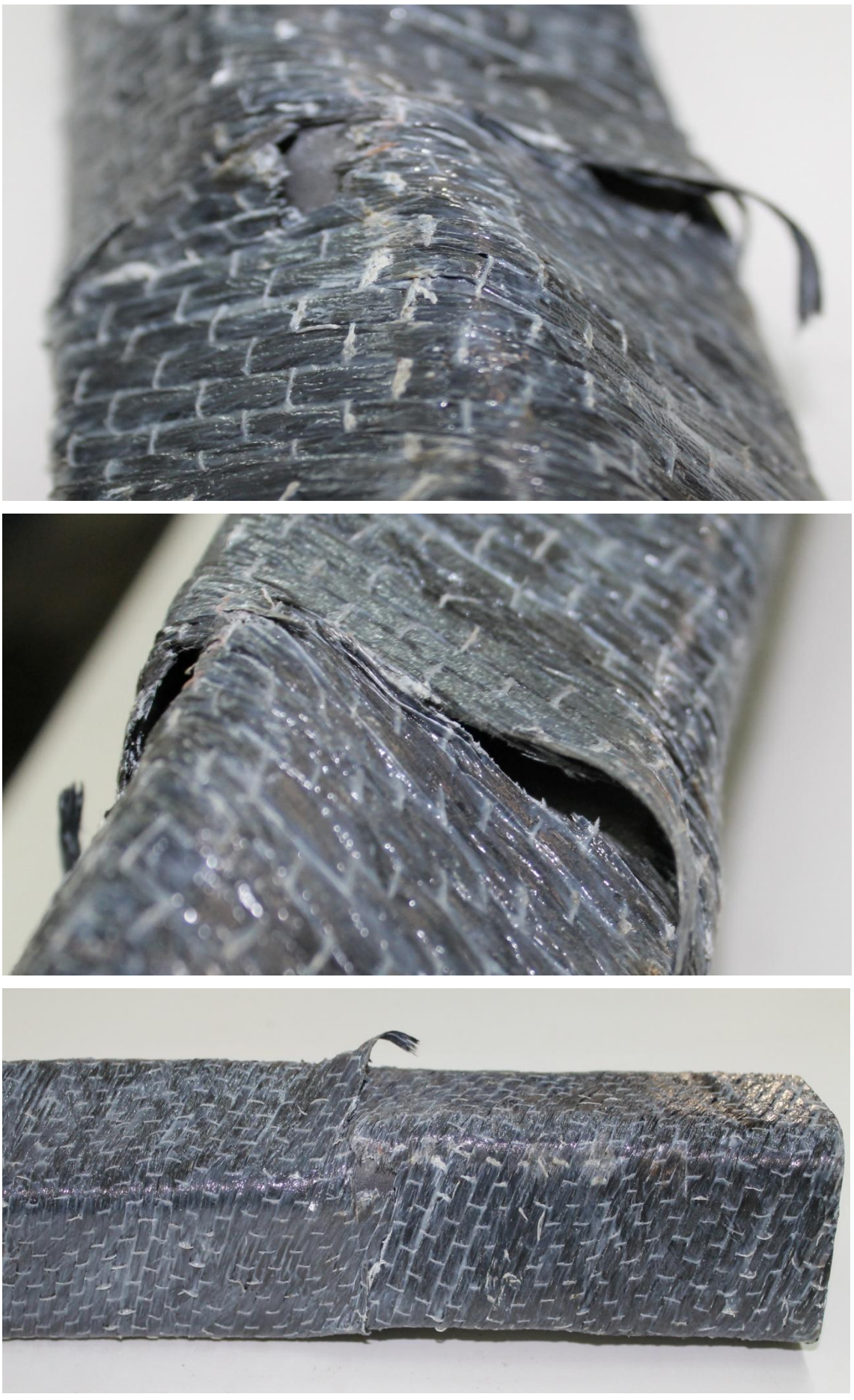

Figure B.4 CFRP rupture and debonding failure modes of $SHS1_{RR60^o}$

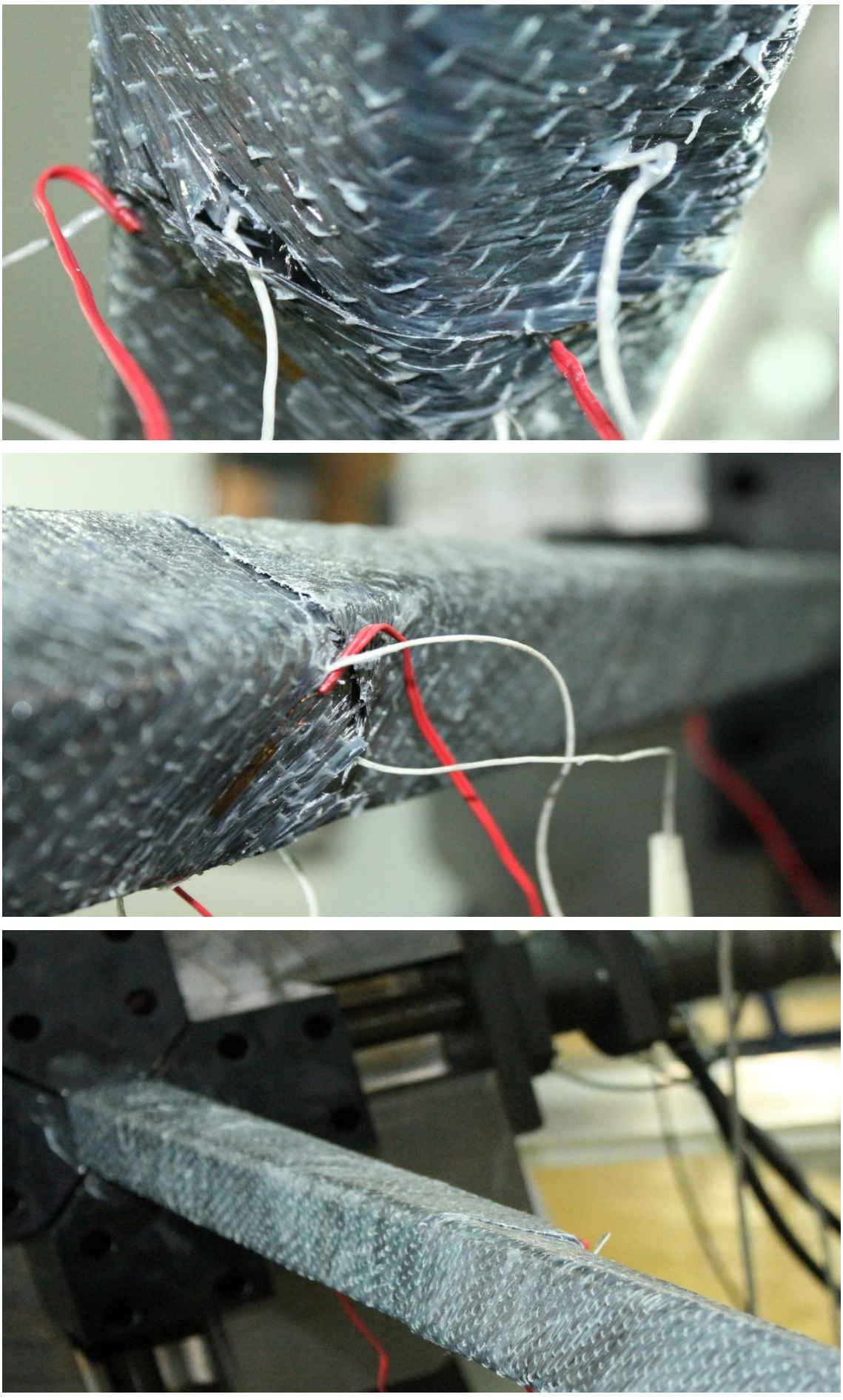

Figure B.5 CFRP rupture and debonding failure modes of $SHS1_{SR60^o}$

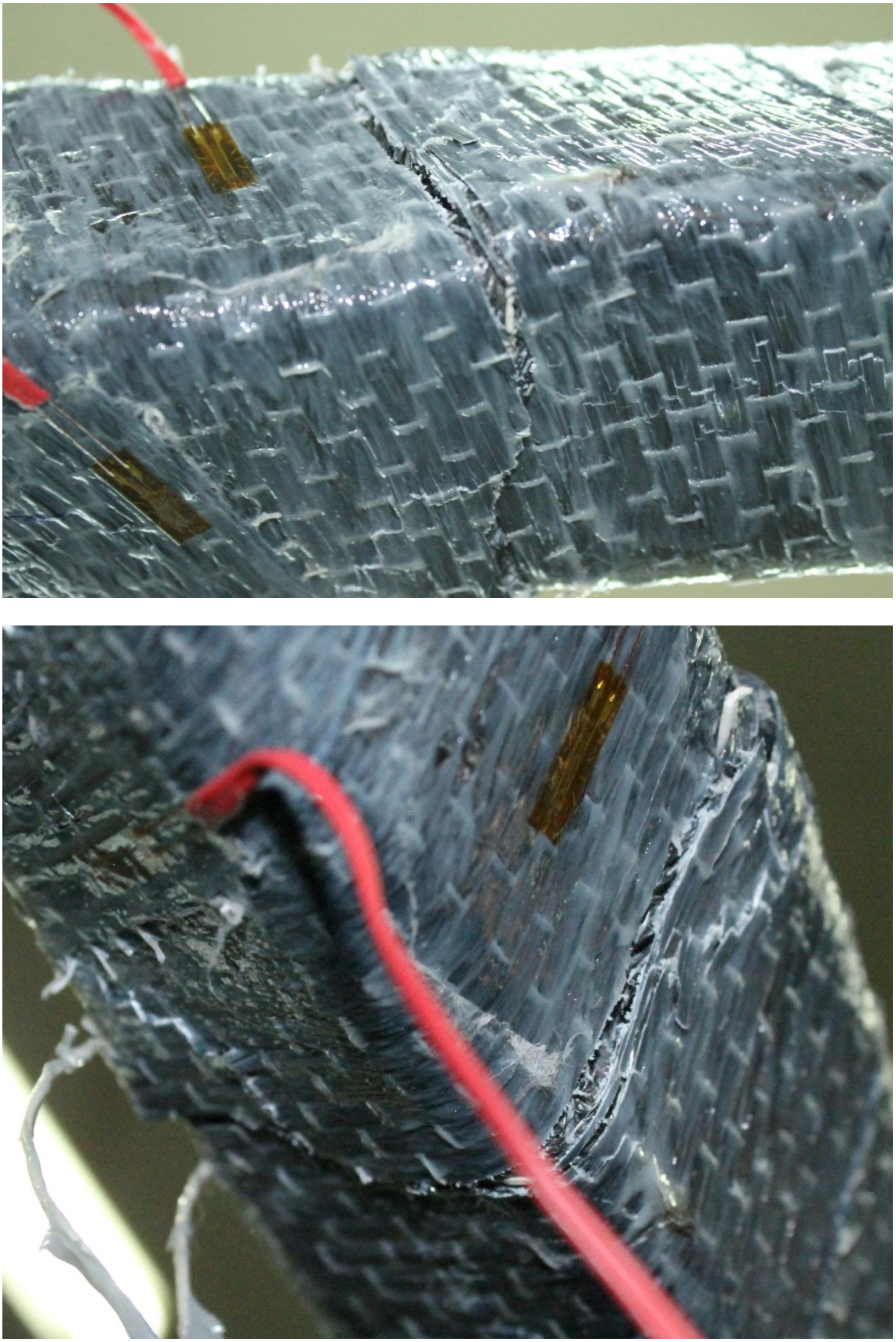

Figure B.6 CFRP splitting failure mode of $SHS1_{SRS60^o}$

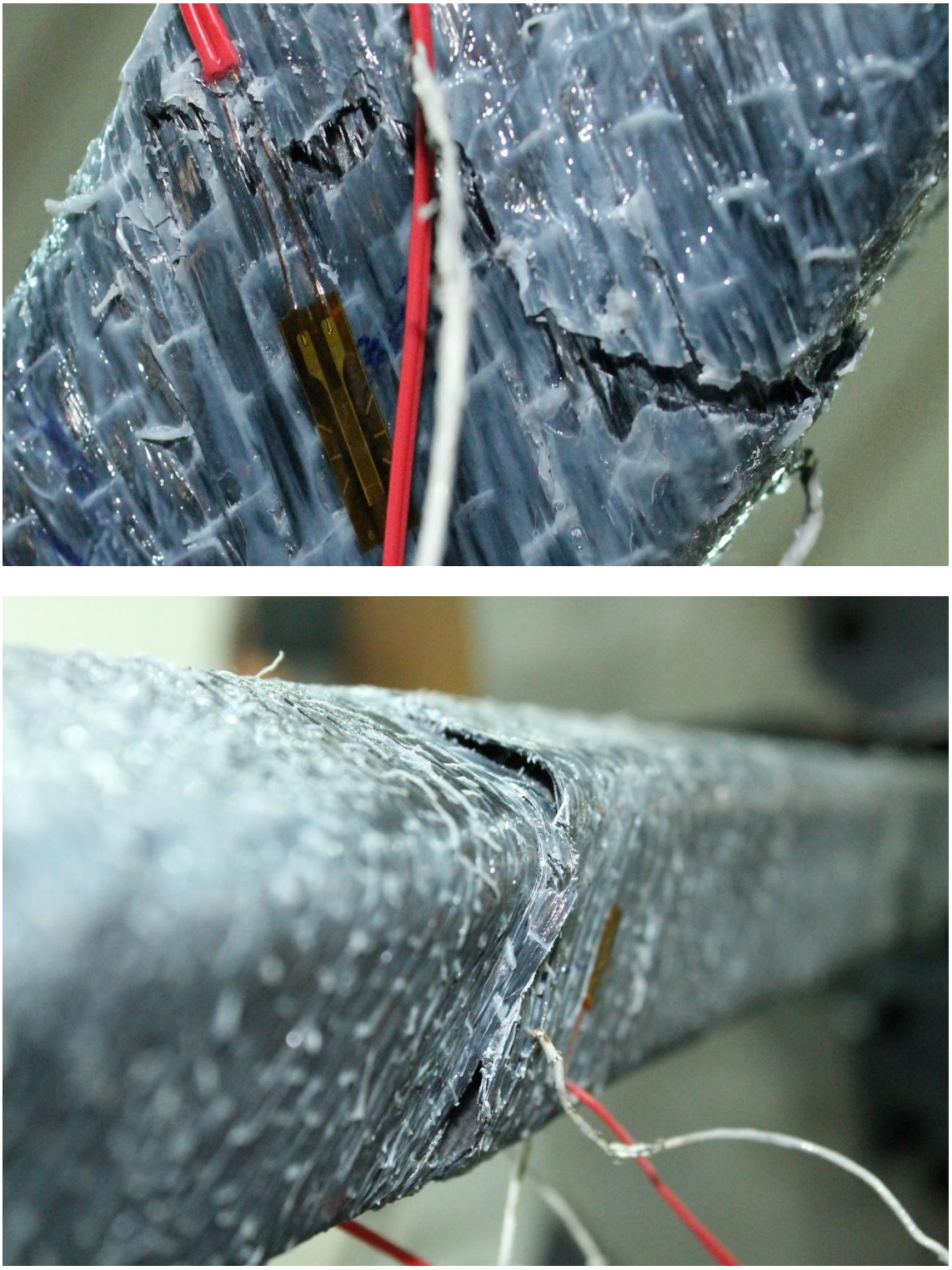

Figure B.7 CFRP rupture and debonding failure mode of $SHS1_{RSR60^o}$

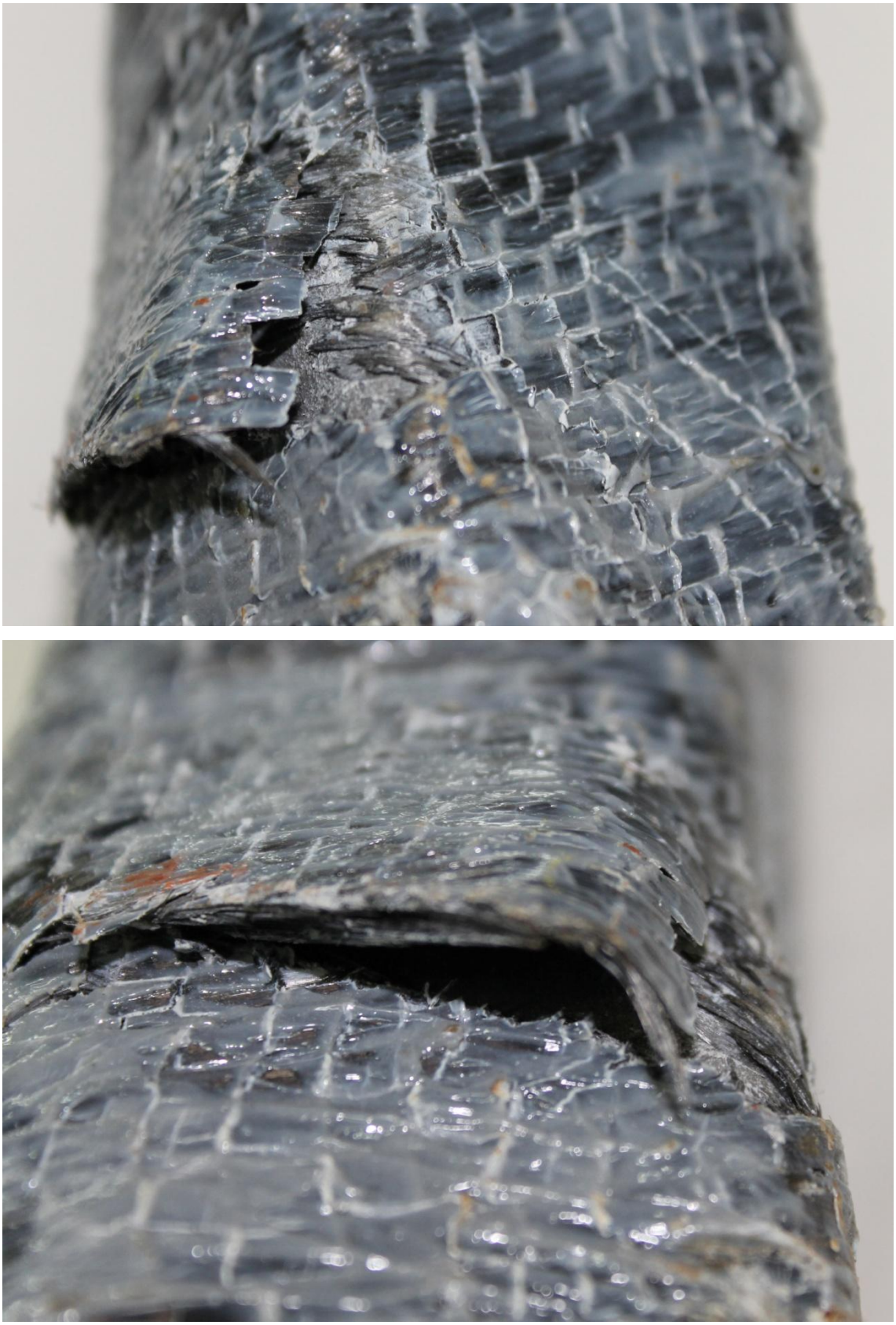

Figure B.8 CFRP rupture and debonding failure mode of $SHS1_{RRRS60^o}$

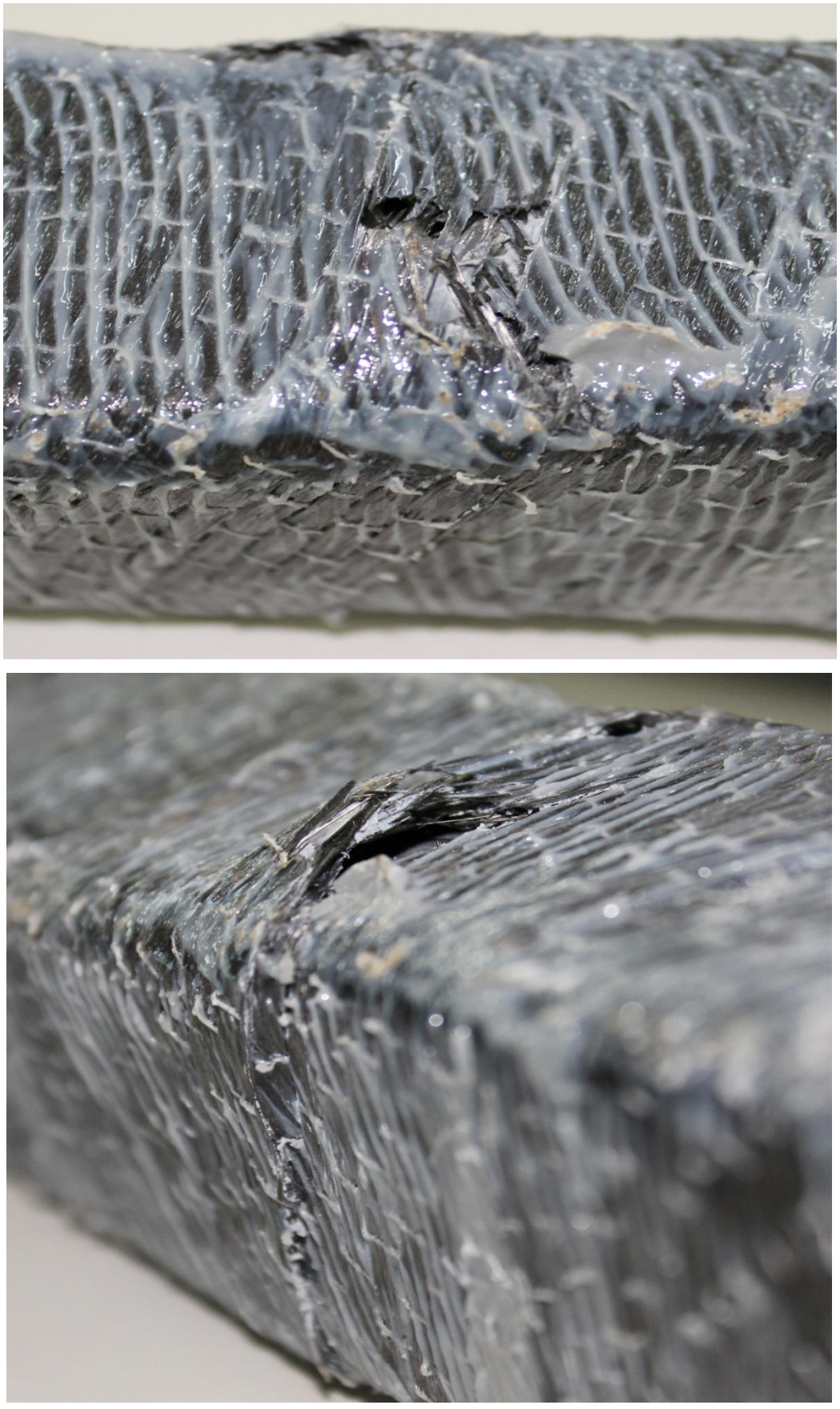

Figure B.9 CFRP rupture and debonding failure mode of $SHS1_{RSRS60^o}$

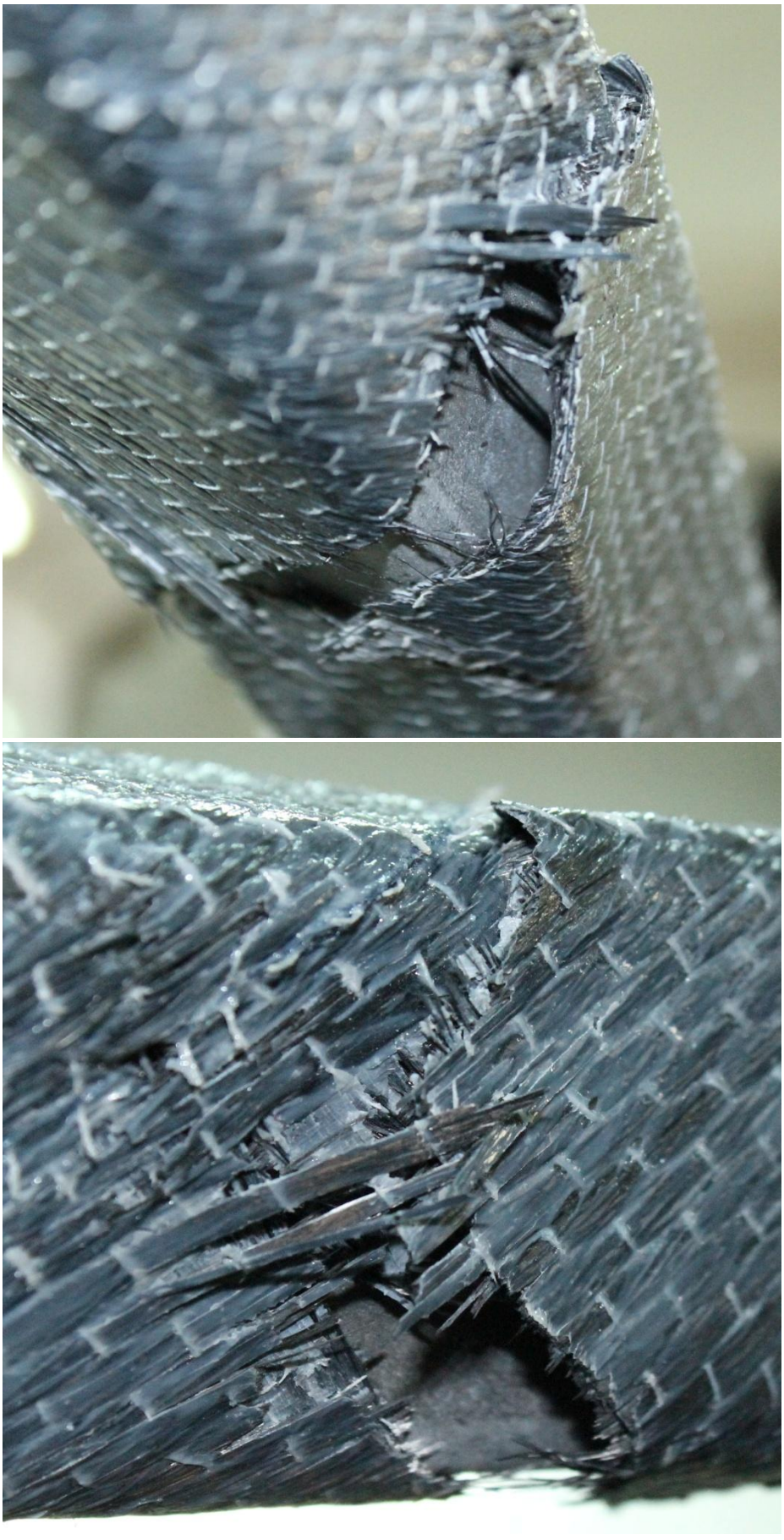

Figure B. 10 CFRP rupture and debonding failure mode of $SHS1_{SRSR45^{\circ}}$

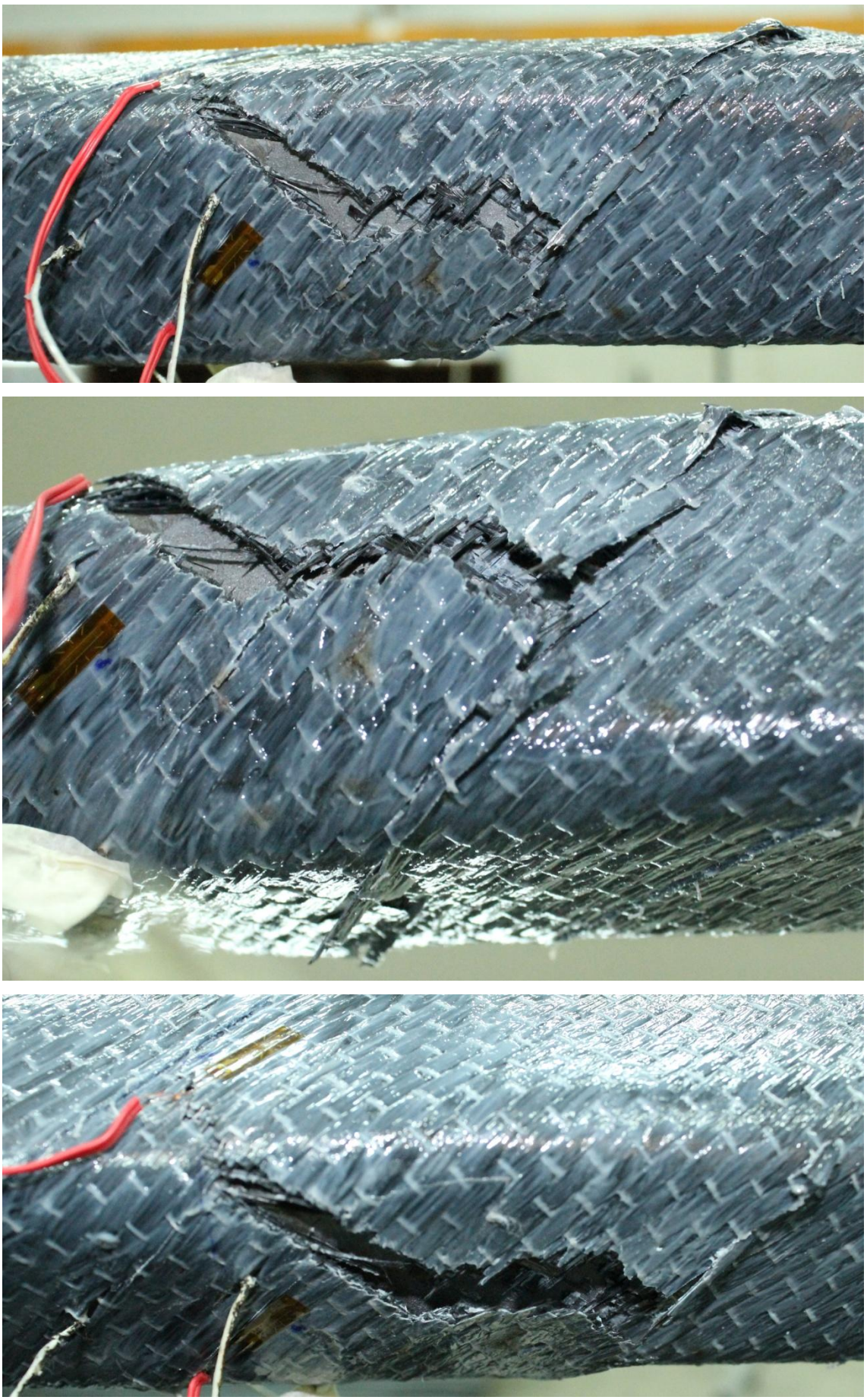

Figure B.11 CFRP rupture and debonding failure mode of $SHS2_{SRSR45^{\circ}}$

PATENT Filed

Title of invention: A REINFORCING SYSTEM FOR A HOLLOW STRUCTURAL MEMBER AND A METHOD THEREOF (*Patent No: PI 2012700851*).

JOURNAL PUBLICATIONS

Abdollahi Chahkand, N., Zamin Jumaat, M., Ramli Sulong, N. H., Zhao, X. L., Mohammadizadeh, M. R. (2013). Experimental and theoretical investigation on torsional behaviour of CFRP strengthened square hollow steel section. *Thin-Walled Structures*, 68: 135-140. (Q1, ISI-Cited Publication).

Abdollahi Chahkand, N., Zamin Jumaat, M., Ramli Sulong, N. H., Zhao, X. L., Shariati, M. (2013). Effects of CFRP strengthening on torsional behavior of SHS. *Journal of Constructional Steel Research*, Ref.No.: JCSR-D-13-00198 (Under Review), (Q1, ISI-Cited Publication).

CONFERENCE PROCEEDINGS

Abdollahi Chahkand, N., Jumaat, M. Z., Ramli Sulong, N. H., Mohammadizadeh, M. R., Asadi, A., & Mojarrad, M. (2012). Experimental investigation on torsional behavior of CFRP strengthened square hollow steel section, *Forensic Engineering 2012:Gateway to a Better Tomorrow Proceedings of the 6th Congress on Forensic Engineering* (ASCE 2013), San Francisco, CA. pp 1101-1110.

Abdollahi Chahkand, N., Jumaat, M. Z., & Ramli Sulong, N. H. (2012). Improving torsional behavior of square hollow section (SHS) with carbon fiber reinforced polymer (CFRP). *7th Asia-Oceania Top University League on Engineering (AOTULE 2012)*, University of Malaya, Kuala Lumpur, Malaysia, Paper ID: 127.

AWARD

The leading international invention and innovation Expo 2013. Innovative method of strengthening steel beam in torsion, Bronze Medal, MTE 2013, 21-23 Feb 2013, Kuala Lumpur, Malaysia.